

## **General Disclaimer**

### **One or more of the Following Statements may affect this Document**

- This document has been reproduced from the best copy furnished by the organizational source. It is being released in the interest of making available as much information as possible.
- This document may contain data, which exceeds the sheet parameters. It was furnished in this condition by the organizational source and is the best copy available.
- This document may contain tone-on-tone or color graphs, charts and/or pictures, which have been reproduced in black and white.
- This document is paginated as submitted by the original source.
- Portions of this document are not fully legible due to the historical nature of some of the material. However, it is the best reproduction available from the original submission.

(NASA-TM-77467) TURBO FLUID MACHINERY AND  
DIFFUSERS (National Aeronautics and Space  
Administration) 220 P HC A10/MF A01

N85-17363

CSCI 131

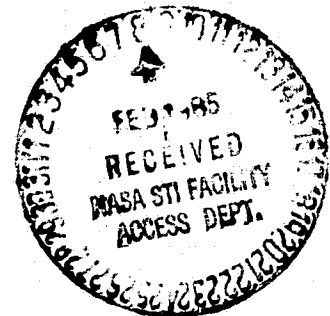
Uncias

G3/37 13523

TURBO FLUID MACHINERY AND DIFFUSERS

Teruo Sakurai

Translation of "Nikkan Kogyo Shinbunsha",  
September 30, 1983, First Edition, pp.  
1-187.



## STANDARD TITLE PAGE

1. Report No. NASA TM-77467	2. Government Accession No.	3. Recipient's Catalog No.	
4. Title and Subtitle TURBO FLUID MACHINERY AND DIFFUSERS		5. Report Date SEPTEMBER 1984	
		6. Performing Organization Code	
7. Author(s) Teruo Sakurai		8. Performing Organization Report No.	
		10. Work Unit No.	
9. Performing Organization Name and Address SCITRAN Box 5456 Santa Barbara, CA 93108		11. Contract or Grant No. NASW 4004	
		12. Type of Report and Period Covered Translation	
12. Sponsoring Agency Name and Address National Aeronautics and Space Administration Washington, D.C. 20546		14. Sponsoring Agency Code	
		13. Supplementary Notes Translation of "Kikkan Kogyo Shinbunsha", September 30, 1983, First Edition, pages 1-187.	
16. Abstract  This book explains the general theory behind turbo devices and diffusers, and discusses problems and the state of research on basic equations of flow, experimental and measuring methods. Conventional centrifugation-type compressor and fan diffusers are primarily examined.			
17. Key Words (Selected by Author(s))		18. Distribution Statement  Unclassified and Unlimited	
19. Security Classif. (of this report) Unclassified	20. Security Classif. (of this page) Unclassified	21. No. of Pages 206	22. Price

## TABLE OF CONTENTS

Introduction	1
Chapter 1. Turbo Fluid Machines and Diffusers	4
1.1. Turbo fluid machines and diffusers	4
1.2. Blade and bladeless diffusers for centrifugal compressor and fans	8
1.3. Application of blade diffusers	13
1.4. Other diffusers used in centrifugation compressors and fans	
1.5. Diffusers used in other fluid machines	19
Chapter 2. Basic Equations for Flow of Turbo Machines	23
2.1. Basic equations	23
2.2. Examples of calculations of the flow and boundary film	40
Chapter 3. Designs for Diffusers and Research Results	51
3.1. Theoretical equation and design of compressors and fans	51
3.2. Diffuser design methods	67
3.3. Problems with diffuser properties Diffuser design tests	73 79
Chapter 4. Experiments and Measurement and Analysis Methods for Diffusers	81
4.1. Experimental device and model structure	81
4.2. Measurement gauges and methods	89
4.3. Theoretical analysis	105
Chapter 5. General Pipe Type Diffuser Properties	108
5.1. Conical diffusers	108
5.2. Two dimensional diffusers	112
5.3. Annular diffusers	116

5.4.	Cross section and center lines	118
5.5.	Form of inlets and outlets	126
5.6.	Inlet boundary layer and boundary layer control	130
5.7.	Effect of Reynolds number and Mach number	136
5.8.	Shear flow and swirl flow effects	139
Chapter 6. Centrifugation Diffuser Properties		145
6.1.	Centrifugation bladed diffusers	145
6.2.	Bladed diffuser	158
6.3.	Bladeless diffusers	168
6.4.	Axially symmetric flow paths	184
6.5.	Effect of fluid dynamic variables	190
Chapter 7. Properties of Turbo Fluid Device Diffusers		198
7.1.	Introduction	198
7.2.	Inspection and adjustment of data	198
7.3.	Tests on inspection results (technological trends)	200
7.4.	Conclusion	205

## INTRODUCTION

/i\*

Turbo fluid machines are of the centrifugal-type, axial flow type, etc., "velocity" fluid machines (machines that convert electrical power to fluid energy and obtain power from fluid energy, that is, compressors, fans, pumps, etc., by acceleration or deceleration of the fluid). Diffusers are conventional means for deceleration of fluids.

Conventional diffusers have fluid path elements, such as wide, cone-shaped pipes, etc., while turbo fluid machines (particularly compressors and fans) can be used for deceleration (fluid paths). This type of fluid machine is characterized by the fact that, in comparison to other types (return movement-type, rotary-types, etc.), the diffuser plays an important role. Turbo-type fluid machines are also characterized by the fact that they can easily be made into high speed, small devices or high speed, large devices. Consequently, they are receiving a great deal of attention in industry, communications, home electronics, etc. Improvements have also been made in the field of diffusers in order to improve the capabilities of these machines and promote energy saving measures. Diffusers are typical hydraulic elements. However, their development has reached a new age and marked results are being obtained (with regard to compressors and fans, the term diffuser has been conventionally used, but the term is only applied to certain parts of pumps). In recent years there has been a move to use the common terminology whenever possible because compressors and fans and pumps operate on the same basic theory. Centrifugal pumps having a diffuser (guide blade) are called diffuser pumps (conventional turbo pumps).

---

\* Numbers in margin indicate pagination of foreign text

There have been many reports on hydraulic engineering (hydraulics) and on fluid machines. However, there have been few reports that give details on diffusers.

Judging from hydraulic engineering or hydraulic technology, it appears that diffusers are one means for deacceleration of fluids. It is also one of the structural elements of hydraulic machines. In comparison to straight currents (uniform velocity current paths) and curved paths, there are problems with the flow used in diffusers in that it is difficult to change the flow to the appropriate direction. Moreover, in comparison to narrow flow paths (accelerated flows), it is difficult to readily produce a deviate flow (deflected flow) or to remove the flow from the walls when the current is deaccelerated.

Moreover, the important parts of the fluid machines differ from the essential sections of conventional machines that provide energy to the fluid (total pressure or increase in total head). Research on diffusers that change the energy of the fluid to static pressure has been carried out. However, in recent years there has been an improvement in fluid machines based on the idea of resources and energy. Marked progress has also been made in evaluation technologies and in methods for theoretical and numerical research.

/ii

From this point, it appears that diffuser technology ("diffuserology") is an important part of fluid technology.

Diffusers are simple flow elements. There are many types of forms that affect the properties of the flow and many types of hydraulic elements (hydraulic variants of the Reynolds' number and other constants). The flow phenomenon is also complex and design technology is therefore very complicated.

This text explains the general theory behind turbo devices and diffusers and comments on problems and the state of research on basic equations of flow, experimental and measuring methods, etc. Moreover, with the exception of simple forms, there are cases where there are many unknown points that must be determined before establishing a policy for the design of diffusers. The reader should also refer to the many references that may be of interest.

In addition, the authors did not mention in detail the phenomenon of high current velocity (ultrasonic diffusers) and unique properties of hydraulic systems (related to diffusers). They instead chose to focus on conventional centrifugation-type compressor and fan diffusers, which is where their point of expertise lies.

This text was prepared as research on fluid machines. /iii  
However, it may also have an important role in the design and use of conventional equipment and structures used in hydraulics.

Furthermore, the authors have used S. I. units whenever possible (mass and density rather than weight).

June 1983

Authors



## TURBO FLUID MACHINES AND DIFFUSERS

1.1 Turbo fluid machines and diffusers

Turbo fluid machines are centrifugal-type or axial flow-type "velocity" fluid machines (machines that convert electrical power to fluid energy and obtain power from fluid energy by acceleration or deacceleration of fluids, that is, compressors, fans, pumps, etc.). Diffusers are generally paths for deacceleration of fluids. In systems, equipment and devices that use fluids, such as gases and liquids, the fluid must be connected from the small cross sectional paths (feed side) to the large cross sectional paths (application side). In this case when there is a direct connection between the small cross sectional side and large cross sectional side, sudden expansion of the surface area occurs. Therefore, the fluid is blown in a spray form to the down current side and a peeling section or still water section is produced, resulting in pressure loss (or energy loss). This loss is one factor that must be avoided in order to solve energy problems. The above mentioned loss may be disregarded in cases where it is small in comparison to the energy possessed by the fluid (cases of high pressure, low current). However, there are cases where the loss cannot be disregarded (cases of intermediate-low pressure high currents). Therefore, in order to prevent this type of loss, a path must be used to steadily increase the cross section area.

/2

Diffusers are paths that introduce a flow while steadily increasing the flow path cross section area. In addition to the above mentioned purpose of:

- (a) introducing a fluid to a desired position with as little as possible pressure loss,
- diffusers also have the following purposes:

- (b) introduction of current to down flow side so that it is uniformly distributed throughout the current path cross section and
- (c) reduction in high pressure of fluid at inlet side (or of velocity energy) and changing the reduction to static pressure increase.

As will be mentioned in Chapter 2, the sum of dynamic pressure and static pressure (total pressure) is constant with ideal flows. Moreover, the dynamic pressure reduction can be changed to an increase in static pressure with actual diffusers, etc.

Furthermore, velocity energy is wasted in cases where the fluid is ultimately emitted to the air or space. Therefore, a reduction in the velocity of the emitted gases (liquids) is related to a reduction in energy loss, that is, efficient operation.

Diffusers come in the shapes shown in Figure 1-1. For instance, there are

- (a) conical diffusers,
- (b) two-dimensional diffusers (one side has a constant cross section, while the other increases in size),
- (c) pyramid diffusers,
- (d) annular diffusers (cross section is concentric) and
- (e) diffuser with nonsimilar end cross sections (cross sections change in shape from round to square).

Moreover, all forms in the figure have a straight central axis and changes in the diameter or width (depth) are simple linear changes. However, there are cases of complex form having a bent central axis (curved diffusers) and where the changes in diameter and width are not linear (for instance, rappa\* diffusers or bell-shaped diffusers), etc., are used. (Complex forms where the

---

\*Translator's note: term unknown; transliteration of phonetic characters.

central axis is bent and the surface area changes are used in diffusers that are used in engines and air conditioners).

Diffusers have wide pipes whose "cross section gradually increases". For instance, the simplest conical diffusers usually have wide pipes (angle formed by two lines) which increase gradually. When the angle becomes too wide, the deaccelerated flow produced a boundary layer (increased pressure flow in above mentioned (c)). The bonding strength between the flow and flow path wall decreases (actually friction stress) and becomes zero. Therefore, the flow peels from the walls and there is a marked deterioration in diffuser properties, that is (a)-(c).

In designing diffusers with a low expansion rate, the total length is long. However, this is uneconomic. Therefore, the friction loss with the flow increases and there is a steady deterioration of diffuser properties. The diffuser is a simple flow element and, therefore, basic deacceleration is essential (flow where peeling and uniform flow velocity distribution readily occurs). Taking changes in the bend and cross section into consideration, it appears that diffusers with good properties in a restricted space represent an important engineering and research problem.

Figure 1.2 shows an example of a diffuser that is used as an element for wind tunnels. The three diffusers of first diffuser 4, second diffuser 10 and wide angle diffuser 14 are used. The wind tunnel is sealed and, therefore, air is circulated repeatedly by fan 9. The flow is deaccelerated by the second diffuser (area ratio of inlet and outlet of 2.98, wide angle of 4 25') and the wide angle diffuser (area ratio of 1.73 and angle of 44 46 '); 4  
three wire nets are set up inside to prevent peeling caused by the wide angle. The current is introduced to regulator 16 at a low speed and then is accelerated by nozzle 17. The current is

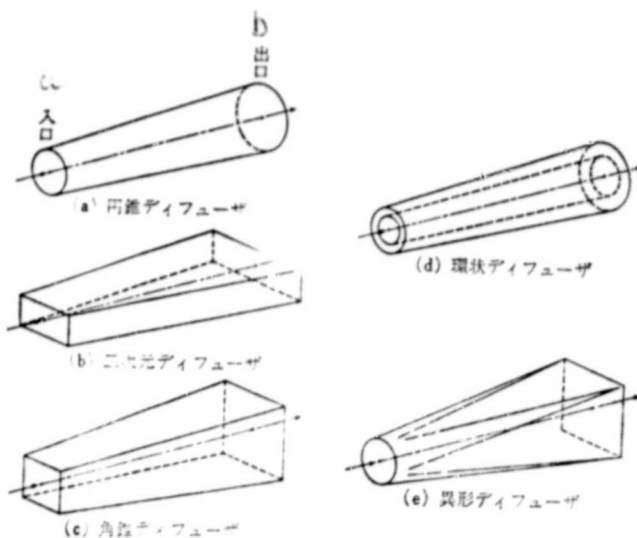


Figure 1.1. Various shapes of diffusers  
 Key: (a) conical diffusers (b) two-dimensional diffuser  
 (c) pyramid diffuser (d) annular diffuser  
 (e) diffuser with non-similar end cross sections  
 a. inlet b. outlet

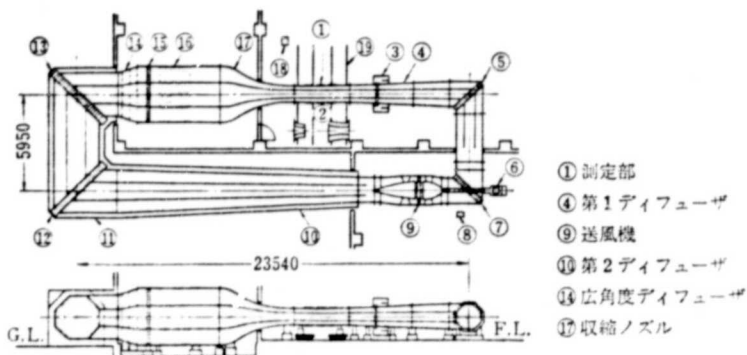


Figure 1.2. Diffuser used in wind tunnels  
 Key: (1) measuring section  
 (4) 1st diffuser  
 (9) fan  
 (10) 2nd diffuser  
 (14) wide angle diffuser  
 (17) nozzle

then passed to measuring section 1. The flow that has passed to the air velocity at the inlet of the fan after it passes through the first diffuser (area ratio of 2.32 and wide angle of 5). It is then presented to the fan section. The diffuser, therefore, plays an important role in presenting a uniform air current at a low speed.

## 1.2 Blade and bladeless diffusers for centrifugal compressor and fans

Fluid machines are machines that convert energy and power of fluids. There are turbines, which convert mechanical energy of fluids or thermal energy to power, compressors, fans<sup>\*</sup>, pumps, etc., which convert the power to fluid energy, etc. The deacceleration section (diffuser) is essential. However, diffusers play a particularly important role in compressors, fans, pumps, etc. Moreover, although the diffusers are also called deacceleration paths, there are different types of diffusers, such as blade diffusers that have blades arranged in a circle, and bladeless diffusers. They are used in centrifugal compressors and fans<sup>\*\*</sup>. These diffusers are the focus of this explanation.

Figure 1.3(a) shows a centrifugal compressor with blades from the axial inlet side (front view).

/5

---

\* The compressors and fans have the same theory and structure. However, they are differentiated by emission pressure. The emission (gauge) pressure of compressors is  $1 \text{ kgf/cm}^2$  (98 kPa) or more, while that of fans is less than  $1 \text{ kgf/cm}^2$  and sometimes less than 1000 mmAq (9.8 kPa).

\*\* Centrifugal-type (also called radial flow-type or horizontal-flow type) compressors and fans provide energy by rotation of blades and introduce pressurized air in a radial or axial direction (perpendicular to the axis with radial types and parallel to the axis in horizontal types). Their intermediate is called an inclined current type. Moreover, these are also called turbo-types (turbo-types means volume-type (return movement-type, rotary-type, etc.)).

ORIGINAL PAGE  
BLACK AND WHITE PHOTOGRAPH

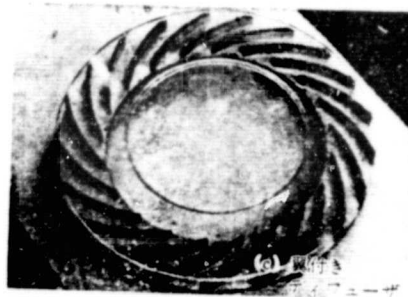
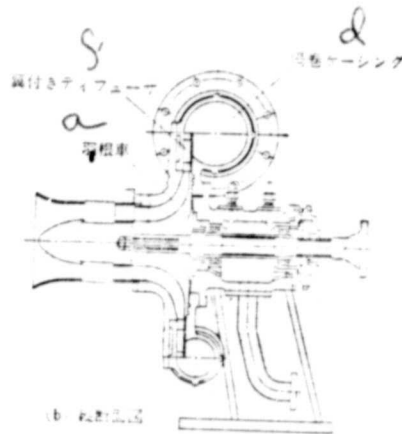
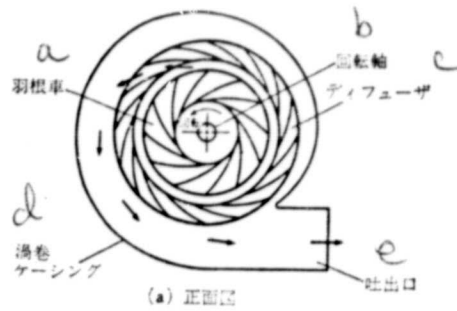


Figure 1.3. Centrifugation-type compressor with blade diffuser  
 Key: (a) front view  
 (b) cross section  
 (c) blade diffuser  
 a--blade car; b--rotation axis; c--diffuser; d--spiral casing;  
 e--outlet; f--blade diffuser

As can be seen in the figure, the diffuser is formed so that grid-like round blades are formed around the blade car (called round blade arrangement). Pressurization and acceleration occur with rotation of the blade car (left side of picture) while deceleration of gases in the flow in a spiral form from around the blade car occurs when the gas passes through the diffuser. Thus, part of the pressure is converted to static pressure. Spiral casings are arranged on the outside of the blade car and diffuser, and gas that is emitted from the diffuser accumulates around the spiral casing and is further decelerated and emitted to the outlet.

A cross section of this type of air compressor is shown in Figure 1.3(b) (includes rotation axis center line). [2]. As can be seen from the figure, the spiral casing has round flow paths. Moreover, Figure 1.3(c) is a photograph showing a blade diffuser.

/6

Figure 1.4 is a cross section of a multistage centrifugation compressor (made by GHH) with a blade diffuser [3]. Guide paths for introduction of the flow to the next stage are set up between the diffuser stages and next stage of the blade car (refer to section 1.4).

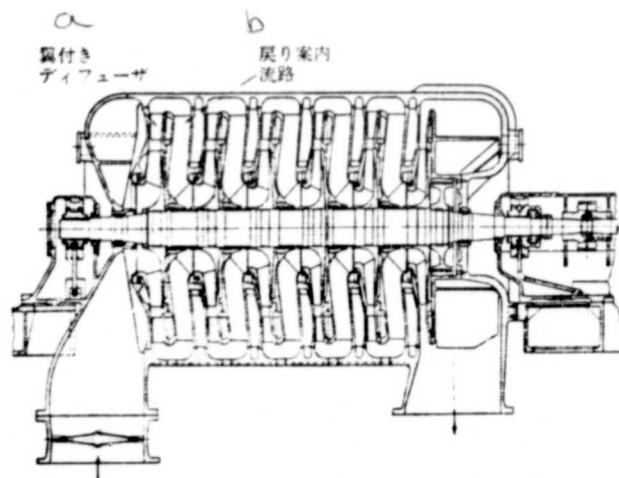


Figure 1.4. Multistage centrifugation compressor with blade diffuser:

Key: a--blade diffuser; b--guide paths

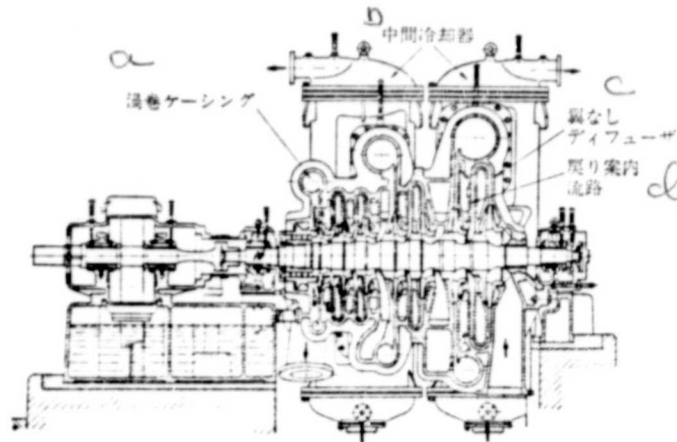


Figure 1.5. Multistage compressor with bladeless diffuser:  
 a--spiral casing; b--cooler; c--bladeless diffuser; d--guide path

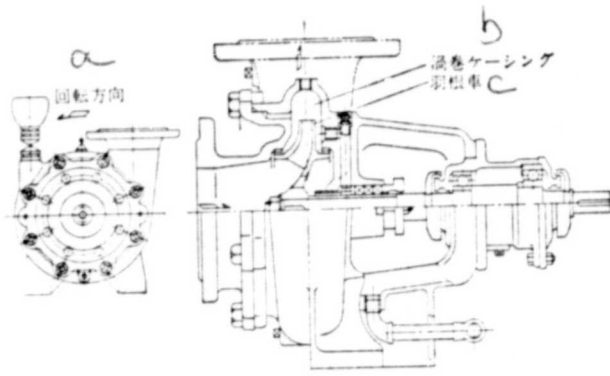


Figure 1.6. Low pressure pump  
 a--rotating direction; b--spiral casing; c--blade car

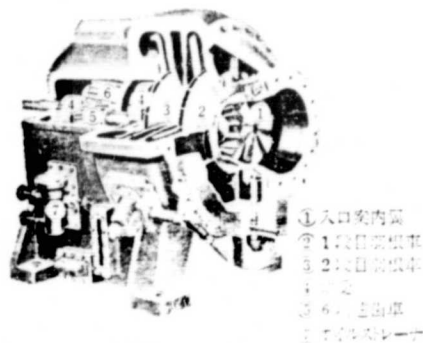


Figure 1.7. 2-stage compressor oblique view  
 1--inlet guide blade; 2--1st stage blade car; 3--2nd stage blade car; 4--axle bearing; 5,6--acceleration gear; 7--foil strainer



Figure 1.5 is a figure showing a multistage centrifugation 17 compressor (made by Escher Wyss) having a bladeless diffuser [4]. It is made from a diffuser with bladeless spaces around the side walls. The bladeless diffuser has a low deacceleration property and the static pressure recovery value is low in comparison to blade diffusers. However, there is a low efficiency and reduction in pressure with changes in the operating current. Therefore, it is characterized by the fact that matching of each stage is good. Moreover, in this example, two coolers are used in between stages and air is introduced to the coolers once it has been recovered. Therefore, two spiral casings are set up in addition to the spiral casing at the outlet.

Figure 1.6 is a low pressure centrifugation pump (low pressure type<sup>\*</sup>) [5]. In this example, the spiral casings are made of ore and the casings is one unit that stores the blade car. In low pressure fans the structure is often the same. Moreover, in fans called low pressure turbo fans, a spiral casing with an angle-type cross section is used. These types of pumps and fans have a simplified structure and can be made into small, light weight devices, thereby reducing cost. 18

Figure 1.7 is an illustration of a cooler-type centrifugation compressor. It is the oblique view of the 2-stage compressor [6]. It has inlet guide blades (axial flow blades) for controlling the amount (flow) in the paths of the blade car. Moreover, it is equipped with one gear for acceleration and a bladeless diffuser. Guide paths are set up in 2-stage compressors.

Figure 1.8 is an example where a blade diffuser is used in centrifugal compressors for electrical devices [7] (called electric fans). This structure has been improved to increase energy

---

\* Low pressure type-pressure increase/density of liquid.

ORIGINAL PAGE  
BLACK AND WHITE PHOTOGRAPH

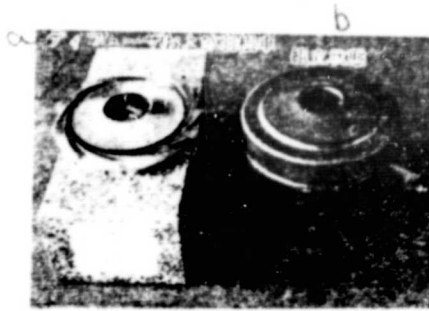


Figure 1.8. Electrical compressor  
Key: a--diffuser and blade car; b--assembled condition

saving measures in recent years. The blade car and diffuser have guide paths on the undersides and are used in the cooling of electric devices.

### 1.3 Application of blade diffuser

A conventional blade (or bladeless) diffuser was explained in the previous section (1.2). However, there are other special types of diffusers.

A movable blade diffuser (Brown Boveri) is shown in Figure 1.9 [8]. Each blade of the diffuser rotates around the axles set up in a parallel direction and the rotation axis of the compressor. This makes the angle of attachment variable. When the operation flow of the compressor is varied, the direction of flow from the blade car can be changed (refer to Chapter 3). Therefore, in conventional static blade diffusers, the direction of the blade cannot be combined with the direction of the current with changes in flow\*. The diffuser efficiency therefore decreases. The example shows that a high compressor capability is obtained by changes in the direction of the flow with changes in the amount of flow because the angle of the blades can be changed.

---

\* In conventional diffusers, the inlet of the blade (blade inlet angle) is combined with the direction of inlet flow during design (inlet flow angle).

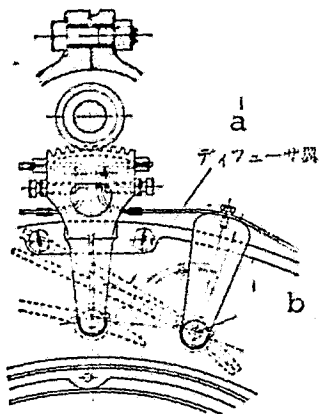


Figure 1.9. Movable blade diffuser.  
a--diffuser blade;  
b--axle

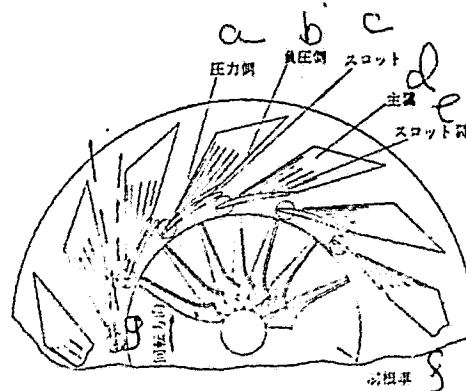


Figure 1.10. Slot blade diffuser  
a--pressure side; b--negative pressure side; c--slot; d--main blade; e--slot blade; f--blade car; g--rotation;

Figure 1.10 is a diffuser with a movable slot blade. The diffuser with a slot blade is set up so that slot blades are arranged on the inlet side of the main blade and when the angle of flow against the main blade (angle of flow) is increased (cases where the operating flow is low), part of the flow moves to the negative pressure side\*. Therefore, a loss of velocity is presented and a reduction in diffuser properties is avoided. As shown by the arrows, and by rotation in the direction shown by the broken lines, it is possible to produce a distance between the slot blade and main blade. Furthermore, there are also cases where a static slot blade is used.

The diffuser shown in Figure 1.11 is called a channel (flow path-type) diffuser [10]. Conventional blade diffusers have blades arranged along the walls at certain distances and the

\* Right side is negative pressure side, left side is pressure side. Blades of airplanes, etc., have inertia due to a difference in pressure on the negative pressure surface (top surface) and pressure surface (bottom surface). Therefore, a pressure difference is produced and the flow changes direction with the blades of the fluid machine.

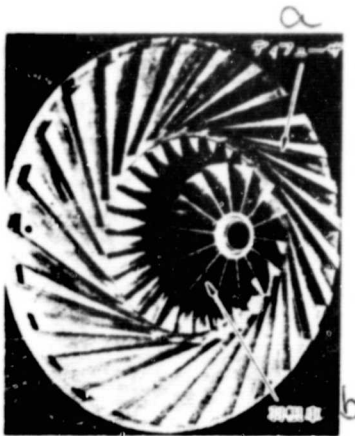


Figure 1.11. Channel-type diffuser  
a--diffuser  
b--blade car



Figure 1.12. Pipe diffuser  
a--outlet; b--inlet

cross section of the flow path around the blade and side walls is made a flat slender shape as it moves toward the outlet side. This is not desirable as a flow path.

In contrast to this, there are flow paths where the flow path is enlarged and an efficient flow path is obtained with a square structure or round structure. This is called a channel-type diffuser. The materials of the flow path are triangular, etc. (blade side). This type of diffuser is often used for improving the high pressure force ratio and features of gas turbines, airplane engines, etc. In this case, properties are superior because the entire unit size and cost is not increased.

The direction of the channel diffuser is further promoted to obtain the pipe diffuser in Figure 1.12 [11]. That is, the inlet is round and the outlet is flat and slender. Flow paths are made in casing blocks to assemble a group of individual flow paths. The diffuser shown in Figure 1.12 is used to rotate the flow at the outlet in the direction of the axis as in the case of Figure 1.16 (for connecting to the combustion device).

1.4. Other diffusers used in centrifugation compressor and fans

/11

The guide paths used in the multistage centrifugation pumps (fans) in Figures 1.4 and 1.5 were previously explained. The guides and blade and bladeless diffuser are made into one unit to make one diffuser. There are also combinations of diffusers. Furthermore, the spiral casing used as the outlet of the centrifugation compressor (fan) has a diffuser effect. However, it is not included in the diffuser and will not be explained in this text.

Figure 1.13 is an illustration showing guide paths used in 2-stage centrifugation compressors [12] tested by the authors (the guide paths are formed from guide blades and flow path walls (side walls) and are divided in two). The guide path is inclined toward the periphery of the inlet (outside). Moreover, it moves in a radial direction at the outlet (inside) side). This enables the flow to be received from the diffusers and move in a radial direction as it is being deaccelerated so that it has no peripheral component (swirl component) and can be introduced to the next blade car.

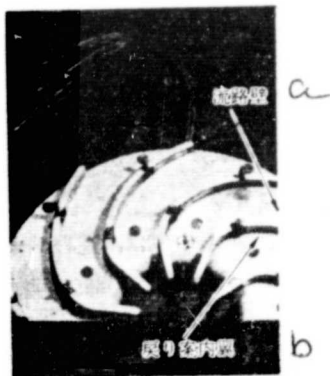


Figure 1.13. Guide flow path and blades of centrifugation pumps  
a--flow paths; b--guide blades

Figure 1.14(a) and (b) show the blade diffuser and guide paths used in centrifugation pumps [13]. (a) is the case where the centrifugation compressor previously explained is used and

/12

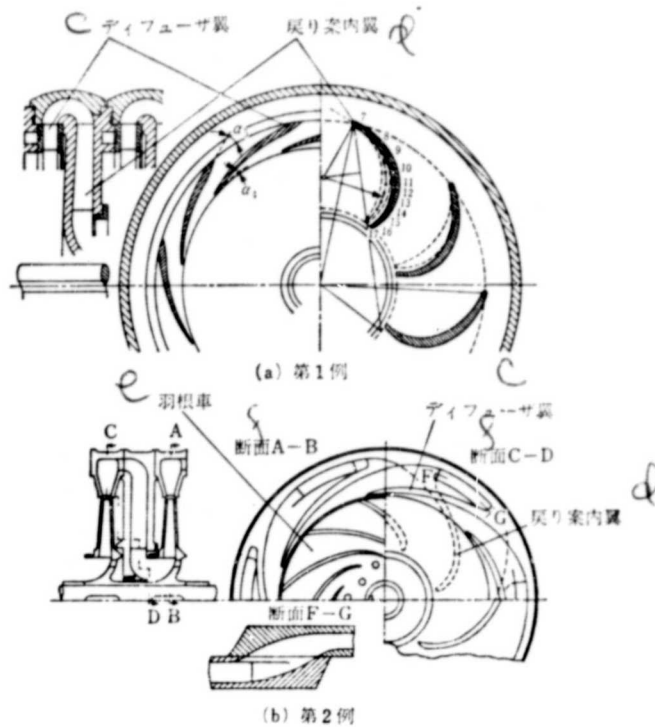


Figure 1.14. Centrifugation pump diffuser and guide paths.  
 (a) 1st example (b) 2nd example  
 c--diffuser blades; d--guide blade; e--blade car; f--cross section

(b) is the case where a series of paths is formed from the casing to the diffuser blades and guide blades. In each case, there is a tendency for the ratio of the outer diameter of the guide paths and the blade car to be less than that seen with compressors and fans.

A bent path is set up so that a U-shaped path is formed between the diffuser and guide path in the cross section of the compressor. Moreover, a bent U-shaped section is formed between the outlet of the guide path and the next blade car (Figure 1.15 [12]). The former is the bent path on the emission side and the latter is the bent path on the inlet side.

The path on the emission side is a uniform speed path (concentric section), as shown in Figures 1.15 and 1.5. The width of the inlet expands from the outlet side of the diffuser. However, it is no wider than in conventional types. The inlet side bent path is a path in which nonuniformity of the velocity distribution readily occurs near the center axis and, therefore, near the next blade car. Consequently, it has a strong effect on the next stage. Determination of the shape must be given 13 careful consideration. There are also many cases where a flow accelerating path is set up to obtain a uniform flow behind the flow path (blade car side). Even in the case of bent flow paths, the curvature radius of the path inside the bend is small and the shape is inconsistent. Therefore, there is a reduction in properties when the flow peels.

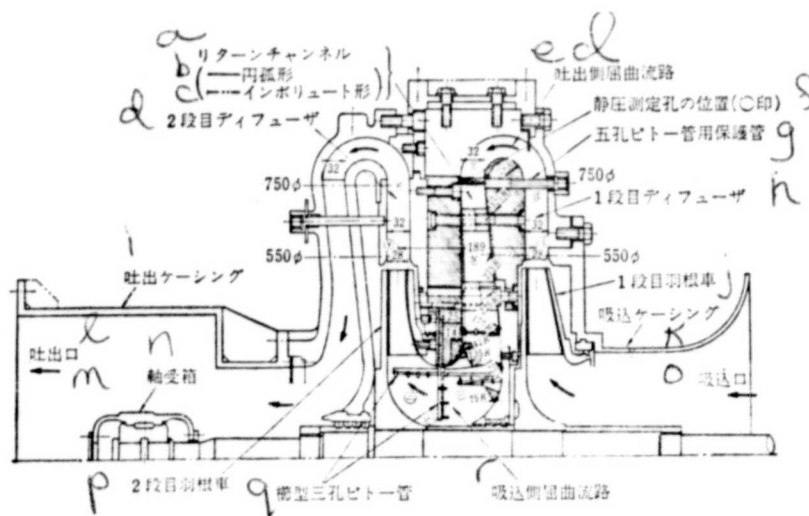


Figure 1.15. 2-stage centrifugation compressor used in tests.

a--retain channel; b--holes; c--inporoyuto shape<sup>\*</sup>; d--2nd stage diffuser; e--emission side curved flow path; f--static pressure determination hole (marked with 0); g--five hole pipe retainer; h--1st stage diffuser; i--emission casing; j--1st stage blade car; k--inlet casing; l--outlet casing; m--emission outlet; n--bearing; o--inlet; p--2nd stage blade; q--three hole pipe; r--inlet side curved flow path

\* Translator's note: term unknown; transliteration of phonetic characters.

## 1.5 Diffuser used in other fluid machines

Figure 1.16 shows a mixed flow-type\* compressor and its diffuser [14]. The blade car of this compressor has an emission angle that is a tilted flow approximating a radial flow. Moreover, the diffuser is divided into two sections, with the first section being a tilted-flow type and the second section being an axial-flow type. Figure 1.17 shows the general structure of an axial flow-type fan. Moving blades (rotating blades) are placed on the up current side and stationary blades (or guides) are placed on the down current side. Moreover, at the top of the illustration these blades are cut into cylindrical surfaces (by the dotted line). Therefore, an example of a straight blade /14 situated in a linear lattice is illustrated. In the figure, the example of moving blades and stationary blades shows that they are both arranged so that the flow can be deaccelerated. This type of arrangement is a deacceleration arrangement. The deacceleration blades are not always part of the diffuser. They are not normally treated as part of the diffuser\*\*. Therefore, they will not be explained in this text.

Figure 1.18 is a cross section showing a multi-stage axial compressor [15]. The elements of a pair of moving blades and stationary blades shown in Figure 1.17 are overlapped. In this device, the gas is fed from the left inlet casing and is pressurized as it passes through the moving blades and stationary blades. It finally passes through the curved flowed diffuser (called emission diffuser) and is stored in emission casings. Then it is emitted in a downward direction. The emission diffuser is characteristic of axial flow compressors and it is

---

\* The mixed-flow type is a type that includes an axial flow section (inlet side) and radial flow section (outlet side). (This is used in combination with tilted flow-types).

\*\* The flow in the flow paths is a flow around the blades and is different in that it is an outside flow.



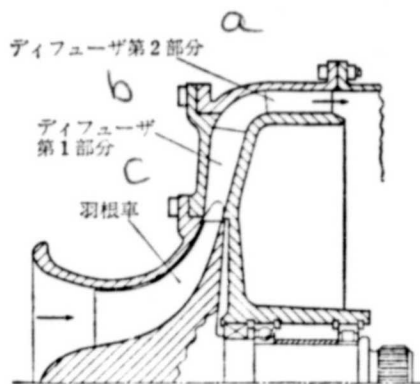


Figure 1.16. Mixed current-type compressor and diffuser  
 a--2nd section of diffuser  
 b--1st section of diffuser  
 c--blade car

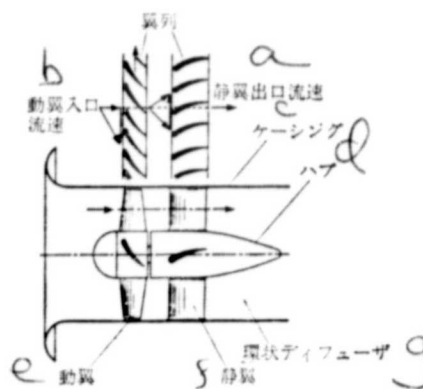


Figure 1.17. Single blade axial flow fan and linear blade  
 a--stationary blade outlet flow velocity; b--movable blade inlet flow velocity; c--casing; d--hub; e--moving blade; f--stationary blade; g--annular diffuser

ORIGINAL PAGE  
 BLACK AND WHITE PHOTOGRAPH

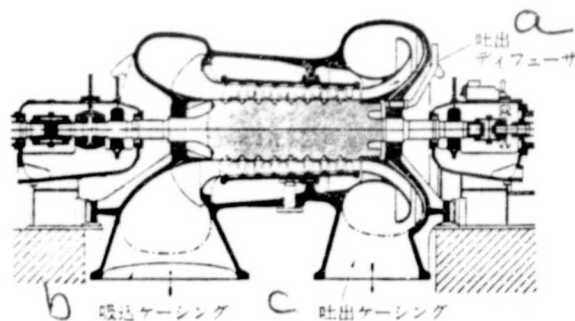


Figure 1.18. Multistage axial flow compressor  
 a--emission diffuser; b--inlet casing; c--outlet casing

used when it is necessary to emit the axial current in a radial direction.

The steam turbine of the axial flow devices uses the same type of emission diffuser. The emission current is deaccelerated at the turbine and is similar to a compressor in that the difference in effective pressure is thereby increased.

Figure 1.17 shows a downward current of an axial flow fan (hub). There are many cases where an annular diffuser (double pipe diffuser) is formed between the outer casing and inner casing. The diffuser operates by deacceleration of a flow that is introduced to ducts. The section in the axial flow fans is one example of the important use of annular diffusers. /15

Figure 1.19 is a radial flow-type water wheel [16]. (a) in the figure is the outside of the main section and (b) is the cross section of the entire unit. The direction of the flow is the opposite of that in pumps and fans. The flow from the left side of the spiral casing in (a) is emitted below the axis after being reversed by blade cars (called runners). Flat duct pipes are attached in a downward direction in (b) so that the water passes through the ducts before being emitted. The emission flow of the water wheel is deaccelerated and waste loss is reduced, thereby increasing efficiency. Therefore, it plays an important role in the output of water wheels.

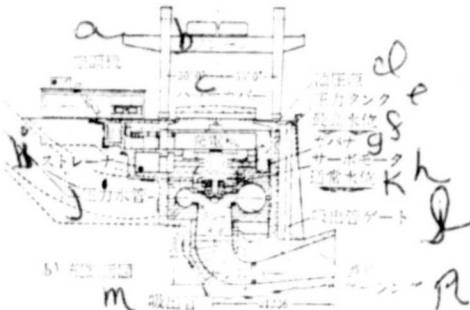
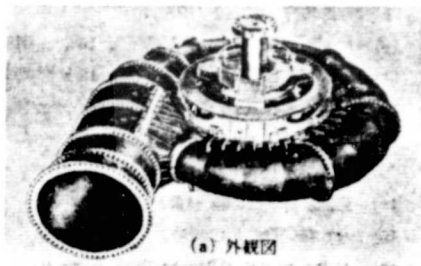


Figure 1.19. Water wheel and emission pipes

(a) external view (b) cross section  
 a--air conditioner; b--crane;  
 c--hatch cover; d--oil pressure  
 source; e--pressure tank; f--max.  
 water level; g--gabana\*; h--servo-  
 motor; i--strainer; j--pressure  
 pipes; k--normal water level; l--  
 outlet pipe gate; m--emission pipe;  
 n--whirlpool casing

ORIGINAL PAGE  
 BLACK AND WHITE PHOTOGRAPH

\*Translator's note: term unknown; transliteration of phonetic characters.

## REFERENCES

- [1] Ito and Komura: Turbo Devices 9-4, p. 25 (4/81)
- [2] Suzuki and Yasudo: Mitsui Shipbuilding Technology Report 27, p. 29
- [3] Eckert, B.: Die Kreiselpumpen fuer Fluessigkeiten und Gase (Turbines for Fluids and Gases), p 369,370 ,(Springer, 1961).
- [4] ibid., p. 279
- [5] Hitachi Catalog (OV Hitachi Small Whirlpool Pump)
- [6] Hitachi Catalog (RF Hitachi Turbo Cooler)
- [7] Shimaen and Mori: Turbo Devices 8-7, p. 21 (7/78)
- [8] Stepanoff (Terada; translator): Turbo Fans, p. 307 (Maruen Publishers) 1958.
- [9] U. S. Patent no. 3957392 (1976)
- [10] Krain, H.: Trans. ASME\*. 103, p. 688 (1981-10)
- [11] Kenny, D. P.: ASME publication 68-GT-38 (1968)
- [12] Sugi: Japan Mechanical Engineers Convention Notes (Hitachi Convention), p. 24 \*11/1965)
- [13] Pfleiderer, C.: Die Kreiselpumpen fuer Fluessigkeiten und Gase, fuenfte Auflage (Turbines for Fluids and Gases) p 369,370 (Springer 1961)
- [14] U. S. patent 3832089 (1974)
- [15] Stepanoff: Turbo Fans, p. 307 (Maruen Publishers) 1958
- [16] Hitachi Catalog (Hitachi Francis Turbine)

## BASIC EQUATIONS FOR FLOW OF TURBO MACHINES

There are many experimental methods for treating the properties of diffusers used in fluid engineering. Therefore, there are many ways of studying hydraulic engineering and theoretical methods. However, equations that are the basis of experiments and calculations on diffusers have been obtained from basic theories of hydraulics and in recent studies, progress has been made on calculations of diffuser flow and boundary layers based on differential calculus equations. In this light, we will explain the basic theory (operation equations, models, Bernoulli's equation, boundary layer theories, high speed flow, etc.) in 2.1 of this chapter and will explain the basic facts of hydraulics in 2.2.

### 2.1 Basic equations [1,2]

#### (1) Operation equations and equations of continuity

When the continuity equation of a general flow (three-dimensional) of noncompressed viscous fluids\* (equation 2.1) is obtained. This is obtained from the components of the fluid.  $u$ ,  $v$  and  $w$  are the axis components  $x$ ,  $y$  and  $z$  respectively of fluid velocity and  $X$ ,  $Y$  and  $Z$  are the  $x$ ,  $y$  and  $z$  axis components of external force per unit mass of the fluid respectively;  $p$ ,  $\rho$  and  $\mu$  are the pressure, density and viscosity coefficient of the fluid respectively and  $t$  represents time (there are cases when

---

\* Although fluid pressure may be used, conventional flows are noncompressed. In the case of gases, noncompressed flows are not used when changes in density are small (for instance, several percent). Noncompressed fluids are treated only when the speed is low.

variants are often used. However, there are also many cases that are actually treated by disregarding the function of time by decreasing the number of dimensions).

$$\begin{aligned}
 & \left. \begin{aligned}
 & \frac{\partial u}{\partial t} + u \frac{\partial u}{\partial x} + v \frac{\partial u}{\partial y} + w \frac{\partial u}{\partial z} \\
 & = X - \frac{1}{\rho} \frac{\partial p}{\partial x} + \frac{\mu}{\rho} \left( \frac{\partial^2 u}{\partial x^2} + \frac{\partial^2 u}{\partial y^2} + \frac{\partial^2 u}{\partial z^2} \right) \\
 & \frac{\partial v}{\partial t} + u \frac{\partial v}{\partial x} + v \frac{\partial v}{\partial y} + w \frac{\partial v}{\partial z} \\
 & = Y - \frac{1}{\rho} \frac{\partial p}{\partial y} + \frac{\mu}{\rho} \left( \frac{\partial^2 v}{\partial x^2} + \frac{\partial^2 v}{\partial y^2} + \frac{\partial^2 v}{\partial z^2} \right) \\
 & \frac{\partial w}{\partial t} + u \frac{\partial w}{\partial x} + v \frac{\partial w}{\partial y} + w \frac{\partial w}{\partial z} \\
 & = Z - \frac{1}{\rho} \frac{\partial p}{\partial z} + \frac{\mu}{\rho} \left( \frac{\partial^2 w}{\partial x^2} + \frac{\partial^2 w}{\partial y^2} + \frac{\partial^2 w}{\partial z^2} \right)
 \end{aligned} \right\} \quad (2.1)
 \end{aligned}$$

Equation (2.1) is called the Navier Stokes equation and can be considered as an equation based on conventional flows\*. Moreover, the equation of continuity for three-dimensional noncompressed flows is as shown in 2.2.

$$\frac{\partial u}{\partial x} + \frac{\partial v}{\partial y} + \frac{\partial w}{\partial z} = 0 \quad \dots\dots\dots (2.2)$$

The operational equation and continuity equations are expressed with a cylindrical coordinate system (r, θ, x). Thus, equation (2.3) and equation (2.4) are obtained. Here V<sub>r</sub>, V<sub>θ</sub> and V<sub>x</sub> are the r, θ and x components of velocity respectively and R, θ and X are the components of external force of r, θ and x respectively (the fluid device is often made with the entire unit being axially symmetric and therefore treatment of the

---

\* This equation requires that Newton fluids be used (fluid where the frictional stress caused by viscosity is proportional to the fluid velocity gradient in a perpendicular direction, refer to reference [4]).

equation with a cylindrical coordinate system is useful).

$$\left. \begin{aligned}
 & \frac{\partial V_r}{\partial t} + V_r \frac{\partial V_r}{\partial r} + \frac{V_\theta}{r} \frac{\partial V_r}{\partial \theta} + V_z \frac{\partial V_r}{\partial x} - \frac{V_\theta^2}{r} \\
 & = R - \frac{1}{\rho} \frac{\partial p}{\partial r} + \frac{\mu}{\rho} \left( \nabla^2 V_r - \frac{V_r}{r^2} - \frac{2}{r^2} \frac{\partial V_\theta}{\partial \theta} \right) \\
 & \frac{\partial V_\theta}{\partial t} + V_r \frac{\partial V_\theta}{\partial r} + \frac{V_\theta}{r} \frac{\partial V_\theta}{\partial \theta} + V_z \frac{\partial V_\theta}{\partial x} + \frac{V_r V_\theta}{r} \\
 & = \Theta - \frac{1}{\rho} \frac{\partial p}{r \partial \theta} + \frac{\mu}{\rho} \left( \nabla^2 V_\theta + \frac{2}{r^2} \frac{\partial V_r}{\partial \theta} - \frac{V_\theta}{r^2} \right) \\
 & \frac{\partial V_z}{\partial t} + V_r \frac{\partial V_z}{\partial r} + \frac{V_\theta}{r} \frac{\partial V_z}{\partial \theta} + V_z \frac{\partial V_z}{\partial x} \\
 & = X - \frac{1}{\rho} \frac{\partial p}{\partial x} + \frac{\mu}{\rho} \nabla^2 V_z
 \end{aligned} \right\} \quad (2.3)$$

/19

however,

$$\begin{aligned}
 \nabla^2 &= \frac{\partial^2}{\partial r^2} + \frac{1}{r} \frac{\partial}{\partial r} + \frac{1}{r^2} \frac{\partial^2}{\partial \theta^2} + \frac{\partial^2}{\partial x^2} \quad (2.4) \\
 \frac{1}{r} \frac{\partial(r V_r)}{\partial r} + \frac{\partial V_\theta}{r \partial \theta} + \frac{\partial V_z}{\partial x} &= 0 \dots\dots\dots
 \end{aligned}$$

Furthermore, the equation of continuity of compressed flows (case where changes in density of the fluid are also considered) becomes equations (2.5) and (2.6) (each used perpendicular and cylindrical equations respectively).

$$\frac{\partial \rho}{\partial t} + \frac{\partial(\rho u)}{\partial x} + \frac{\partial(\rho v)}{\partial y} + \frac{\partial(\rho w)}{\partial z} = 0 \dots\dots\dots (2.5)$$

$$\frac{\partial \rho}{\partial t} + \frac{1}{r} \frac{\partial(\rho r V_r)}{\partial r} + \frac{\partial(\rho V_\theta)}{r \partial \theta} + \frac{\partial(\rho V_z)}{\partial x} = 0 \dots\dots\dots (2.6)$$

When  $\frac{\partial}{\partial t} = 0$  in equations (2.1) and (2.6), the flow shows no changes in time (constant flow) and there are many problems. Changes in time must be considered and, therefore, the flow is inconsistent.

(2) Whirlpool, potential flow, conformal transformation

Two-dimensional flows will be considered. When the components of the fluid are turned (whirlpool motion) so that they revolve around 1 point in an (x,y) plane,  $\zeta$  expressed by equation (2.7) is called the vorticity and the vorticity is two times the rotation angle velocity.

$$\zeta = \left( \frac{\partial v}{\partial x} - \frac{\partial u}{\partial y} \right) \dots \dots \dots (2.7)$$

The strength of the whirlpool motion is called circulation and is represented by equation (2.8) ( $\Gamma$  is the circulation,  $V$  is the component of velocity reflected at the closed curve surrounding the whirlpool and  $ds$  is the short length along the above-mentioned closed curve).

$$\Gamma = \int V \cdot ds \dots \dots \dots (2.8)$$

Taking the fact that the closed curve from equation (2.8) is a circle with radius  $r$ ,

$$V = \frac{\Gamma}{2\pi r} \dots \dots \dots (2.9)$$

that is, the velocity induced at distance  $r$  from the whirlpool by strength  $\Gamma$  is  $\Gamma/2\pi r$ , equation (2.10) is obtained from equation (2.7) with flows where there is no whirlpool motion /20

$$\frac{\partial v}{\partial x} - \frac{\partial u}{\partial y} = 0 \dots \dots \dots (2.10)$$

and here

$$u = \frac{\partial \phi}{\partial x}, \quad v = \frac{\partial \phi}{\partial y} \dots \dots \dots (2.11)$$

Therefore, when function  $\phi$  is taken into consideration, equation (2.10) is satisfied by equation (2.11). That is, the above-mentioned function  $\phi$  (velocity potential) is present in flows without vorticity (or flows that are potential flows). The equation of two-dimension continuity

$$\frac{\partial u}{\partial x} + \frac{\partial v}{\partial y} = 0 \dots \dots \dots (2.2')$$

can be replaced for (2.11) to establish (2.12) (this is called the differential equation of Laplace).

$$\frac{\partial^2 \phi}{\partial x^2} + \frac{\partial^2 \phi}{\partial y^2} = 0 \dots \dots \dots (2.12) *$$

$\phi =$  a constant line called a constant potential line.

Next,

$$u = \frac{\partial \phi}{\partial x}, \quad v = -\frac{\partial \phi}{\partial y} \dots \dots \dots (2.13) *$$

\* Equations (2.13), (2.12) and (2.14) are equations (2.13'), (2.12) and (2.14) in axially symmetric cylindrical coordinate systems.

$$V_z = \frac{1}{r} \frac{\partial \phi}{\partial r}, \quad V_r = -\frac{1}{r} \frac{\partial \phi}{\partial x} \dots \dots \dots (2.13')$$

$$\frac{\partial^2 \phi}{\partial x^2} + \frac{1}{r} \frac{\partial \phi}{\partial r} + \frac{\partial^2 \phi}{\partial r^2} = 0 \dots \dots \dots (2.12')$$

$$\frac{\partial^2 \phi}{\partial x^2} - \frac{1}{r} \frac{\partial \phi}{\partial r} + \frac{\partial^2 \phi}{\partial r^2} = 0 \dots \dots \dots (2.14')$$

is obtained and when we consider function  $\psi$ , equation (2.2') is satisfied by equation (2.13). This type of function is called a flow function and  $\psi = \text{constant}$  curve is the flow curve (curve where the direction of the flow velocity is the direction of the curve). Therefore, the flow curve and equal potential curve intersect--the difference between the value with regard to 2 flow curves is the amount of flow of a liquid that flows between the two curves. When equation (2.13) is replaced by equation (2.10), which is a nonvortex equation, equation (2.14) is established (this is also a differential equation of Laplace). /21

$$\frac{\partial^2 \psi}{\partial x^2} + \frac{\partial^2 \psi}{\partial y^2} = 0 \dots\dots\dots (2.14)^*$$

Now, the complex numbers

$$z = x + iy \dots\dots\dots (2.15)$$

represent the surface and the complex function (complex potential) is represented by

$$W = \phi + i\psi \dots\dots\dots (2.16)$$

The following function (equation (2.17)) represents the potential flow of the plane (x,y)

$$W = f(z) \dots\dots\dots (2.17)$$

Example 1

$$W = Uz \dots\dots\dots (2.18)$$

This equation represents the flow parallel to the x axis with a constant U velocity ( $\phi = Ux$ ,  $\psi = Uy$  when the actual numbers are used to replace equations (2.15) and (2.16) with equation (2.18). Refer to Figure 2.1).

Example 2

$$W = \frac{Q}{2\pi} \log z \dots\dots\dots (2.19)$$



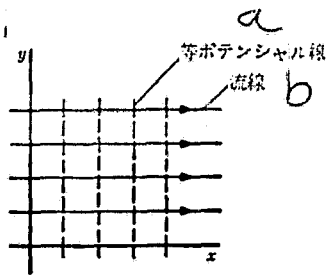


Figure 2.1.  
Parallel flow  
a--potential curve  
b--flow curve

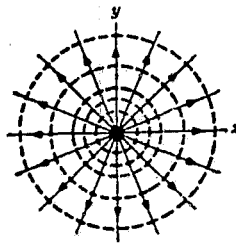


Figure 2.2  
Emission flow

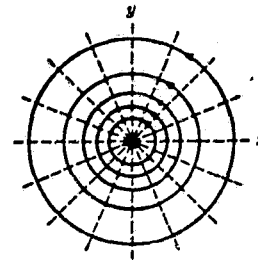


Figure 2.3  
Whirlpool

This represents the radiating flow from the starting point (when  $z = re^{i\theta}$  is replaced in equation (2.15),

$$\phi = \frac{Q}{2\pi} \log r, \quad \psi = \frac{Q\theta}{2\pi}$$

/22

and the potential curve becomes round and the flow curve becomes radiating. Refer to Figure 2.2). The central point is the emission point\* and  $Q$  is the strength of emission.

Example 3

$$W = \frac{\Gamma}{2\pi i} \log z \dots \tag{2.20}$$

This is the whirlpool movement at strength  $\Gamma$  centering around the starting point. (As in example 2,

$$\phi = \frac{\Gamma\theta}{2\pi}, \quad \psi = -\frac{\Gamma}{2\pi} \log r.$$

that is, there is a current curve with a concentric shape and a potential curve with a radiating shape; refer to Figure 2.3).

Next, two planes represented by the two complex numbers  $\zeta = \xi + i\eta$  and  $z = x + iy$  will be considered. We will consider the case where the correlation in (2.21) exists between  $\zeta$  and  $z$ .

$$\zeta = f(z) \dots \tag{2.21}$$

\* This is a flow that enters one point from four directions (called center point).

The diagram above the  $z$  plane is copied onto the diagram of the  $\zeta$  plane by this equation so that the correlation is integrated. This function is called the conformal transformation. For instance, since

$$\zeta = z + \frac{a^2}{z} \dots\dots (2.22)$$

the circle with radius  $a$  having a center at the starting point above the  $z$  plane is transformed to the flat blade with length  $4a$  which has no thickness at plane (refer to Figure 2.4(a)). Then the same circle having a center at the  $y$  axis is made so that it is transformed to the blade of length  $4a$  with no thickness above plane  $\zeta$  (refer to figure (b)). Moreover, the circle having center in plane  $z$  is transformed to the blade having a thickness (Figure (c)).

The complex potential that represents the circle (cylinder) with radius  $a$  in this flow is represented by equation (2.23) and the complex potential of the flow having circulation  $\Gamma^*$  around the circle is represented by equation (2.24).

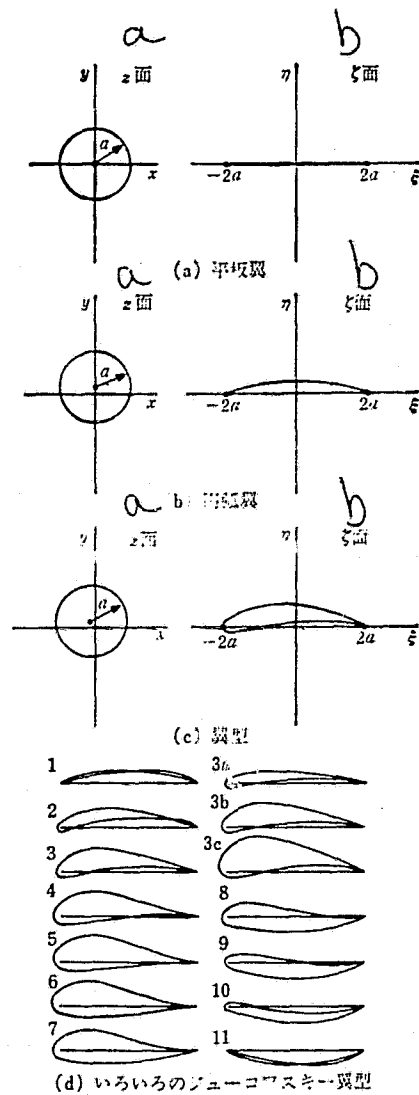


Figure 2.4. Circle ( $z$  plane) and transformation (plane) (a)--flat blade; (b)--round blade; (c)--blade; (d)--various Joukovsky's airfoils. a.  $z$  plane b. plane

\* This blade at the circle has the same circulation  $\Gamma$  and the force is expressed as  $\rho\Gamma U$  (based on Kutta-Joukowski hypothesis).

$$W = Uz + \frac{Ua^2}{z} \dots\dots\dots (2.23)$$

$$W = Uz + \frac{Ua^2}{z} - \frac{\Gamma}{2\pi i} \log z \dots\dots\dots (2.24)$$

The velocity distribution above the circle (cylinder) can be determined from the above-mentioned equation and the velocity above the blade in  $\zeta$  plane can be found by multiplying this times the inverse of the rate of transformation of the corresponding point ( $d\zeta/dz$ ) (refer to equation (2.25)). Furthermore,  $dW/d\zeta$  and  $dW/dz$  is called the conjugate complex velocity and the absolute value represents the velocity.

$$\frac{dW}{d\zeta} = \frac{dW}{dz} \cdot \frac{dz}{d\zeta} \dots\dots\dots (2.25)$$

The blade shown in Figure 2.4(c) is called the Joukowski blade and is rarely used. However, many practical methods for transformation are being developed. (Figure (d) shows the Joukowski blade model obtained by transformation [3]).

(3) Euler's equation, Bernoulli's equation and the momentum theory

The case where items representing the viscosity in the above-mentioned Navier-Stokes equation can be disregarded is called the Euler equation. It is shown below using perpendicular coordinates ( $x$ ,  $y$  and  $z$ ).

$$\left. \begin{aligned} \frac{\partial u}{\partial t} + u \frac{\partial u}{\partial x} + v \frac{\partial u}{\partial y} + w \frac{\partial u}{\partial z} &= X - \frac{1}{\rho} \frac{\partial p}{\partial x} \\ \frac{\partial v}{\partial t} + u \frac{\partial v}{\partial x} + v \frac{\partial v}{\partial y} + w \frac{\partial v}{\partial z} &= Y - \frac{1}{\rho} \frac{\partial p}{\partial y} \\ \frac{\partial w}{\partial t} + u \frac{\partial w}{\partial x} + v \frac{\partial w}{\partial y} + w \frac{\partial w}{\partial z} &= Z - \frac{1}{\rho} \frac{\partial p}{\partial z} \end{aligned} \right\} \dots\dots\dots (2.26)$$

The above mentioned equation is a general curve and represents the flow inside pipes having a finite cross section (pipes where the surface is formed from flow lines) (refer to (2.27)). Here  $U$  is the velocity,  $s$  is the distance along the flow, and  $F$  is external force.

$$\frac{\partial U}{\partial t} + U \frac{\partial U}{\partial s} = F - \frac{1}{\rho} \frac{\partial p}{\partial s} \dots\dots\dots (2.27)$$

The constant flow ( $\frac{\partial}{\partial t}=0$ ) is treated by equation (2.27) and when using  $s$ , the following equation (2.28) is obtained.

$$\frac{1}{2}U^2 + \frac{p}{\rho} - \int F ds = \text{constant} \dots\dots\dots (2.28)$$

Moreover, when external force is made gravity, equation (2.29) or (2.30) is obtained ( $y$  is the perpendicular distance).

$$\frac{1}{2}U^2 + \frac{p}{\rho} + gy = \text{constant} \dots\dots\dots (2.29)$$

$$\frac{\rho}{2}U^2 + p + \rho gy = \text{constant} \dots\dots\dots (2.30)$$

Equations (2.29) or (2.30) are called Bernoulli's equations (or energy equations and the total of the velocity head, pressure head, and position head, which are items 1, 2 and 3 on the left side of equation (2.29) are the total head. The sum of dynamic pressure (velocity pressure) and static pressure, which are items 1 and 2 respectively on the left side of equation (2.30), is the total pressure (there are many cases where static pressure is simply called pressure)\*. Furthermore, when equation (2.29) is determined, equation (2.31) can be obtained in cases where  $\frac{\partial U}{\partial t}$  is disregarded (same with equation (2.30)).

$$\frac{1}{2}U^2 + \frac{p}{\rho} + gy + \int \frac{\partial U}{\partial t} ds = \text{constant} \dots\dots\dots (2.31)$$

---

\* Equation (2.29) is the case where the flow of liquids are treated and equation (2.30) is used to treat gases. There are many cases where item 3 on the left side can be disregarded when gases are treated. The head represents energy per unit mass of fluid.

This equation is called the energy equation for abnormal /25 flows. Equations (2.29) or (2.30) are introduced with flows where there is no loss, and the pressure or pressure heads can, therefore, be constant. In actual flows, there is pressure loss and, therefore, when we consider the fact that head loss  $\Delta h$  and pressure loss  $\Delta p$  ( $= \rho \Delta h$ ) are added to the right side of the equation. These sums are constant in equations (2.29) and (2.30).

$$\frac{1}{2}U^2 + \frac{p}{\rho} + gy + \Delta h = \text{constant} \dots \dots \dots (2.29')$$

$$\frac{\rho}{2}U^2 + p + \rho gy + \Delta p = \text{constant} \dots \dots \dots (2.30')$$

As an example of pressure loss (or head loss) during flow of a fluid in the flow path, pressure loss of a flow in a straight round pipe (friction loss) is illustrated. Equation (2.32) is obtained.  $l$  in the equation is length, and  $d$  is diameter of the pipe.

$$\Delta p = \lambda \frac{l}{d} \frac{\rho}{2} U^2 \dots \dots \dots (2.32)$$

is called the pipe friction coefficient and the Reynolds' number  $Re$  shown in 2.5 [1] is used as the function of relative coarseness inside the pipe ( $= \frac{Ud}{\nu}$ ,  $\nu = \frac{\mu}{\rho}$  is the dynamic viscosity coefficient of the fluid).

The pressure loss produced inside the diffuser is not represented as in the case of round pipes. However, the properties of the diffuser are defined using  $\zeta$ , the loss coefficient, and the static pressure recovery efficiency (called diffuser efficiency)  $\eta$ . ( $A$  is the cross section perpendicular to the flow and letter 1 shows the inlet area and 2 is the outlet area).

$$\zeta = \frac{\Delta p}{\frac{\rho}{2} U_1^2} \dots \dots \dots (2.33)$$

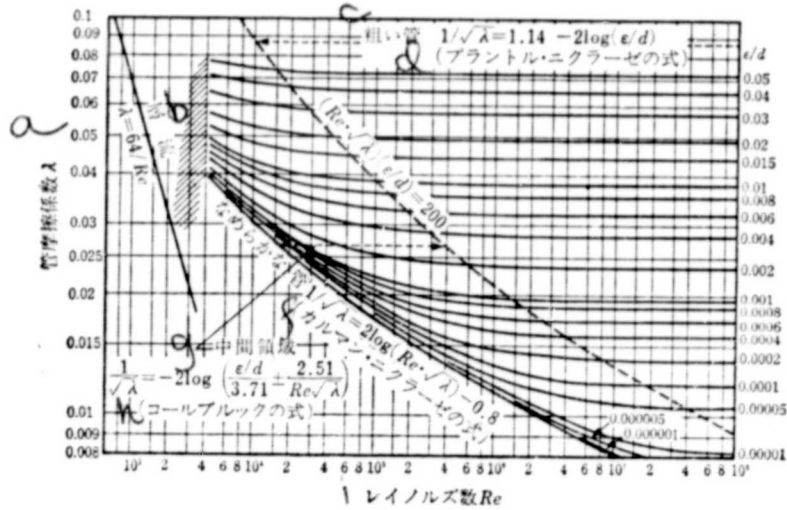


Figure 2.5. Pipe coefficient of friction in cylinder.

a--pipe coefficient of friction; b--layer; c--rough pipe; d--equation of Plant and Nicholase); f--equation of Carmen and Nicholase); g--intermediate region; h--Coalplack equation; i--Reynolds' number

$$\eta = \frac{\frac{\rho}{2} U_1^2 - \frac{\rho}{2} U_2^2 - \Delta p}{\frac{\rho}{2} U_1^2 - \frac{\rho}{2} U_2^2} \dots \dots \dots /26 \quad (2.34) *$$

Moreover,

$$\eta = 1 - \frac{\Delta p}{\frac{\rho}{2} U_1^2 \left( 1 - \left( \frac{A_1}{A_2} \right)^2 \right)} \dots \dots \dots (2.34') *$$

Next, as was previously mentioned, the mass momentum theory will be discussed. That is, 1, 2 inspection planes in 2 areas in the pipes were considered and the correlation of mass momentum of the fluid was used (powder is the time integral of mass momentum). The following equation (2.35) was obtained (Q is flow).

\* Equations (2.34) and (2.34') used  $U_1 A_1 = U_2 A_2$  (there is a correlation). Moreover,  $\Delta p$  is the total pressure loss. When static pressure reduction is considered, the velocity in the path is constant.

$$F = \rho Q(U_2 - U_1) \dots \dots \dots (2.35)$$

In the above-mentioned equation, power F is the total of the force exerted in the direction of fluid flow (pressure difference, frictional force, etc.). Regardless of whether viscosity of the fluid and compressibility are used, the mass momentum theory can be applied under these conditions. Therefore, it is very convenient.

(4) Boundary layer theory

The boundary layer is produced at the surface of the substance in the flow or at the flow path wall. The boundary layer is relatively thin in cases of ideal flow paths. The main flow is similar to a potential flow. In this case, the loss is treated as that produced only in the boundary layer. Therefore, it is very large\*.

The momentum equation of Navier and Stokes is restricted to cases of two-dimensions and when the direction of flow is x, and the direction perpendicular to flow walls is made y, the following equation is established.

$$\left. \begin{aligned} & \frac{\partial u}{\partial t} + u \frac{\partial u}{\partial x} + v \frac{\partial u}{\partial y} = -\frac{1}{\rho} \frac{\partial p}{\partial x} + \nu \left( \frac{\partial^2 u}{\partial x^2} + \frac{\partial^2 u}{\partial y^2} \right) \end{aligned} \right\} (2.1')$$

Equation of continuity

$$\frac{\partial u}{\partial x} + \frac{\partial v}{\partial y} = 0 \dots \dots \dots (2.2')$$

---

\* The actual boundary layer is limited to cases where a flow path and substance can be designed. However, the fact that tests on the velocity distribution and boundary layer of potential flows are being carried out is very important in understanding loss and peeling.

Here the boundary layer is a thin layer and, therefore, the items on a small order, such as

$$v \ll u, \quad \frac{\partial^2 u}{\partial x^2} \ll \frac{\partial^2 u}{\partial y^2}$$

are omitted to obtain equation (2.36) as long as (constant flow)

$$\left. \begin{aligned} u \frac{\partial u}{\partial x} + v \frac{\partial u}{\partial y} &= -\frac{1}{\rho} \frac{\partial p}{\partial x} + \nu \frac{\partial^2 u}{\partial y^2} \\ \frac{\partial p}{\partial y} &= 0, \quad \frac{\partial u}{\partial x} + \frac{\partial v}{\partial y} = 0 \end{aligned} \right\} \dots\dots\dots (2.36)$$

Equation (2.36) is called the boundary layer equation. The pressure  $p$  remains constant in the direction of  $y$ . The outside of the boundary layer is

$$v=0, \quad \frac{\partial}{\partial y} = \frac{\partial^2}{\partial y^2} = 0, \quad u=U$$

and, therefore, the first equation in (2.36) is written as follows.

$$U \frac{\partial U}{\partial x} = -\frac{1}{\rho} \frac{\partial p}{\partial x} \dots\dots\dots (2.37)$$

This equation is solved as (2.36) when boundary layers are set. The  $\nu \frac{\partial^2 u}{\partial y^2}$  in the first equation on the right side of (2.36) can /28 be written as  $\frac{1}{\rho} \frac{\partial \tau}{\partial y}$  and, therefore, when the boundary layer is used, the correlation between the friction stress ( $\tau$ ) and viscosity coefficient ( $\mu$ ) with a Newton fluid\* is used (equation (2.38)).

$$\tau = \mu \frac{\partial u}{\partial y} \dots\dots\dots (2.38)$$

In the case of a disrupted flow boundary layer\*\*, the following equation is established.

\* Refer to equation (2.1).

\*\* As is well known, the boundary flow becomes disrupted in some cases and transition to a disrupted flow from a boundary layer in round pipes is seen with a Reynolds' number of approximately 2300 or more. The condition of the boundary flow in the boundary layer is the layer flow boundary layer, and the case of a disrupted flow in the boundary layer is called disrupted flow boundary layer. Transition of the boundary layer occurs with a main flow Reynolds' number on the order of  $10^5$  or more.



$$\tau = \mu \frac{\partial \bar{u}}{\partial y} - \rho \bar{u}' \bar{v}' \dots \dots \dots (2.39)$$

In the above equation,  $\bar{u}$  is the mean time of velocity and  $\bar{u}'$  is the changing component.  $-\rho \bar{u}' \bar{v}'$  is the Reynolds' stress. The friction stress of the disrupted boundary layer uses various experimental equations. For instance, the following is one example.

$$\tau = 0.0225 \rho U^2 \left( \frac{U \delta}{y} \right)^{-1/4} \dots \dots \dots (2.40)$$

In the above-mentioned equation,  $\delta$  is the thickness of the boundary equation. The  $u$  and  $y$  direction distribution of velocity in the boundary layer is approximately the main current velocity  $U$ . Therefore, the size of  $\delta$  is impossible to determine. Consequently, thickness  $\delta^*$  and mass momentum thickness  $\vartheta$  are defined and used for the above-mentioned purpose.

$$\delta^* = \int_0^\infty \left( 1 - \frac{u}{U} \right) dy \dots \dots \dots (2.41)$$

$$\vartheta = \int_0^\infty \frac{u}{U} \left( 1 - \frac{u}{U} \right) dy \dots \dots \dots (2.42)$$

From the above-mentioned definition, mass momentum  $\rho U \delta^*$  is lost due to the formation of the boundary layer and  $\rho U^2 \vartheta$  is the mass momentum that is lost. The form coefficient  $H$  is defined as follows:

$$H = \frac{\delta^*}{\vartheta} \dots \dots \dots (2.43)$$

Form coefficient  $H$  varies with the distribution  $u$  of the boundary layer and, therefore, it is used in peeling of the disrupted boundary layer (in the case of layer flow boundary layers,  $\tau = 0$  when the boundary layer equation is directly solved).

The items in the first equation of the boundary layer equation (2.36) are integrated up to a sufficient size from  $y = 0$  and when varied, the following equation (2.44) is obtained.

$$\frac{d\theta}{dx} + \frac{\theta}{U} \frac{dU}{dx} (2+H) = \frac{\tau}{\rho U^2} \dots \dots \dots (2.44)$$

This is called the mass momentum integration of the boundary layer [4,5] and when combined with the experimental equations for frictional stress, such as (2.40), it is used as an approximation of the boundary layer.

(5) High speed flow (subsonic speed)

In flows of high speed or high pressure treated by centrifugation compressors, the flow must be explained using the compressibility of the gas, and this case will therefore be described. The equation for perfect gases\* is represented by equation (2.45) and the equation for changes in adiabatic properties\*\* are given with equation (2.46). Here R is the gas constant, T is absolute temperature and k is the specific heat ratio of the gas (ratio of constant pressure specific heat and constant volume specific heat).

$$\frac{p}{\rho} = RT \dots \dots \dots (2.45)$$

$$\frac{p}{\rho^k} = \text{constant} \dots \dots \dots (2.46)$$

From equations (2.45) and (2.46), it is possible to establish the following correlation between pressure p, temperature T and density ρ by using the changes in conditions (1) and (2). ((1) and (2) are attached).

---

\* Air can be treated as a perfect gas. However, there are many gases and coolants that cannot be treated with this equation and in this case, it is therefore necessary to determine changes in density.

\*\* The flow of gases is adiabatic (no loss or introduction of heat) and therefore changes in adiabatic properties are used as the standard (Chapter 3). Moreover, the correlation between total pressure and dynamic pressure and total temperature and dynamic pressure is also adiabatic.

$$\frac{p_1}{p_2} = \left(\frac{\rho_1}{\rho_2}\right)^k, \quad \frac{T_1}{T_2} = \left(\frac{p_1}{p_2}\right)^{\frac{k-1}{k}}, \quad \frac{T_1}{T_2} = \left(\frac{\rho_1}{\rho_2}\right)^{k-1} \dots \dots \dots (2.47)$$

The flow of gases with temperature T and velocity U is considered. The speed energy is converted adiabatically to heat, thereby resulting in an increase in temperature. This relationship is shown in equation (2.48).

$$T_t = T + \frac{1}{R} \frac{k-1}{k} \frac{U^2}{2} \dots \dots \dots (2.48) \quad \underline{/30}$$

The T in the first item on the right side is static temperature and the second item is dynamic pressure. Their sum is  $T_t$  of the total temperature. The static pressure, dynamic pressure and total pressure show a similar correlation in item (3). Equation (2.48) is represented by equations (2.51) and (2.51') when the velocity of pressure changes in the gas and the subvelocity a or Mach number M are used.

$$a = \sqrt{\frac{k p}{\rho}} \dots \dots \dots (2.49)$$

$$a = \sqrt{kRT} \dots \dots \dots (2.49')$$

$$M = \frac{U}{a} \dots \dots \dots (2.50)$$

$$T_t = T \left[ 1 + \frac{k-1}{2} \left( \frac{U}{a} \right)^2 \right] \dots \dots \dots (2.51)$$

$$T_t = T \left( 1 + \frac{k-1}{2} M^2 \right) \dots \dots \dots (2.51')$$

When equations (2.47) and (2.51') are used, the following correlation is obtained ( $p_t$  is total pressure and  $\rho_t$  is the density).

$$\frac{T_t}{T} = \left( \frac{p_t}{p} \right)^{\frac{k-1}{k}} \dots \dots \dots (2.52)$$

$$\frac{p_t}{p} = \left( \frac{\rho_t}{\rho} \right)^k \dots \dots \dots (2.53)$$

$$\frac{p_t}{p} = \left( 1 + \frac{k-1}{2} M^2 \right)^{\frac{k}{k-1}} \dots \dots \dots (2.54)$$

$$\frac{\rho_t}{\rho} = \left( 1 + \frac{k-1}{2} M^2 \right)^{\frac{1}{k-1}} \dots \dots \dots (2.55)$$

When equation (2.54) is developed, (2.56) is obtained. If the second items in the right side are omitted, the correlation between dynamic pressure, static pressure and total pressure for noncompressible flows in item (3) is the same.

$$p_t - p = \frac{\rho}{2} U^2 \left( 1 + \frac{M^2}{4} + \frac{2-k}{24} M^4 + \dots \right) \dots \dots \dots (2.56)$$

/31

Moreover, the equation (2.57) is obtained by changing equation (2.48) and this is the correlation equation for Bernoulli's equation in item (3) (right side is the total head)

$$\frac{U^2}{2} + \frac{k}{k-1} \frac{p}{\rho} = \text{constant} \dots \dots \dots (2.57)$$

(6) Law of similarity

This law states that when there are n number of changes in the physical phenomenon (n > 3), the number of basic units (mass, length and time) is three and therefore it is assumed that a correlation equation is drawn up by combining several variations (numbers). In this case, there are (n-3) non-dimensional (values). This is hypothesized as π. For instance, the variables pertaining to pressure loss of flow inside pipes Δp are pipe diameter d, pipe length l, fluid density ρ, viscosity coefficient μ, velocity U and length of pipe walls ε. Thus, the Δp is represented as equation (2.32) by

$$\Delta p = \frac{\rho}{2} U^2 \frac{l}{d} f \left( \frac{Ud}{\mu}, \frac{\epsilon}{d} \right) \dots \dots \dots (2.32')$$

and the nondimensional values of l/d, ε/d and  $\frac{Ud}{\mu} (= \frac{Ud}{\nu})$  are obtained. The equation (2.32') is the correlation of similarity with regard to pressure loss of pipes and is restricted to constant values of l/d (pipe length ratio), ε/d (relative roughness) and  $\frac{Ud}{\nu}$  (Reynolds' number). The correlation between Δp and  $\frac{\rho}{2} U^2$  is constant and similarity between two or more flows is established regardless of the size of the flow path or velocity.

In order to determine the similarity correlation (law), it is necessary to establish similarity with regard to the geometric and hydraulic properties (pressure, gravity, frictional force) and velocity of two flows in a model. Moreover, the variables must be correct. The flow in the diffuser has non-dimensional variables, such as the above-mentioned Reynolds' number  $Re$  and Mach number  $M$ . Other examples of nondimensional numbers are the nondimensional numbers pertaining to heat transfer (for instance, Prandtl number), the variables pertaining to vibrations (Struhal numbers) and the nondimensional numbers of fluid phenomena pertaining to gravity) Froude numbers).

## 2.2 Examples of calculations of the flow and boundary film

In this section, we will explain the simple calculations of the authors on the distribution of potential flow as well as the boundary film. As was noted in Chapter 3, the design of a diffuser with flow paths and guide blades is important, yet simple. However, tests and numerical calculations are necessary and, therefore, design guide lines are needed.

In addition, the authors used the direct method for the flow in the flow path. However, the inverse method is used as a method for determining flow path conditions from velocity (or pressure) distribution. This will be mentioned briefly in another chapter.

### (1) Conformal transformation method

The round blade forming the bladed diffuser ( $z$  plane) is transformed to a straight blade ( $\zeta$  plane) by transformation coefficient  $\zeta = \log z$  (or  $\log z = e$ ). Figure 2.6 shows this. The lattice made from circle and radiating lines above the  $z$  plane is changed to a lattice consisting of vertical and

horizontal lines in the plane<sup>\*</sup>. The advantage of transformation to a straight blade is that with the straight blade the calculations are simpler (the flow line method and relaxation method can be used).

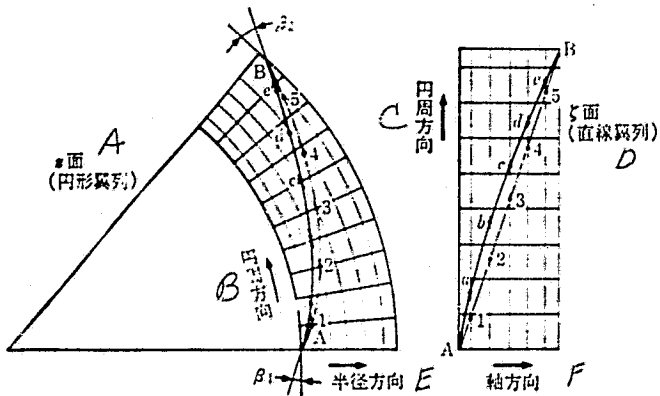


Figure 2.6 Transformation of the round blade to the straight blade. A--Z plane (round blade); B--Circumferential direction; C--Circumferential direction; D--S plane (straight blade); E--Radius direction; F--Axis direction

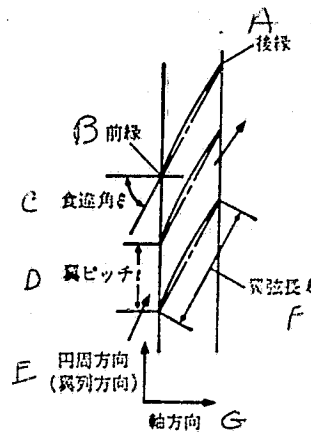


Figure 2.7 Illustration of the straight blade. A--Front connection; B--back connection; C--Feed angle  $\xi$ ; D--pitch; E--Circumferential direction (blade direction); F--length  $l$ ; G--axis direction.

The authors used the method whereby the straight blade is transformed to a concentric double circle and then the velocity distribution above the blades is determined [16].

/33

In general, when a bladed diffuser is used and transformed to a straight blade example, the chord ratio (ratio of pitch  $t$  to length  $l$ )  $t/l$  is low and the feed angle (angle of blade in horizontal direction)  $\xi$  is large (Figure 2.6). This type of blade shows a very uneven distribution of velocity in calculations and it is therefore necessary that  $t/l \cos \xi$  be greater

\* Figure 2.6 is an example of a case where the direction of the round blades and the straight blades differ. Moreover, in this case the concave section is the pressure surface and the concave section is negative pressure (normally the opposite with single blades and straight blades).

than 0.4. When the angle of the blade inlet is large and there are few blades, the calculations on diffuser design by conformal transformation are restricted. Therefore, long slender flow paths should be treated by the following flow line analytical method.

## (2) Flow line analysis

Flow line analysis involves drawing the flow line and potential curves on a flow path chart to obtain intersecting curves. Their positions are then changed to satisfy fluid engineering conditions. Figure 2.8 shows an example of an axial flow turbine [7].

The authors used the flow line analysis method with an axially symmetric example. The results are mentioned below [8]. The flow path was a flow path used in compressors (fans) (Chapter 1). As can be seen in Figure 2.9(a), it is a flow path with two curves a and b as the walls that are enclosed in a circle with the center being above the center line of the flow path (dotted line). The product of the diameter of the circle and the distance  $r$  from the center is constant and the flow path has a constant cross section area (uniform speed when viewed as a unit). The boundary conditions were calculated as follows.

- (a) c-c symmetric.
- (b) intersection between potential curve and flow line (including walls). Flow line is constant at a fixed flow ratio.
- (c) the distance of the flow line measured along the potential curve is  $dn$ , the length of the flow line along the two potential curves is  $ds$  and velocity is  $u$ . The amount of flow between the two curves  $Q$  is as follows.

/35





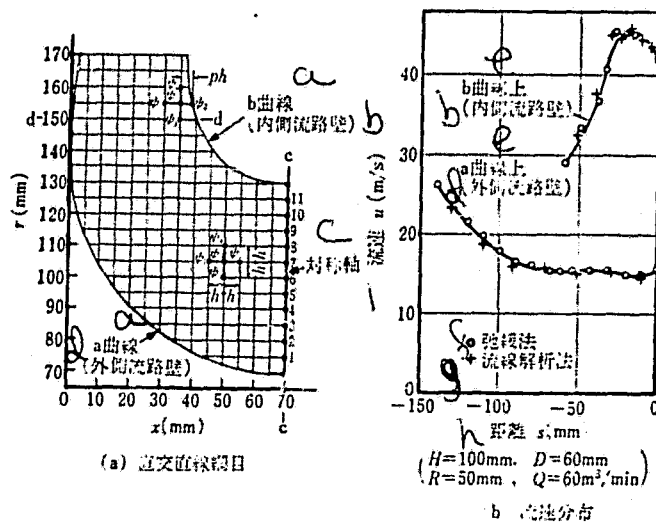


Figure 2.10. Relaxation calculations of axially symmetric flow path  
 (a) lattice (b) velocity distribution  
 a--curve b (inside flow path walls); c--symmetric axis;  
 d--(outside flow path walls); e--above curve; f--relaxation method;  
 g--flow line analysis; h--distance; i--velocity

(3) Relaxation method (or difference method)

This method involves the use of a flow path chart. It is suitable for repeated calculations on a computer. It is known that this method can be used for two-dimensional graphs [9]. The authors used it for the above-mentioned symmetric axis flow path [8]. As shown in Figure 2.10(1), a parallel lattice (distance between lines = h) is drawn on the coordinate axis (x,r) and the function  $\psi$  of flow along any point in the path is made  $\psi_0$  and that along those of the left, right, bottom and top are made  $\psi_2, \psi_1, \psi_3$  and  $\psi_4$ . When  $\psi_1 - \psi_4$  are developed, equation (2.61) is obtained.

$$\left. \begin{aligned} \frac{\partial^2 \psi}{\partial x^2} &= \frac{\psi_1 + \psi_2 - 2\psi_0}{h^2}, & \frac{\partial^2 \psi}{\partial r^2} &= \frac{\psi_3 + \psi_4 - 2\psi_0}{h^2} \\ \frac{\partial \psi}{\partial r} &= \frac{\psi_4 - \psi_3}{2h} \end{aligned} \right\} \dots \dots \quad (2.61)$$

These equations are used to obtain (2.62) with (2.14').

$$\psi_0 = \frac{1}{4}(\psi_1 + \psi_2 + \psi_3 + \psi_4) + \frac{h}{8r}(\psi_3 - \psi_4) \dots\dots\dots \quad (2.62) \quad \frac{/37}{*}$$

Equation (2.63) is obtained for (2.62) when the distance up to the flow path walls is made  $ph(0 < p < 1)$ . This is also true of other cases.

$$\psi_0 = \frac{1}{1+p} \left\{ \frac{p\psi_1 + \psi_2}{1+p} + \frac{p(\psi_3 + \psi_4)}{2} + \frac{ph(\psi_3 - \psi_4)}{4r} \right\} \dots\dots \quad (2.63) \quad *$$

The boundary conditions of the flow are as follows:

- (a) c-c symmetric.
- (b) distribution of velocity in the upper left is constant ( $\psi$  changes linearly in a horizontal direction).
- (c)  $\psi = 0$  along outside flow wall a and  $\psi = Q$  (desired flow) along inside flow path wall b.

Under these conditions, the  $\psi$  equations (2.62) and (2.63) can be satisfied for all points in the lattice and the distribution of  $\psi$  is therefore determined<sup>\*\*</sup>. The velocity (including the flow path wall) of each point can be determined using equation (2.13'). The results in section (2) are shown in Figure 2.10(b). These calculations coincided with one another.

Next, the calculations of two-dimensional flow paths will be explained. Figure 2.11(a) is a flow path of a model device (Chapter 4). The flow moves from the left to right. There are the rectifier, the central section for acceleration (nozzle) and the diffuser. A double spiral form was used.

In addition, the outlet of the diffuser is used in the calculations in a shorter form than in actual models. The same

---

\* In the case of two-dimensional paths (for instance, Figure 2.11),  $r$  is not included.

\*\* The calculations are repeated several times for accuracy. However, some functions are multiplied in order to curtail time.

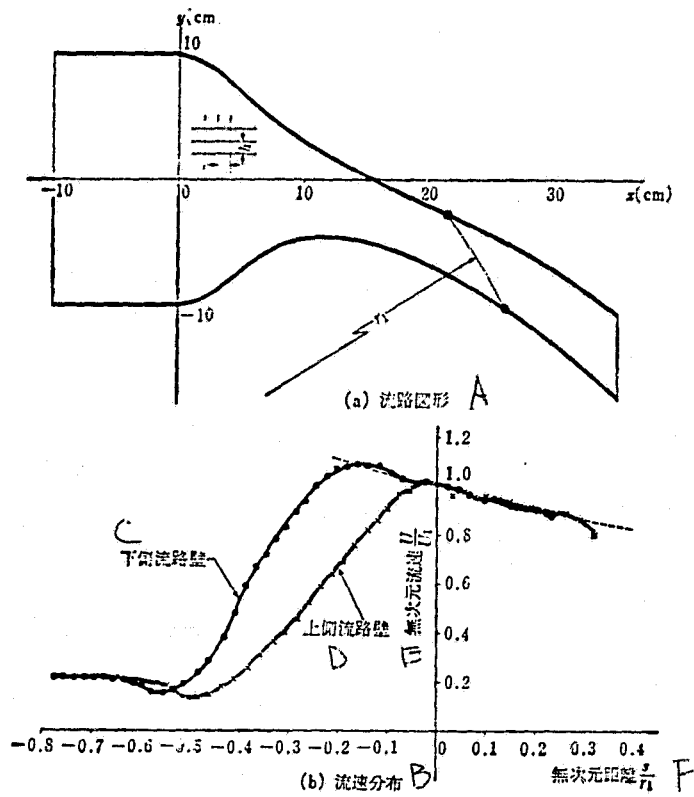


Figure 2.11 Calculations of two-dimensional flow paths

- A-- (a) Flow path of a model device;
- B-- (b) Velocity distribution
- C-- Lower flow path
- D-- Upper flow path
- E-- Nondimensional velocity  $\frac{U}{U_1}$
- F-- Nondimensional distance  $\frac{x}{r_1}$

is true in cases where the boundary conditions are set. The velocity distribution is shown in Figure 2.11(b). The axis /38 of the abscissa in the figure is the standard point of intersection at the inlet circle (distance above flow path wall). A nondimensional  $s/r_1$  ( $s$  is distance) is used. This is made dimensionless by radius  $r_1$  of the inlet. The axis of the ordinates is the velocity made dimensionless by velocity  $U_1$  and is written as  $U/u_1$  ( $U$  is velocity). The broken lines in the figures show the velocity of potential flows and  $U/U_1 = 1$  at the inlet ( $\frac{s}{r_1} = 0$ ). The spiral potential flow at the outlet is therefore similar.

Next, by the flow analysis method and relaxation method the velocity obtained in calculations showed some variations. This may have been due to a lack of time in calculations of errors made in readings ( $p$  in equation (2.63)). However, when calculations were repeated, there was little improvement.

#### (4) Boundary calculations

In order to determine the distribution of potential flow in flow paths (particularly along the top of the flow walls), it is necessary to determine whether there is a boundary layer and whether it separates.

When the main distribution of velocity is given (correlation between distance  $x$  and main velocity  $U$ ), the method of continuity differentiation recorded in 2.1 (4) can be used to calculate the boundary layer. The method of Buri is one example for disrupted flow boundary layers [10,11]. The variable  $Z$  in equation (2.64) is obtained for solving the /39 equation (2.44). Moreover, when equation (2.65) is used for the frictional force, the equation (2.44) is changed to differential equation (2.66) for  $Z$ .

$$Z = g \left( \frac{Ug}{\nu} \right)^{\frac{1}{n}} \dots \dots \dots (2.64)$$

$$\frac{\tau}{\rho U^2} = \frac{k}{\left( \frac{Ug}{\nu} \right)^{\frac{1}{n}}} \dots \dots \dots (2.65)$$

$$\frac{dZ}{dx} + \frac{Z}{U} \frac{dU}{dx} - A = \frac{k}{\frac{n}{n+1}} \dots \dots \dots (2.66)$$

Provided that,

$$A = \frac{H+2 - \frac{1}{n+1}}{\frac{n}{n+1}} \dots \dots \dots (2.67)$$

the following equation can be used to solve (2.66)

$$Z = \frac{1}{U^A} \left[ \frac{k(n+1)}{n} \int U^A dx + C \right] \quad (C - \text{constant}) \quad (2.68)$$

Buri introduced the following boundary layer parameter  $\Gamma$  and used  $\Gamma \leq -0.06$  as the separation conditions. When  $\Gamma$  is used, (2.68) is represented by equation (2.70)

$$\Gamma = \frac{g}{U} \frac{dU}{dx} \left( \frac{Ug}{\nu} \right)^{\frac{1}{n}} \dots \dots \dots (2.69)$$

$$\Gamma = \frac{1}{U^{A+1}} \frac{dU}{dx} \left[ \frac{k(n+1)}{n} \int U^A dx + C \right] \dots \dots \dots (2.70)$$

Moreover, equation (2.71) is obtained by solving with (2.69).

$$g = \left( \frac{\Gamma U^{\frac{n-1}{n}} \nu^{\frac{1}{n}}}{\frac{dU}{dx}} \right)^{\frac{n}{n+1}} \dots \dots \dots (2.71)$$

Here  $k$  is 0.01256,  $n$  is 4, and  $H$  is 1.4. Therefore,  $A$  is 4. Moreover, equations (2.70) and (2.71) are represented by (2.70') and (2.71'). (The minimum points are represented with 0).

$$\Gamma = \frac{1}{U^5} \frac{dU}{dx} \left[ 0.016 \int_x^x U^4 dx + \frac{\Gamma_0 U_0^5}{\left( \frac{dU}{dx} \right)_0} \right] \dots \dots \dots (2.70')$$

$$g = \left( \frac{\Gamma U^{\frac{1}{4}} \nu^{\frac{1}{4}}}{\frac{dU}{dx}} \right)^{\frac{4}{5}} \dots \dots \dots (2.71') \quad /40$$

Furthermore, (2.70) is represented by (2.70'') with axially symmetric flows.

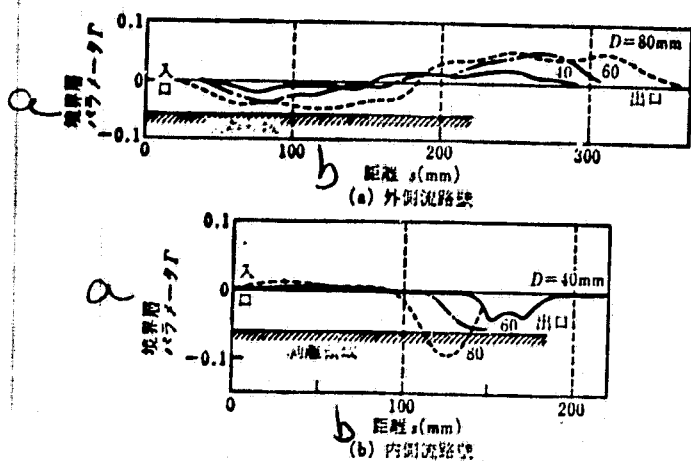


Figure 2.12. Calculations of boundary layer parameters (R = 50 mm and H = 100 mm)  
 (a) outside wall (b) inside wall  
 a---boundary layer parameter; b---distance

$$\Gamma = \frac{\frac{dU}{dx}}{U^{\frac{3}{2}} r^{\frac{1}{2}}} \left[ 0.016 \int_s^x U^{\frac{1}{2}} r^{\frac{1}{2}} dx + \frac{\Gamma_0 U_0^{\frac{1}{2}} r_0^{\frac{1}{2}}}{\left(\frac{dU}{dx}\right)_0} \right] \dots \dots \dots (2.70'')$$

The authors have calculated  $\Gamma$  along the inside and outside of the flow walls using the model in Figure 2.9(a) and the results are shown in Figure 2.12(a). The calculations are obtained by using U shaped flow. As shown in the figure, when D (width of flow path) is small,  $\Gamma$  changes very little and when D is large, the changes in  $\Gamma$  are large. Moreover, the changes in  $\Gamma$  are greater on the inside of the path. U shaped components have a chance of showing peeling, as in Figure 2.10. Therefore, the back of the flow path starts to peel in Figure 2.12(b) when D is 80 mm. This fact is also seen in model experiment results (determinations of flow path pressure distribution).

In addition to the Buri  $\Gamma$ , the H of Doenhoff, the  $\eta$  of Gruschwits, and the L of Truckenbrodt may be used [13] but the same results are obtained by all of these methods when the flow is a decelerated flow.

## REFERENCES

- [1] Japan Mechanical Engineering Society: Mechanical Engineering (ed. 6), volume 8, 5/1976.
- [2] for instance Harada: Engineering with Fluids (Maruen, 1962).
- [3] Eckert, B.: Axialkompressoren und Radialkompressoren (Axial Compressors and Radial Compressors), p. 222 (Springer, 1953).
- [4] Tamaki: Fluid Dynamics II (lecture 16), p. 49 197=60.
- [5] Schlichting, H.: Boundary layer theory, p. 137 (McGraw Hill, 1962).
- [6] Hyakushoku: Mechanical Engineering Soc. of Japan Preprints no. 43, p. 33 (4/1961).
- [7] Uchida: Fluid Engineering, p. 126 (1957).
- [8] Sugii: Japan Society of Mechanical Engineering Convention, 32-240, p. 182 (8/1966).
- [9] same as in [8], p. 123.
- [10] Buri, A.: Diss Zurich (1931).
- [11] same as [5], p. 569.
- [12] same as [8], p. 1286.
- [13] same as [5], p. 570.

## DESIGNS FOR DIFFUSERS AND RESEARCH RESULTS

In this section, we will give the theoretical equations for centrifugation compressors and fans and then explain the design of diffusers (as flow paths and fluid machines). The explanations are basic ones and the effects of form and use are explained in Chapter 5. The problems with diffuser properties are also mentioned.

### 3.1 Theoretical equations and design of compressors and fans

#### (1) Theory of mass momentum [1]

The law of mass momentum explained in 2.1 is used to "make the momentum at a certain point equal to the time component of momentum of the objects at this point". Here the force momentum is the product of distance  $r$  between the point (center point) and the operating point and the force is a peripheral direction (component perpendicular to radius from center point). The mass momentum is the product of the above-mentioned  $r$  and the mass component of the object in a peripheral direction of  $mu_u$  ( $m$  is mass and  $c_u$  is velocity).

The above-mentioned correlation is used for swirl flows of fluids. 1 is attached to the point at the inlet of the flow and 2 to the point at the outlet to obtain the correlation in 3.1 for equation (2.35). Here  $T$  is torque (momentum),  $\rho$  is density of the fluid, and  $Q$  is the flow (Figure 3.1)

$$T = \rho Q (c_{u2} r_2 - c_{u1} r_1) \dots\dots\dots (3.1)$$

The runners in compressors and fans increase the momentum of the fluid by torque and thereby increase energy of the fluid. Next, the force applied to the runner without loss is



made L and when the correlations in 3.2 and equation (3.3) are realized, equation (3.4) is obtained ( $\omega$  is the angle velocity of the runner and  $u$  is the peripheral velocity).

$$L = T\omega \dots\dots\dots (3.2)$$

$$L = \rho QH \dots\dots\dots (3.3)$$

$$H = u_2 c_{u2} - u_1 c_{u1} \dots\dots\dots (3.4)$$

The above-mentioned H is the weight of the substance and is the same as the head in the energy equation in Chapter 2 (energy per unit mass of the fluid). It is called the head (head without a loss). That is, force added to the runner produces head H and mass flow  $\rho Q$ .

Next, in diffusers in a stationary path (called diffusers without or with blades), the force is not exerted on the fluid and a head is not seen. In two-dimensional flows without friction (or constant flow path width),  $T = 0$  and thus, equation (3.5) is obtained.

$$c_{u2}r_2 = c_{u1}r_1 = c_u r \text{ (一定)} \dots\dots\dots (3.5)$$

That is, in the above-mentioned flow the velocity  $c_u$  is proportional to the radius  $r$  and the radius component  $c_r$  of velocity is proportional to  $r$  according to equation (3.6) continuity correlation

$$c_{r2}r_2 = c_{r1}r_1 = c_r r = \text{constant} \dots\dots\dots (3.6)$$

(3.8) is established from 3.5 and 3.6 and 3.7. ( $\alpha$  is the angle of the flow toward the periphery (flow angle)

$$\tan \alpha = \frac{c_u}{c_r} \dots\dots\dots (3.7)$$

$$\alpha_1 = \alpha_2 = \alpha = \text{constant} \dots\dots\dots (3.8)$$

That is, angle  $\alpha$  of the swirl flow in a two-dimensional potential flow is constant and this type of flow line is a logarithmic spiral (or conformal spiral). Moreover, the flow established by equation (3.5) is called a free spiral flow. As is clear in equations (3.5) and (3.6), the size  $c$  of the velocity is proportional to radius  $r$  and the surface  $A_r$  is the same as the ratio of outlet and inlet diameter.

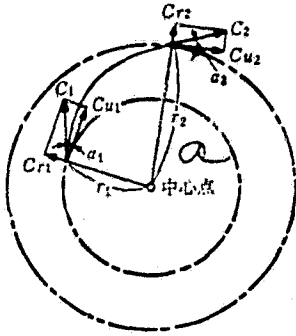


Figure 3.1. Swirl flow.  
a--central point

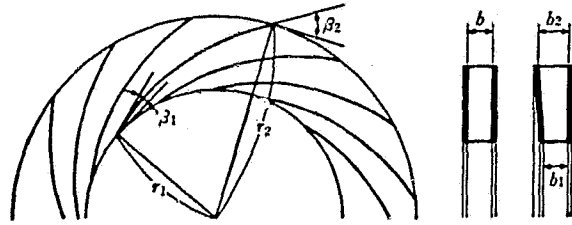


Figure 3.2. Bladed diffuser

$$A_r = \frac{r_2}{r_1} \dots \dots \dots (3.9)$$

The value of  $c_{u2}$  is less than the correlation shown in equation (3.5) (and therefore, the size of  $c$  is also smaller). The surface area of the diffuser  $A_r$  is represented by (3.10) (here  $\beta$  is the angle of the blade in a peripheral direction (blade angle))<sup>\*</sup>.

$$A_r = \frac{r_2 \sin \beta_2}{r_1 \sin \beta_1} \dots \dots \dots (3.10)$$

\* The width of the axis ( $b$ ) is constant in (3.10). When the width changes,

$$A_r = \frac{b_2 r_2 \sin \beta_2}{b_1 r_1 \sin \beta_1} \dots \dots \dots (3.10')$$

(refer to Figure 3.2). In any equation, the flow is the flow along the blade angle.

$\beta_2 > \beta_1$  in equation (3.10). The surface area ratio  $A_r$  is greater than that of bladeless diffusers. A head is not seen. However, torque is produced as in equation (3.1) and therefore the force is applied as bending force on the blades.

## (2) Design of centrifugation compressor

Here the design method of the centrifugation compressor will be explained with changes in the density of the fluid (changes with a high velocity flow). These equations are simplified and compressibility has little effect. Moreover, it is simple to use these equations for compressors and pumps (refer to page 58). In addition, the effects of compressibility are not sufficiently treated by the fluid path itself. However, when viewed as a structural element, it is necessary to use calculations for determining the dynamic pressure at the inlet and flow angle. 46

First of all, the symbols in the calculations are summarized using those in section (1) and the preceding chapter. In addition, Figure 3.3 shows the diffusers, the runners and the spiral casing [2]. The diffuser is a diffuser with no blades immediately behind the runner (called inlet-bladeless diffuser below)\*. (A guide path is sometimes used in place of the spiral casing).

---

\* Noise and pressure changes are produced near the runner outlet in bladed runners. Therefore, there are many cases where the blades separate from the runners. This is particularly true in cases where the flow emitted from the runner is at ultrasonic velocity. Therefore, the velocity is reduced to subsonic velocity.

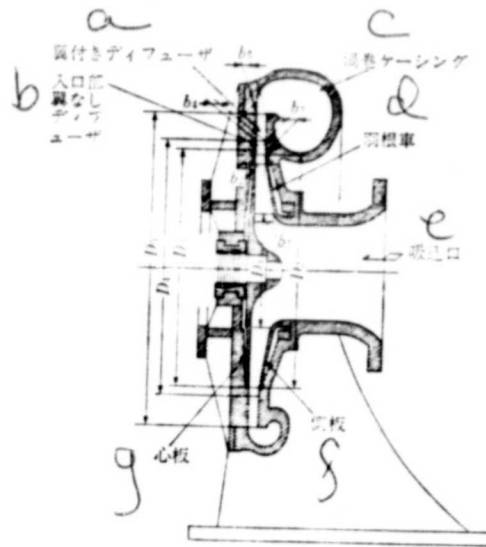


Figure 3.3. Centrifugation compressor  
 a--bladed diffuser; b--inlet-bladeless diffuser; c--spiral casing; d--runner; e--inlet; f--side plate; g--central plate

Q: inlet flow

H: head

p: pressure

T: absolute temperature

u: peripheral velocity

c: current velocity

$\rho$ : fluid density

$\alpha$ : flow angle

$\beta$ : blade angle

$\epsilon$ : ratio occupied by blade thickness

$\lambda$ : wall friction coefficient (same as pipe friction coefficient)

$\eta$ : efficiency

$\zeta$ : loss coefficient

$\mu$ : smoothness

$\Lambda$ : reverse degree

M: Mach number

a: sonic speed

k: specific heat ratio

R: gas constant

D: diameter ( $=2r$ )

b: current path (axial) width

A: path surface area

Letters

- th, i: no loss
- ∞: no smoothness (infinite number of runners)
- ad: adiabatic heat
- t: total (total temperature, pressure)
- s: static (temperature and pressure)
- r: radial
- u: peripheral
- 1: runner inlet
- 2: runner outlet
- 3: inlet-bladeless diffuser inlet
- 4: bladed diffuser inlet
- 5: bladed diffuser outlet
- 6: spiral casing outlet (- compressor outlet)
- R: runner
- e: inlet-bladeless diffuser
- d: bladed diffuser
- c: spiral casing

Next, the properties of the compressor and efficiency are defined below:

smoothness\* 
$$\mu = \frac{H_{th}}{H_{th\infty}} \dots\dots\dots (3.11)$$

adiabatic heat efficiency 
$$\eta_{ad} = \frac{H_{ad}}{H_{th}} \dots\dots\dots (3.12)$$

runner adiabatic efficiency 
$$\eta_{adR} = \frac{H_{adR}}{H_{th}} \dots\dots\dots (3.13)$$

head without loss of smoothness\* 
$$H_{th\infty} = u_2 c_{u2\infty} = u_2 \left( u_2 - \frac{c_{r2}}{\tan \beta_2} \right) \dots\dots\dots (3.14)$$

adiabatic head 
$$H_{ad} = \frac{kRT_{t1}}{k-1} \left\{ \left( \frac{p_{t5}}{p_{t1}} \right)^{\frac{k-1}{k}} - 1 \right\} \dots\dots\dots (3.15)$$

runner adiabatic head 
$$H_{adR} = \frac{kRT_{t1}}{k-1} \left\{ \left( \frac{p_{t2}}{p_{t1}} \right)^{\frac{k-1}{k}} - 1 \right\} \dots\dots\dots (3.16)$$

---

\* Smoothness is the phenomenon where angle  $\beta_2$  at the runner outlet is small due to a secondary flow and the head is smaller than "the head with an ideal runner with an infinite number of blades".

Here, equation (3.14) is obtained by using the correlation in Figure 3.4 with the second item on the left of 3.4 being 0<sup>\*\*</sup>. Moreover, the adiabatic head is a head that is provided to gases when the gas is adiabatically compressed. It is obtained from equations (2.45) and (2.46).

Efficiency of inlet-bladeless diffuser (called efficiency below, the same as recorded in (2.34), etc.)

$$\eta_c = \frac{p_{s4} - p_{s3}}{p_{s4i} - p_{s3}} \dots\dots\dots (3.17)$$

Total pressure loss coefficient (called loss coefficient; same as in (2.33))

$$\zeta_e = \frac{p_{t3} - p_{t4}}{\frac{\rho_{s3}}{2} c_3^2} \dots\dots\dots (3.18)$$

Efficiency of bladed diffuser

$$\eta_d = \frac{p_{s5} - p_{s4}}{p_{s5i} - p_{s4}} \dots\dots\dots (3.19)$$

total loss coefficient  $\zeta_d = \frac{p_{t1} - p_{t5}}{\frac{\rho_{s1}}{2} c_4^2} \dots\dots\dots (3.20)$

spiral casing coefficient  $\eta_c = \frac{p_{s6} - p_{s5}}{p_{s6i} - p_{s5}} \dots\dots\dots (3.21)$

same loss coefficient  $\zeta_c = \frac{p_{t5} - p_{t6}}{\frac{\rho_{s5}}{2} c_5^2} \dots\dots\dots (3.22)$

reverse degrees  $A = \frac{p_{s2} - p_{s1}}{p_{s6} - p_{s1}} \dots\dots\dots (3.23)$

or  $A = \frac{p_{s2} - p_{s1}}{p_{t2} - p_{t1}} \dots\dots\dots (3.23')$

Mach number of runner outlet (3.24)

$$M_2 = \frac{c_2}{a_2} = \frac{c_2}{\sqrt{kRT_{t2}}} \dots\dots\dots$$

The values are determined for steps 1-6 using data obtained from each element (diffuser, etc.). Then 1-6 are repeated for the entire unit to obtain the desired dimensions and form.

---

<sup>\*\*</sup> In order to increase head efficiency, the value is usually  $\mu_{tCul} = 0$  (nonswirling flow).

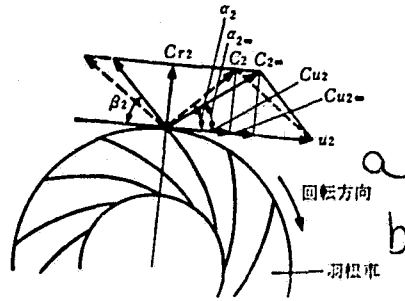


Figure 3.4. Velocity triangle at runner outlet ( $\infty$  represents no smoothness when there are infinite numbers of runners)  
 a--rotation direction; b---runner

1. Runner blade inlet: The gas conditions  $p_{t1}$  and  $T_{t1}$  at the inlet of the diffuser and  $R$  and flow  $Q$  are given /50

$$\left. \begin{aligned} \rho_{t1} &= \frac{p_{t1}}{RT_{t1}}, \quad c_1 = \frac{Q\rho_{t1}}{A_1\rho_{s1}}, \\ \text{ただし, } A_1 &= \pi b_1 D_1 (1 - \epsilon_1) \\ p_{s1} &= p_{t1} \left( 1 - \frac{k-1}{kRT_{t1}} \cdot \frac{c_1^2}{2} \right)^{\frac{k}{k-1}} \\ T_{t1} &= T_{s1} \left( \frac{p_{t1}}{p_{s1}} \right)^{\frac{\gamma-1}{\gamma}}, \quad \rho_{s1} = \frac{p_{s1}}{RT_{s1}} \end{aligned} \right\} \dots (3.25) *$$

\* The low pressure fans use  $T_1$  regardless of the difference between  $T_{s1}$  and  $T_1$ . Moreover, the equation is simplified using dynamic pressure, static pressure, total pressure at a low velocity (same as in 2, but  $\rho$  is increased with each stage.

$$\rho_1 = \frac{p_{t1}}{RT_1}, \quad c_1 = \frac{Q}{A_1}, \quad p_{s1} = p_{t1} - \frac{\rho_1}{2} c_1^2 \dots \dots \dots (3.25')$$

There are changes in  $\rho$  at each stage in pumps and any  $\rho$  is considered.

(2) Runner outlet: In compressors the pressure is given with the above-mentioned inlet conditions ( $p_{t6}$  or  $p_{s6}$ ).  $H_{th}$  is determined from equations (3.15) and (3.12) and (3.11).  $u_2$  and  $c_{u2}$  are given so that (3.14) is satisfied.

$$\left. \begin{aligned}
 c_{r2} &= \frac{Q \rho_{t1}}{\rho_{t2} A_2}, \quad \text{ただし } A_2 = \pi b_2 D_2 (1 - \epsilon_2) \\
 c_{u2} &= \mu \left( u_2 - \frac{c_{r2}}{\tan \beta_2} \right), \quad c_2 = \sqrt{c_{r2}^2 + c_{u2}^2} \\
 p_{t2} &= p_{t1} \left( \frac{\rho_{t2} R}{R T_{t1}} \cdot \frac{k-1}{k} u_2 c_{u2} + 1 \right)^{\frac{k}{k-1}} \\
 T_{t2} &= T_{t1} + \frac{k-1}{kR} u_2 c_{u2} \\
 p_{t2} &= p_{t1} \left( 1 - \frac{k-1}{kR T_{t2}} \cdot \frac{c_2^2}{2} \right)^{\frac{k}{k-1}} \\
 T_{t2} &= T_{t2} \left( \frac{p_{t2}}{p_{t2}} \right)^{\frac{k-1}{k}}, \quad \rho_{t2} = \frac{p_{t2}}{R T_{t2}}
 \end{aligned} \right\} \dots \dots \dots (3.26)$$

51

$$\alpha_2 = \tan^{-1} \frac{c_{r2}}{c_{u2}} \dots \dots \dots (3.27)$$

(3) Inlet-bladeless diffuser: As in (2)  
 $c_{r3}, c_{u3}, c_3, p_{t3}, T_{t3}, p_{s3}, T_{s3}, \dots \dots \dots (3.28)$

$\rho_{s3}$  are established  
 $\alpha_3 = \tan^{-1} \frac{c_{r3}}{c_{u3}} \dots \dots \dots (3.29)$

The above-mentioned  $\alpha_3$  is the angle of flow of the gas in a bladeless diffuser (this value is as large as the amount of flow as in the first equation in (3.26)).

(4i) Bladed diffuser inlet (assuming no loss between 3 and 4)

$c_{r4i}, c_{u4i}, c_{4i}, p_{t4i}, T_{t4i}, p_{s4i}, T_{s4i}, \rho_{s4i}$  established consecutively (3.30)

$$\alpha_{4i} = \tan^{-1} \frac{c_{r4i}}{c_{u4i}} \dots \dots \dots (3.31)$$

(4) Bladed diffuser inlet  
 $\alpha_4 = \alpha_{4i} + \Delta \alpha_4$   
 provided that  
 $\Delta \alpha_4 = \tan^{-1} \left\{ \tan \alpha_3 + \frac{\lambda(D_4 - D_3)}{8b_3} \right\} - \alpha_3$  } ..... (3.32)



(Here  $\Delta\alpha_4$  is the increase in the flow angle with friction between (3) and (4) [3]. The inlet angle  $\beta_4$  of the diffuser blade is equal to  $\alpha_4$ ).

$$\left. \begin{aligned} c_{r4} &= \frac{Q\rho_{t1}}{\rho_{t4}A_4}, \quad c_4 = \frac{c_{r4}}{\sin \alpha_4} \\ T_{t4} &= T_{t2}, \quad p_{t4} = \eta_e(p_{s1t} - p_{t3}) + p_{t3} \\ p_{t4} &= p_{s1} \left( 1 - \frac{k-1}{kRT_{t4}} \cdot \frac{c_4^2}{2} \right)^{\frac{k}{k-1}} \\ T_{s1} &= T_{t4} \left( \frac{p_{s1}}{p_{t4}} \right)^{\frac{k-1}{k}}, \quad \rho_{s1} = \frac{p_{s1}}{RT_{s1}} \end{aligned} \right\} \dots \dots \dots (3.33)$$

The above-mentioned are solved consecutively.

$$\zeta_e = \frac{p_{t3} - p_{t4}}{\frac{\rho_{t3}}{2} c_3^2} \dots \dots \dots (3.18) \quad /52$$

In (3.33), the efficiency  $\eta_e$  of the diffuser is obtained from experimental data. When the loss coefficient  $\zeta_e$  is known,  $\eta_e$  is determined ( $\eta_d$  and  $\zeta_d$  and  $\eta_c$  and  $\zeta_c$  also).

(5i\*) Outlet of bladed diffuser (no loss between(4) and (5)) provided that

$$\left. \begin{aligned} c_{r5i} &= \frac{Q\rho_{t1}}{\rho_{s5i}A_5}, \quad \text{for } A_5 = \pi b_5 D_5 (1 - \varepsilon_5) \\ &\quad \text{(is the calculated)} \\ \alpha_5 &= \beta_5 - \Delta\alpha_5 \quad \Delta\alpha_5 \text{ potential flow. It is} \\ &\quad \text{the same as the angle of deflection} \\ c_{s5i} &= \frac{c_{r5i}}{\sin \alpha_5}, \quad p_{s5i} = p_{t4} \\ T_{s5i} &= T_{t2} \\ p_{s5i} &= p_{s5i} \left( 1 - \frac{k-1}{kRT_{s5i}} \cdot \frac{c_{s5i}^2}{2} \right)^{\frac{k}{k-1}} \\ T_{s5i} &= T_{s5i} \left( \frac{p_{s5i}}{p_{t5i}} \right)^{\frac{k-1}{k}}, \quad \rho_{s5i} = \frac{p_{s5i}}{RT_{s5i}} \end{aligned} \right\} \dots \dots \dots (3.34)$$

The above-mentioned are solved consecutively.

---

\* 5i and 5 are omitted for compressors with diffusers and (4) is used for the diffuser. Then proceed to 6i and 6. Moreover, a flow path is used in place of the spiral casing. In addition, the same equation is used for bladed diffusers (refer to Eckert [3]).

(5) Outlet of bladed diffuser

$$\left. \begin{aligned} c_{r5} &= \frac{Q \rho_{t1}}{\rho_{t5} A_5}, \quad c_5 = \frac{c_{r5}}{\sin \alpha_5} \\ p_{t5} &= \eta_d (p_{t5i} - p_{t4}) + p_{t4}, \quad T_{t5} = T_{t2} \\ p_{t5} &= p_{t5} \left( 1 - \frac{k-1}{k R T_{t5}} \cdot \frac{c_5^2}{2} \right)^{-\frac{k}{k-1}} \\ T_{t5} &= T_{t5} \left( \frac{p_{t5}}{p_{t5}} \right)^{\frac{k-1}{k}}, \quad \rho_{t5} = \frac{p_{t5}}{R T_{t5}} \end{aligned} \right\} \dots \dots \dots (3.35)$$

The above-mentioned are solved consecutively.

$$\zeta_d = \frac{p_{t4} - p_{t5}}{\frac{\rho_{t4}}{2} \cdot c_4^2} \dots \dots \dots (3.20) \quad /53$$

The area of the diffuser is determined from  $\alpha_5, \alpha_4, D_4, D_5, b_4$  and  $b_5$ .

(6i) Spiral casing outlet (case where no loss is seen between (5) and (6))

$$c_{6i}, p_{t6i}, T_{t6i}, p_{s6i}, T_{s6i}, \rho_{s6i} \dots \dots \dots (3.36)$$

(6) Outlet of spiral casing

$$c_6, p_{t6}, T_{t6}, p_{s6}, T_{s6}, \rho_{s6} \dots \dots \dots (3.37)$$

$$\zeta_c = \frac{p_{t5} - p_{t6}}{\frac{\rho_{t5}}{2} \cdot c_5^2} \dots \dots \dots (3.22)$$

If  $p_{t6}$  and  $p_{s6}$  are the desired values (design standards) in equation (3.37), it is possible to adjust the dimensions (efficiency and loss) and then repeat the above-mentioned computations until the design values are the same as the calculated values. Moreover, a single flow (design flow) is recorded and the flow is changed in the calculations.

Figure 3.5 shows the calculation results of the authors (centrifugal compressor). The properties of the bladed diffuser are shown (correlation between angle of flow  $\alpha_4$  and efficiency  $\eta_d$  and loss coefficient  $\zeta_d$ ). From the figure, it is possible to obtain a good efficiency (that is, flow range (mentioned in Chapter 6)).

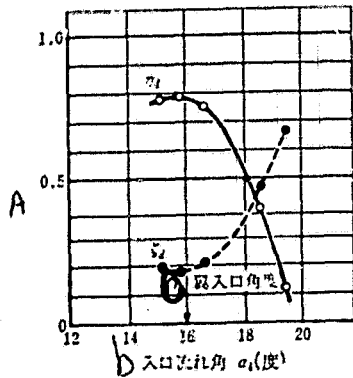


Figure 3.5. Properties of centrifugation compressor diffuser  
 a--diffuser efficiency  $\eta_4$ ,  
 loss efficiency  $\zeta_4$ ,  
 b--inlet flow angle  $\alpha_1$  degrees,  
 c--inlet angle

### (3) Form of round blades

The round blades are formed in runners and bladed diffusers of centrifugal compressors (fans).

/54

The inlet radius  $r_1$ , outlet radius  $r_2$ , inlet angle  $\beta_1$  and outlet angle  $\beta_2$  are given and a curve can be drawn (for instance, spiral [4], etc., curves). The simplest method uses a circle. The actual results are obtained by this method.

Next, we will use the method where 1 curve is drawn\*. Now, with radius  $R$  and  $r_D$  from the center of the round blade, equations (3.38) and (3.39) are established based on  $\Delta OAP$  and  $\Delta OBP$  in Figure 3.6.

$$R = \frac{r_2 - r_1^2}{2(r_2 \cos \beta_2 - r_1 \cos \beta_1)} \dots \dots \dots (3.38)$$

$$r_D = \sqrt{r_2^2 + R^2 - 2r_2 R \cos \beta_2} \dots \dots \dots (3.39)$$

Next, by using a triangle, it is possible to obtain angle  $\phi_3$  with regard to center  $O$  at both ends  $AB$  of a blade as well as  $\phi_1, \phi_2$  with equations (3.40) and (3.42).

$$\phi_1 = \sin^{-1} \left( \frac{R}{r_D} \sin \beta_1 \right) \dots \dots \dots (3.40)$$

(provided that  $R^2 \geq r_1^2 + r_D^2$  is inclined in accordance with  $\phi_1$ ).

$$\phi_2 = \sin^{-1} \left( \frac{R}{r_D} \sin \beta_2 \right) \dots \dots \dots (3.41)$$

(provided that  $R^2 \geq r_2^2 + r_D^2$  is inclined in accordance with  $\phi_2$ ).

$$\phi_3 = \phi_1 - \phi_2 \dots \dots \dots (3.42)$$

\* This graph uses the center line of the blade with no thickness. There are cases where thin blades are used and, therefore, the blade angle considered with regard to the pressure surface or pressure surface of the blade (inlet angle, outlet angle), etc., also varies little with the center axis.

The above-mentioned degrees  $\phi_3$  are common to the size of the angle of 1 pitch of the blade ( $\phi = 2\pi / \text{blade with } Z \text{ number of blades}$ ). (This is the importance of the blade). The suitable values are obtained with  $\phi_3/\phi$  and this can be adjusted by selection of the number of blades.

Next, equations (3.43)-(3.45) are established for the angle with regard to curve AB and the curve efficiency center P, as well as  $r_2, r_1$  in the figures. Length  $l$  from these curves is given by equation (3.46).

$$r_1 = \sin^{-1} \left( \frac{r_1}{r_D} \sin \beta_1 \right) \dots\dots\dots (3.43)$$

$$r_2 = \sin^{-1} \left( \frac{r_2}{r_D} \sin \beta_2 \right) \dots\dots\dots (3.44)$$

( $r_1, r_2$  are both inclined as in equations (3.40) and (3.41)).

$$\gamma = r_2 - r_1 \dots\dots\dots (3.45)$$

$$l = R\gamma \dots\dots\dots (3.46)$$

The surface area ratio  $A_r$  obtained here is given in equation (3.10). However, it is clear that when angle  $\beta_1$  and radius ratio  $\frac{r_2}{r_1}$  are given, the maximum surface area is limited by the angle  $\beta_2$  ( $\sin \beta_2 = 1$ ) and therefore  $r_2 r_1 \sin \beta_1$  is the maximum. (That is, in cases where the outer diameter is set, the outlet width  $b_2$  of the flow path does not increase and the surface area ratio cannot be any larger than the above-mentioned value ).

In equation (3.38),  $r=r_2$  and  $\beta=\beta_2$ . Equation (3.47) is established for  $\beta$ .

$$\beta = \cos^{-1} \left( \frac{r^2 - r_1^2}{2Rr} + \frac{r_1}{r} \cos \beta_1 \right) \dots\dots\dots (3.47)$$

From the above-mentioned equations, it is possible to determine the correlation between the diameter position of the blade ( $r$ ) and the angle at this position ( $\beta$ ).  $r$  and  $\beta$  are not linearly related and when  $r$  is on the axis of abscissa,  $\beta$  is often a convex curve. This tendency is not noted when angle  $\beta_1$  is large and area  $A_r$  is low. However, it is marked

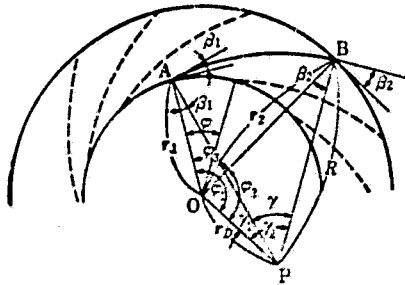


Figure 3.6. Diagrammatical relations of circular blade diffusers.

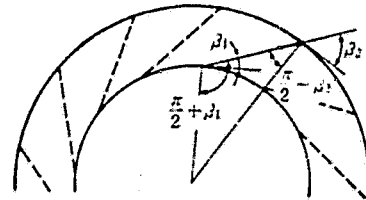


Figure 3.7. Correlations in linear blade diffuser

when  $\beta_1$  is small and  $A_r$  is large (pumps and air conditioners). Therefore, it is preferred that the curve be formed from two circles (in this case length  $l$  is long and there are few numbers of blades  $Z$ ).

In order to simplify the form of the blades, they may be determined with curves (Figure 3.7). In this case, the correlation between inlet angle  $\beta_1$  and outlet angle  $\beta_2$  is given with equation (3.48).

$$\cos \beta_2 = \frac{r_1}{r_2} \cos \beta_1 \dots\dots\dots (3.48)$$

With a straight blade diffuser, it is possible to give a larger surface area than with the round blade diffuser and, therefore, it is often used for diffusers with a small diameter ratio (compressors, etc.).

(4) Law of similarity

The main properties are flow and head in the law of similarity (as was previously mentioned). Therefore, flow  $Q$  produced by a fluid machine is proportional to the product of the typical flow path cross section area  $A$  and velocity  $c$ . Above-mentioned  $A$  is proportional to the square of the typical dimension (such as diameter  $D_2$  of the runner) and the velocity

c is proportional to the velocity of the runner  $u_2$  and  $D_2 N$  (N is the r.p.n.). The following two equations are obtained. The equation (3.49) is called the flow coefficient and is a nondimensional parameter. However, it is usually treated as the flow equation with (3.50).

$$\phi = \frac{Q}{A u} = \text{constant} \dots\dots\dots (3.49)$$

or

$$\frac{Q}{D_2^3 N} = \text{constant} \dots\dots\dots (3.50)$$

The head H produced by fluid machines is proportional to the square of the velocity  $u_2$  as in equation (3.14). (It can be proportional to  $(D_2^2 N^2)$ ). Consequently, the following two equations are obtained and are called nondimensional parameters with equation (3.51) (head coefficient<sup>\*</sup>). As previously mentioned, there are cases where equation (3.52) deals with the head coefficient.

$$\psi = \frac{H}{\frac{u_2^2}{2}} = \text{constant} \dots\dots\dots (3.51) \quad \underline{/57}$$

or

---

\* The increase in pressure is used in place of the head and is sometimes called the pressure coefficient.

or 
$$\frac{H}{D_2^2 N^2} = \text{constant} \dots\dots\dots (3.52)$$

The similarity of force L is determined by equations (3.53) and (3.54) using equation (3.3) ( $\tau$  is the output coefficient)

$$\tau = \frac{L}{\frac{\rho}{2} A u_2^3} = \text{constant} \dots\dots\dots (3.53)$$

or

$$\frac{L}{\rho D_2^5 N^3} = \text{constant} \dots\dots\dots (3.54)$$

Next,  $D_2$  is eliminated from (3.50) and (3.52) to obtain equation (3.55).

$$\frac{NQ^{\frac{1}{2}}}{H^{\frac{1}{2}}} = \text{constant} = n_s \dots\dots\dots (3.55)$$

The above-mentioned  $n_s$  is the relative velocity and is the same value for the fluid device\*. The specific velocity is the number present as the type of fluid device (high pressure or large flow type, etc.) and is generally used to establish a correlation with total efficiency  $\eta_T$  of the type of compressor (= fluid output/driving force, called efficiency) [5,6] (Figure 3.8). This type of figure shows that the curve is obtained by calculating the maximum efficiency of the device at each relative velocity. Moreover, this total efficiency is the efficiency including that of the runner, diffuser, spiral casing, etc., and cannot be represented individually.

The diffusers treated in this test are fluid machines with similar relative velocities. The form of each can be geometrically regulated so that tests can be carried out on the general

---

\* The calculations of specific velocity  $n_2$  are usually done using individual units (for instance,  $N(\text{rpm}), H(\text{m}),$  etc.).  $n_2$  is therefore different depending on the number of dimensions, etc.  $n_2$  is nondimensional when series are used (for instance  $Q(\text{m}^3/\text{s}), N(1/\text{s}), H(\text{m}^2/\text{s}^2),$  defined as energy per unit mass).

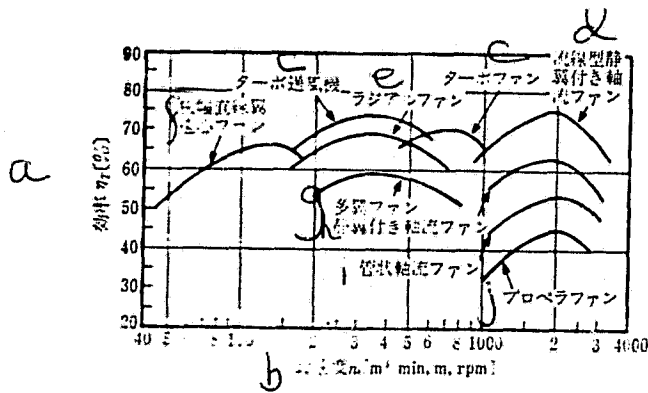


Figure 3.8. Correlation between relative velocity and efficiency  
 a--efficiency; b--relative velocity; c--turbofan; d--current line-type static bladed axial flow fan; e--radial fan; f--centrifugal fan; g--multiblade fan; h--static bladed axial flow fan; i--tube axial flow fan; j--blower fan

hydraulic parameters (Reynolds' numbers, etc.).

### 3.2. Diffuser design methods

In the previous section, we described methods for designing general fluid machines, including diffusers. However, in this section, we will give the basic policies for designing diffusers themselves.

#### (1) General pipe flow type diffusers

The elements defining the forms of diffusers were previously mentioned. The method for defining simple diffusers will be explained here and problems will be mentioned.

Research has been carried out for many years on conical two-dimensional diffusers, etc. Here we will explain the theory of Patterson [1]. Moreover, we will consider the final research results. Figure 3.9 gives the experimental data of Patterson, Gibson [8] and Peters [9] and the axis of the abscissa shows the angle  $2\theta$  (refer to figures) of the diffusers and the axis



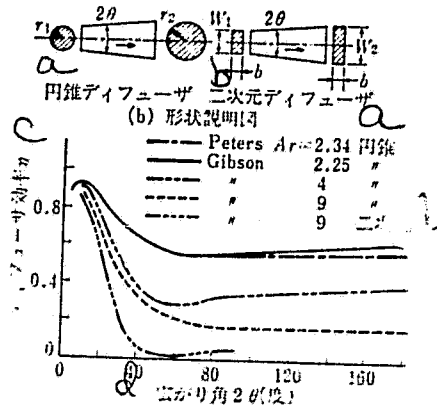


Figure 3.9. Angle and efficiency of diffuser (Patterson)  
 (a) properties of diffuser (b) form  
 a--conical; b--two-dimensional; c--diffuser efficiency  $\eta$ ;  
 d--angle  $2\theta$  (degrees)

of the ordinate shows the efficiency of the diffusers (static return efficiency  $\eta$  (equation 3.56))\*. Furthermore, efficiency is related to the total force coefficient (equation (3.57))  $C_p$  of the diffuser, as well as the total loss coefficient  $\zeta$  (equation (3.58)). (U is velocity, p is static pressure,  $\Delta p$  is total pressure loss,  $\rho$  is fluid density, A is current path area and attached numbers 1 is the diffuser inlet and 2 is the outlet).

/59

\* Equation (3.56) is the equation for the inlet and outlet of the diffuser and gives the velocity as constant values ( $U_1$  and  $U_2$ ). However, a velocity distribution is actually used and therefore the following equations are used [7,10]. (u is the velocity of the cross section, Q is the flow and  $U_1$  and  $U_2$  are the mean velocities). However, from a practical viewpoint, only the equations in (3.56) and (3.56') can be used to determine the dimensions of the diffuser.

$$\eta = \frac{p_2 - p_1}{\frac{\rho}{2} U_1^2 \left\{ \bar{\beta}_1 - \bar{\beta}_2 \left( \frac{A_1}{A_2} \right)^2 \right\}}$$

where

$$\left. \begin{aligned} \bar{\beta}_1 &= \int_{A_1} \frac{1}{2} \rho u^2 dA / \frac{1}{2} \rho U_1^2 Q \\ \bar{\beta}_2 &= \int_{A_2} \frac{1}{2} \rho u^2 dA / \frac{1}{2} \rho U_2^2 Q \end{aligned} \right\} \dots \dots \dots (3.56')$$

$$\eta = \frac{p_2 - p_1}{\frac{\rho}{2} U_1^2 - \frac{\rho}{2} U_2^2} \dots (3.56)$$

$$r = \frac{p_2 - p_1}{\frac{\rho}{2} U_1^2 \left( 1 - \frac{A_1}{A_2} \right)} \dots (3.56')$$

$$C_p = \frac{p_2 - p_1}{\frac{\rho}{2} U_1^2} \dots (3.57)$$

$$\zeta = \frac{\Delta p}{\frac{\rho}{2} U_1^2} \dots (3.58)$$

Patterson showed that the maximum angle of the conical diffuser with an area ratio of 2.3-9 is 6-8 degrees (angle with the maximum efficiency and minimum loss coefficient). However, according to Gibson, the angle is approximately 6 degrees with a square diffuser (ratio of 4) and Biston and Vedernikov [11] showed that the angle was approximately 11 degrees with two-dimensional diffusers (ratio of 4, etc.).

/60

Recently, there have been tests on conical diffusers by BHRA (British Hydraulic Research Association) (refer to (3.10)) [10,12]. They showed that when the ratio of length of the diffuser  $\frac{l}{r_1}$  ( $l$  is length and  $r_1$  is radius of inlet) is on the axis of abscissas and the surface ratio  $A = \frac{r_2^2}{r_1^2}$  is on the axis of the ordinates, the pressure coefficient  $C_p$  or loss coefficient  $\zeta$  can be obtained. However, the ratio  $A_r$  is constant in some cases and the maximum angle  $2\theta$  (angle where the connecting point of  $C_p$  and the line parallel to the axis of abscissas) is approximately 8 degrees. Therefore, when the length ratio  $\frac{l}{r_1}$  is constant, the angle is calculated based on diffuser designs (angle where the  $C_p$  intersect that parallel line on the axis of ordinates. The angle is larger at approximately 12 degrees. From the above-mentioned, it appears that the calculations are more detailed than those of the BHRA. Moreover, in most cases, the conical diffuser designs can be used (refer to Diffuser Design Tests). In addition, according to experiments on two-dimensional diffusers by Stanford University,

the maximum angle with a two-dimensional diffuser is approximately 8 degrees, and the length ratio  $\frac{l}{W_1}$  ( $W_1$  is small and the maximum angle is large) (Figure 3.11 [10,13] and the maximum angle is larger than that of Patterson. In addition, it appears that the design chart for two-dimensional diffusers is used by this research group.

The optimum for most diffusers is obtained by studying the changes in fluid hydraulic conditions (Reynolds' number, inlet boundary layer thickness, capillaries at outlet, etc.). The data and design standards must be used. Moreover, there is a tendency to use conventional conservative designs (angle of 5 degrees). However, it is more economic to use designs that are more efficient.

/61

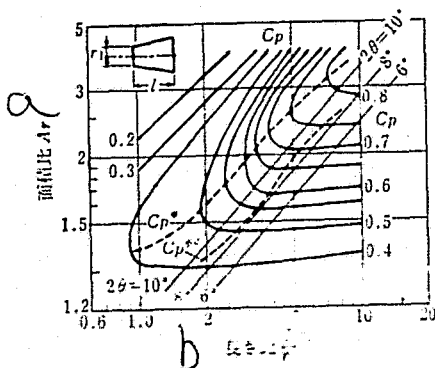


Figure 3.10. Properties of conical diffusers ( $C_p$  is the coefficient of maximum pressure with a constant  $\frac{l}{r_1}$  and  $C_p^{**}$  is the maximum pressure coefficient with a constant  $A_r$ )

a--surface area ratio  $A_r$ ;  
b--length ratio

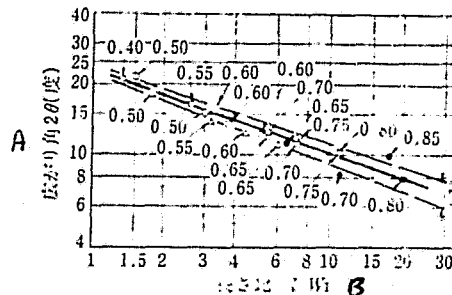


Figure 3.11. two-dimensional diffuser optimum angle (Reneau). The  $C_p$  in the figure is represented by the added number. a--angle  $2\theta$  (degrees); b--length ratio ( $l/W_1$ )

Next, the design of a diffuser will be explained with examples. Sprenger [14] has given the cases where experiments were carried out on various diffusers by changing the cross section form (Figure 3.12).

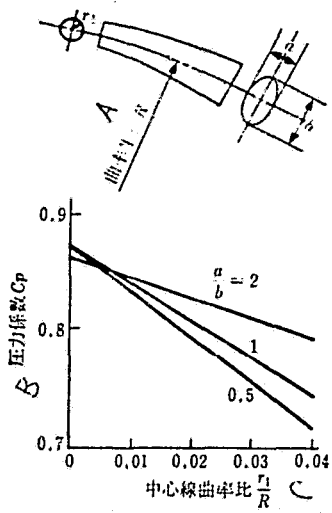


Figure 3.12. Form and performance of bend diffusers.

A--Radius of the center line R;  
 B--Pressure coefficient; C--Bend in the center axis  $\frac{r_1}{R}$ .

Prechter [15] has evaluated experimental results and shown that there is a correlation between the bend in the center axis  $\frac{r_1}{R}$  (R is the radius of the center line) and the inclination (a/b) of the outlet (a is the diameter of the perpendicular cross section with regard to radius and b is the horizontal diameter with respect to radius) and the pressure coefficient  $C_p$  (Figure 3.12). Moreover, the following correlation is established in these experiments.

$$C_p = C_{p(R=\infty)} - \frac{r_1}{R} \left( 4.72 - 1.44 \frac{a}{b} \right) \dots \dots \dots (3.59)$$

(  $\frac{a}{b} = 0.5 \sim 2, 2\theta = 8^\circ, A_r = 4$  )

Therefore, it is clear that there is a reduction in properties (pressure coefficient with a large curve in the center line and that the reduction in properties varies with the shape of the outlet cross section (reduction is marked with long slender cross section). The fact that the cross section is thin in the radial direction shows that the pressure differences (or production of secondary flow\*) are reduced. This is used for emission of water wheels, etc. (Chapter 1). /62

(2) Diffusers of centrifugal compressors and fans (centrifugal diffusers)

The bladeless diffusers of compressors, etc., have few

\* The secondary flow is a flow produced by a perpendicular component (eddy produced in flow path).

difficulties in designs (there are cases where the surface area ratio is constant). Therefore, we will give the design equations for bladed diffusers. The following are the design rules (manuals, etc.).

(a) The following are indicated in the manual of Stepanoff [16].

i) the flow path width is equal to  $b_2$  the width of the outlet of the runner or is somewhat larger (1.05-1.1 fold);

(ii) the outer diameter of the diffuser is 1.35-1.6 fold the outer diameter of the runner  $D_2$ ;

(iii) the angle of the flow path is equal to the optimum in the case of straight diffusers (eight with round cross section, six with square cross section, 11 with constant flow path width (two-dimensional)); these are the standards of Patterson, or somewhat smaller. However, it is difficult to use these designs with conical cross sections;

(iv) the blade thickness in Figure 3.13 shows that the length  $l$  of the blade is four times the inlet width  $a$  (width seen from the front of the flow; in this case the angle is 8.5 and the area ratio  $b/a$  is 1.6);

(v) the angle is constant with  $Z$  number of blades (angle is  $2\pi/Z$ ).

(b) The designs below are those of Eckert [17]:

(i) the flow angle at the outlet of the runner  $\alpha_2$  is less than 20 and the bladed diffusers must be used;

(ii) the width of the diffuser path is 1-2 mm larger than the width of the runner outlet  $b_2$  (including bladeless sections). The diameter of the blade inlet is 7-20% larger than that of the runner outlet;

(iii) the angle of the flow path is usually 8-10 for long slender cross section (test by Wedernikoff\*) and 7-9 degrees

---

\* Same as above-mentioned Vedernikov (Russian spelling changed).

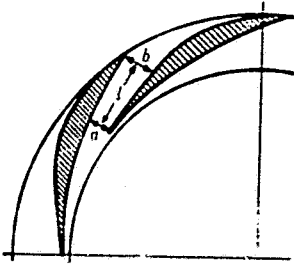


Figure 3.13. Thick blade diffuser

with conical cross section (tests by Andres);

(iv) the area ratio can be 2.5-4 (same as in equations (3.10) and (3.10')). The angle and area ratio may be given with  $Z$  number of blades. Eckert uses the case where the correlation between the inlet and outlet diameter ratio and number of blades is given with the various ratios and angles.

follows [16].

(c) The Stepanoff design is as

(i) the flow path width is constant in the radial direction. The bladed diffuser paths are narrow;

(ii) the distance between the runner outlet and diffuser blade inlet is 5-12% of the runner outer diameter  $D_2$  (10-30 mm);

(iii) the blade inlet angle is equal to the flow angle of the runner outlet. The outlet angle is made the inlet angle + (12-18°). The angle should not exceed 20°;

(iv) the angle of the diffuser flow path is 8-10° (should not exceed 12°). The number of blades is usually between 15-36.

From the above-mentioned designs, it appears that most two-dimensional diffuser designs are based on experimental data and that the policies are conservative. Moreover, there is room for further improvement. These models will be explained in detail later.

### 3.3 Problems with diffuser properties [19]

/64

The problems with centrifugal diffuser properties will be summarized here (refer to Chapters 5 and 6 for details). The elemental problems of diffusers and hydraulic problems will not be discussed. However, the problems will be divided into two areas for convenience. Moreover, there are many common problems

with conventional and contrifugal diffusers and tests will be carried out on particular problems.

(1) Problems related to form.

(a) conical diffuser. There are many problems that have been previously mentioned;

(b) angle diffusers. There are many diffusers that are used in practice. However, few have been tested;

(c) two-dimensional diffusers. As was previously mentioned, many studies have been performed. These diffusers have width  $b$  of the flow path (also called depth) and the ratio of depth and width (for instance  $b/W_1$ , is the aspect ratio) must be considered;

(d) annular diffusers. There are many diffusers that are being used and there has been a great deal of research (Chapter 1);

(e) the cross section of diffusers (profile). By making the cross section including the center axis a curve, it is possible to improve properties (mirror type);

(f) changes in flow path cross section. Diffusers whose cross section is changed can be used;

(g) curve of center axis (curved diffuser). The curved diffuser is made by attaching the cross section diagram to the periphery of the center axis with the center axis being curved in a circle (refer to Sprenger research). There are few examples of studies because this form is so complex;

(h) space curve diffuser. The center axis of this diffuser is curved;

(i) capillaries. The capillaries in Figure 3.4 are attached to the diffuser outlet (called pipes) and free emission is provided. Moreover, there is a considerable difference in properties;

(j) short or enlarged diffuser. The diffuser is a conical diffuser with a large expansion angle. As shown in Figure 3.15, the outlet is expanded with the diameter of the pipes being large (short type diffuser);

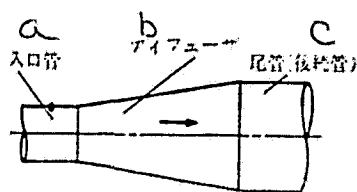


Figure 3.14. Inlet and capillaries  
a--inlet pipes;  
b--diffuser;  
c--capillaries (back pipes)

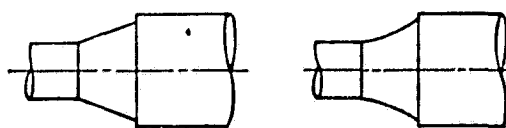


Figure 3.15. Expanded diffusers  
(a) straight type (conical);  
(b) curved type (rappa\*)

(k) center (guide) blades. Center (guide) blades are used in this type of diffuser. There may be one or more of these guides. The flow path is divided at the small angle section and separation and secondary flows are prevented;

(l) rough sections or grooves in flow walls. Rough sections or grooves in flow path walls are made (Figure 3.16) to permit mixing of the fluid in the boundary layer and prevent separation. Next, the features of centrifugal types will be mentioned;

(m) blade diffuser. Blades are set up so that they are inclined several degrees in the direction of the periphery (inlet angle). The inlet of the flow path is slanted toward the flow. The number of variables determining the shape of the bladed diffuser is usually seven and of these, five are important. The number of form elements is usually high and testing is very important; /66

(n) channel diffuser (island models). With this type of diffuser, the cross section of the flow path may be square. However, the flow at the outlet must be efficient;

(o) pipe diffuser. This is a combination of above-mentioned (n) and is hydraulically efficient when the flow paths are conical;

(p) tandem or slot diffusers<sup>\*\*</sup>. When deceleration is high (or when the flow angle is high, peeling is prevented by

\* Translator's note: term unknown; phonetic characters.

\*\* The blades on the inlet side and the blades on the outlet side are tandem-types, with the inlet blades being smaller than the outlet blades. The former is called the slot-type.



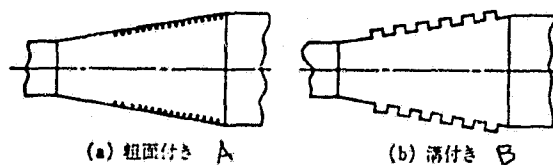


Figure 3.16. Rough sections or grooves in diffuser flow walls. A--rough sections; B--grooves

the boundary film control function;

(q) bladeless diffusers. Many studies have been performed on these diffusers. The elements that determine the form of the diffuser is the diameter ratio of the inlet and outlet  $(\frac{r_2}{r_1})$ . However, actually, the flow path width (b) has an effect and is the variable  $b/r_1$ ;

(r) inclined flow (bladed or bladeless) diffuser. The /67 problems are similar to those in (d). There are many elements that are important in bladed diffusers, and they are therefore complex;

(s) axially symmetric flow paths. There are many forms of diffusers that are used for axial flow compressors, etc., and, therefore, generalization is very difficult.

## (2) Fluid engineering problems

The effect of fluid hydraulics in diffusers is very important. The effects control the value of the data and should be noted in evaluations of other researchers.

(a) Reynolds number. This is normally represented by the typical dimensions of the inlet (inlet diameter  $D_1$  or width  $W_1$ ), the inlet mean velocity and the kinematic viscosity of the fluid. The diffuser is a deceleration path and behavior of the flow path boundary layer is important. Therefore, the Reynolds' number is important;

(b) Mach number. With a high velocity, the Mach number (inlet value) is very important. When the inlet flow exceeds ultrasonic velocity, choking and reduction in the flow may occur.

Cavitation also occurs with a reduction in pressure;

(c) thickness of inlet boundary layer. The boundary layer at the inlet has a large effect on properties;

(d) shear flow at inlet; the flow from the runner is very important and is called a shear flow when it is fast on the center plate side and the side plate side\*. (This is a flow with a velocity gradient). This should be studied further with regard to diffuser properties;

/68

(e) swirling at inlet. As a result of prevention of peeling by using a swirling effect, the efficiency of the diffuser is improved;

(f) disruption of flow. The disrupted flow is a flow with a variable velocity. The flow is disrupted to prevent peeling. Furthermore, there are cases where the flow is varied on a large scale (sizing, swirling, etc.);

(g) rotation. There are cases where the angle flow path is made so that the runner also rotates (diffuser rotation). In rotating paths, the effects of the centrifugation power differ from stationary paths);

(h) boundary layer control. The boundary layer is controlled and properties are thereby improved. Suctioning, swirling, etc., of the boundary layer are used. Moreover, tandem blades or slot blades are sometimes used;

(i) angle of bladed diffusers. The flow angle is changed with changes in the amount of flow (large angle with large flow, small angle with low flow). Therefore, there is a difference between the flow angle and diffuser blade angle (angle difference). When the angle difference is large, separation occurs and there is a marked reduction in efficiency. This leads to a loss of swirling. Moreover, calculation examples were given in 3.1.

---

\*The round plate attached to the rotation axis of the runner is the center plate and the plate on the inlet side is the side plate (Figure 3.3).

## REFERENCES

/69

- [1] for instance, Harada: Fluid Mechanics (Lecture 7), p. 9, 1960.
- [2] Sugii; Mechanical Engineering Lecture Notes, No. 153 , p. 219 4/1966)
- [3] Eckert, B.: Axialkompressoren und Radialkompressoren (Axial and Radial Compressors), p. 342 (Springer, 1953).
- [4] Sugii: Kiron, 32-237, 731 (5/1966)
- [5] same as 1, p. 111
- [6] Kotake: Air Devices (lecture 23), p. 63, 1959)
- [7] Patterson, G. N.: Aircraft Engineering, Vol. X, p. 267 (1938).
- [8] Gibson, A. H.: Proc. Roy. Soc., Ser. A., Vol. 83 (1910).
- [9] Peters, H.: Ing. Arch<sup>\*</sup>, 11-1 (1931-33).
- [10] Japan Mechanical Engineering Society: Technological Report on Fluid Resistance of Pipes and Ducts (1979)
- [11] Vedernikov, A. N.: Trans. of the Central Aero-Hydrodynamic Institute, Moscow, No. 137 (1926).
- [12] BHRA: Internal Flow--A guide to losses in pipe and duct system. Part II, Performance of Straight-Wall Diffusers (1971).
- [13] Reneau, L. R., et al.: Trans. ASME, Ser. D, 89-1, p. 141, (1967-3).
- [14] Sprenger, H.: Diss Zurich, No. 2803 (1959).
- [15] Prechter, H. Maschinenmarkt 67-82, p. 19 (1961).
- [16] Stepanoff (Teruda, translator: Turbofans, p. 161 (1958).
- [17] same as in [3], p. 341
- [18] Stechkin (Hamajima, translator): Jet Engine Theory p. 100 (Corona, 1965).
- [19] for instance, Wakeda, et al.: Turbo Devices 10-1, p. 7 (1.82)

---

\* Ing. Arch: Ingenieur Archiv

In this text, we give the experimental results as dimensionless. Therefore, the following calculations will be shown:

$\text{efficiency of diffuser } (\eta) = \frac{\text{static pressure increase}}{\text{dynamic pressure of flow at inlet} - \text{dynamic pressure of outlet}}$ $\text{pressure coefficient of diffuser } (C_p) = \frac{\text{static pressure increase}}{\text{dynamic pressure of inlet}}$
--

(1) With conical diffusers with an inlet radius  $r_1$  of 10 cm, what is the static pressure  $\Delta p$  obtained with an inlet velocity of  $U_1 = 30$  m/s, inlet density  $\rho = 1.2$  kg/m<sup>3</sup> area ratio (outlet/inlet) of  $A_r = 2$  and efficiency  $\eta$  of 0.8 (or pressure coefficient of  $C_p = 0.6$ )?

$$\text{inlet dynamic pressure} = \frac{\rho}{2} U_1^2 = \frac{1.2}{2} \times 30^2 = 540 \text{ Pa} \quad (\text{Pascal})$$

$$(1 \text{ Pa} = 0.102 \text{ kgf/m}^2 = 0.102 \text{ mmAq})$$

$$\text{outlet dynamic pressure} = \frac{\rho}{2} U_1^2 \times \frac{1}{A_r^2} = 135 \text{ Pa}$$

$$\text{static pressure increase } \Delta p = \eta \frac{\rho}{2} U_1^2 \left(1 - \frac{1}{A_r^2}\right) = 0.8 \times (540 - 135) = 324 \text{ Pa}$$

or

$$\Delta p = C_p \frac{\rho}{2} U_1^2 = 0.6 \times 540 = 324 \text{ Pa}$$

(2) The static pressure increase and form where the maximum static pressure increase is obtained can be determined when the area ratio is  $A_r = 2$  and the  $r_1$  is 10 cm in conical diffusers.

A straight line is drawn from  $A_r = 2$  in Figure 3.10 and the intersection at  $C_p^{**}$  is read.  $\frac{l}{r_1} = 5.2$ , and  $C_p$  is 0.685. /71  
 Therefore,  $l = r_1 \times 5.2 = 52$  cm. Moreover, the expansion angle in Figure 5.1 is  $2\theta = 9.1^\circ$  and the conditions of the inlet flow are the same as in 1. Therefore,  $\Delta p = 0.685 \times 540 = 370$  Pa.

(3) When the length ratio  $\frac{l}{r_1}=4$ , the static pressure increase and the form where the maximum static pressure increase is provided is determined.

A perpendicular line is drawn from  $\frac{l}{r_1}=4$  in Figure 3.10. Then the  $C_p^*$  curve intersection is read.  $A_r = 2.25$  and  $C_p = 0.70$ . Therefore,  $\Delta p = 0.70 \times 540 = 378 \text{ Pa}$ . Moreover, from Figure 5.1  $2\theta = 14.3^\circ$  ( $\tan \theta = (\sqrt{A_r} - 1) / \frac{l}{r_1}$  to obtain  $2\theta$ ).

EXPERIMENTS AND MEASUREMENT [1-3]  
AND ANALYSIS METHODS FOR DIFFUSERS

There are no special differences between experimental diffusers and other experimental fluid machines. However, as noted in the previous chapter, there are many cases where the properties of the diffuser are affected by fluid dynamic conditions. Therefore, precise studies are necessary. The same pertains to measurement devices. The use of gauges has an effect on measurement accuracy and diffuser properties.

In this chapter, we will review experimental devices and measurement methods for diffusers and special subjects will be mentioned in Chapters 5 and 6.

#### 4.1 Experimental device and model structure

##### (1) General pipe diffuser

The fluid hydraulic properties when the flow consists of a body (for instance, construction) and air resistance (pressure) are measured using devices inside the small models. However, diffusers are flow paths (problem of internal treatment) and therefore the experimental model for testing diffusers is different. The basic structure of a wind tunnel was shown in Figure 1.2 of Chapter 1. The position of the structural section is used in diffuser models also.

Air source (fan) → deacceleration section (diffuser) → regulation section → acceleration section (nozzle) → model (test diffuser). That is, there are many changes and the distribution is made so that the flow is uniform.



two acrylic resin plates. This is the acceleration section (in this model, the relaxation calculations in Chapter 2 were also used).

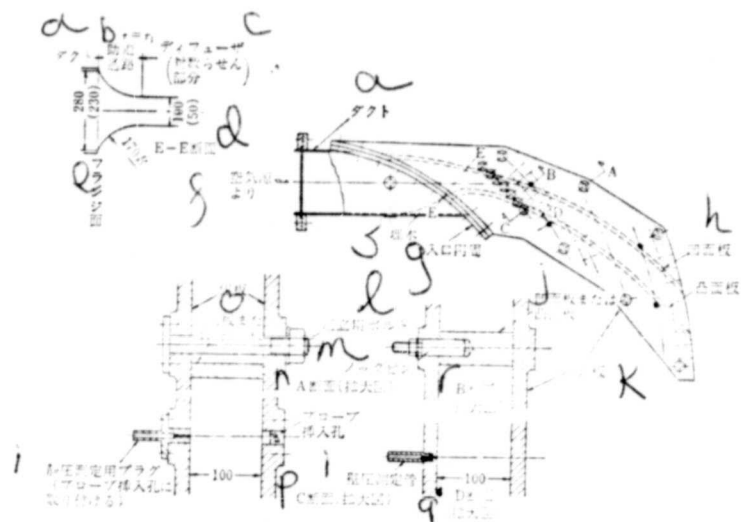


Figure 4.2. Model of diffuser flow paths (large model)

a--duct; b--auxiliary path; c--diffuser (spirals); d--E-E cross section; e--flange; f--from air source; g--inlet periphery; h--concave plate; i--convex plate; i--static pressure determination flux (attached to plug insertion hole); j--convex or concave plate; k--side plates; l--assembly bolts; m--socket pin; n--A Section (enlarged); o--wall pressure pipe; p--C Section (enlarged); q--D Section (enlarged); r--B Section (enlarged) prop insertion hole; s--support

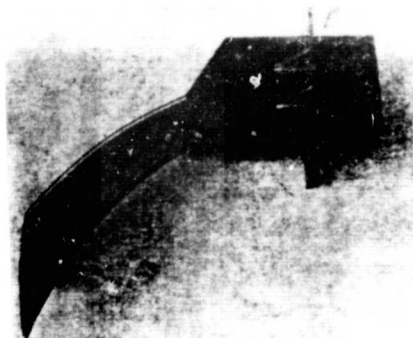


Figure 4.3. Diffuser flow path model (small model)

ORIGINAL PAGE  
BLACK AND WHITE PHOTOGRAPH



The model of the diffuser is used to accurately determine the proper form. The size of the static pressure determination hole is not as large as necessary (diameter of 1 mm is suitable for manometers). Moreover, the top (mentioned later) insertion hole should be made so that the flow path surface is as smooth as possible.

(2) Centrifugal diffuser (case of partial fluid machine)

The static pressure determination hole is made in the /76  
structural component of diffusers used for centrifugal compressors and fans, and the hole may have a prop (flow determination gauge). Then experiments can be carried out. Figure 1.3(b) in Chapter 1 is an example. Moreover, when measurements of total properties of the entire fluid machine are performed, the diffuser results are determined as a whole. However, in order to determine the individual properties of the diffuser, it is necessary to determine static pressure and fluid hydraulic properties as well as rational properties of the entire unit.

For instance, even with single stage compressors, the casing is attached to the outlet and loss of symmetry of the flow (in peripheral direction) is prevented\*. Next, we will explain an example of a designed device.

Figure 4.4 is a device used in the studies of Senoo [9]. The outlet of the diffuser is open. Figure 4.5 is an example of the experimental device used by the authors [10]. This is a diffuser used in single stage fans and the outlet of the guide flow path is axially symmetric.

---

\* The spiral casing is set up so that distribution is even. However, nonuniformity is marked in other design flows.

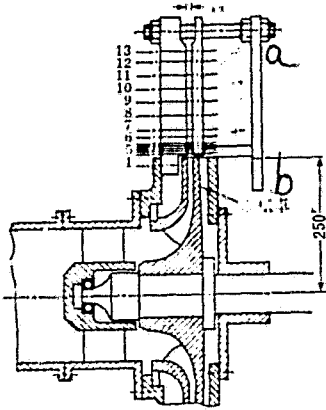


Figure 4.4. Bladeless diffuser model (1)  
a--diffuser; b--runner

from the runner is not uniform in the flow path width direction (shear flow) and there are changes over time with the passage through the runner. Moreover, the inlet flow of the diffuser should be uniform over time and space. As is seen in experiments and bladed wind tunnels [11], the swirl flow must be produced by the device (round blade wind tunnel). Various tests have been carried out.

Figure 4.6 is the experimental device of Jansen [12]. Here the rotation screen (net) is used to make the flow swirl. Moreover, a boundary layer emission device is used and, therefore, the boundary layer flow and two-dimensional flow can be produced. However, it is felt that a great deal of expertise is necessary to actually realize this type of flow. Figures 4.7 and 4.8 [13] show the two devices for swirl flow used by the authors to test bladed diffusers. The device 1 in Figure 4.7 and device 2 in Figure 4.8 both can produce a stable flow. However, the flows are not sufficiently uniform in the direction of flow path width\*.

\* There is a three-dimensional flow with these devices (including axial flow and radial flow) and it is therefore difficult to produce a uniform swirl flow in the direction of flow path width.

The test diffuser (models) used in these tests is the same as in (c). Therefore, the reader should refer to (3).

(3) Centrifugation diffuser  
(model tests)

The centrifugation defuser is set up directly behind the runner. Therefore, it is actually combined with the runner. There are many examples of experimental devices. However, the flow

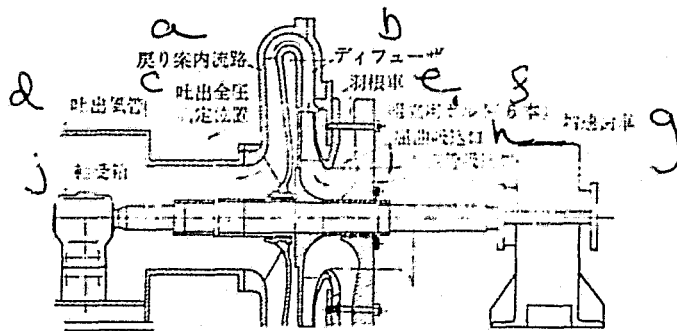


Figure 4.5. Centrifugation fan used in flow path tests. a--guide path; b--diffuser; c--emission pipes; d--emission pressure measurement position; e--runners; f--assembly bolts (6); g--acceleration gears; h--outlet; i--inlet j--bearing case

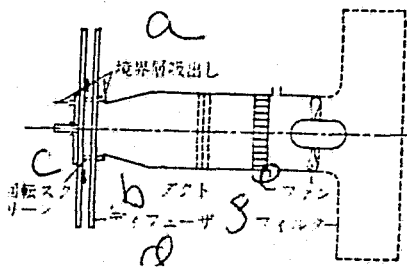


Figure 4.6. Bladeless diffuser test device (2) a--boundary layer emission; b--rotation screen; c--duct; d--diffuser; e--fan; f--filter

When devices 1 and 2 are compared, it appears that the former makes tests within a low flow angle possible and that device 2 has a very small radial width distance between the guides and test diffuser. However, the angle of flow is small (approximately  $10^\circ$ ) and therefore the distance to be measured in the flow line direction is long, which has detrimental effects on the guides and blades. /78

Figure 4.9 is the device used by Feirereisen [14] in tests on bladeless diffusers (no swirl). It has a flow that rotates in a radial direction from the two directions of the axis. Therefore, a symmetric flow is obtained in the direction of width.

Figures 4.10 and 4.11 show the diffuser models made by the authors [13,15]. Figure 4.10(1) is the thin plate diffuser for centrifugation compressors (fans) and (b) is the same thick blade

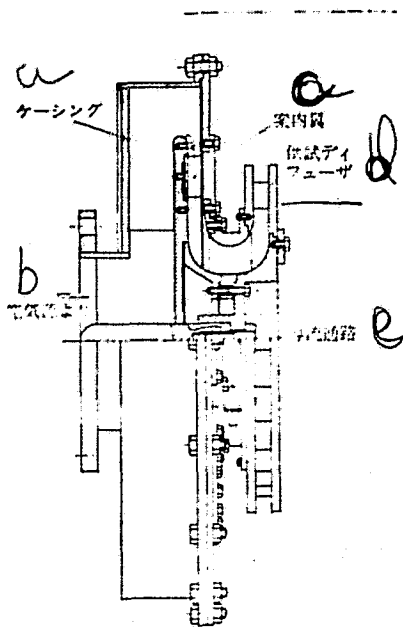


Figure 4.7. Bladed diffuser test device (1)  
 a--casing; b--air source;  
 c--guides; d--test diffuser; e--flow path

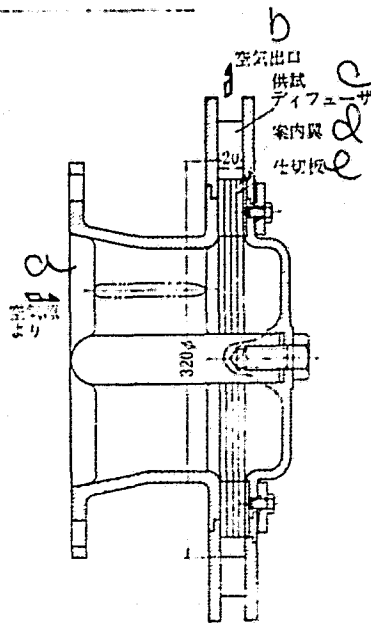


Figure 4.8. Bladed diffuser test device (2)  
 a--from air source; b--air outlet; c--sample diffuser; d--guide; e--plate

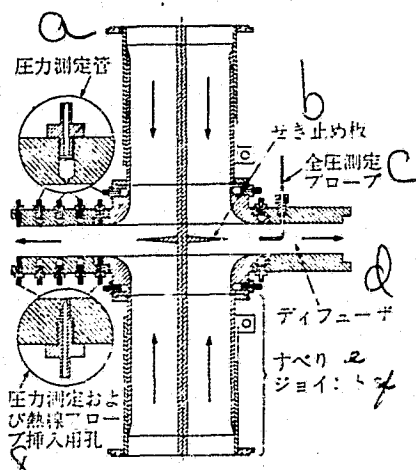


Figure 4.9. Bladeless diffuser test device (3)  
 a--pressure measurement pipe; b--suspension plate; c--total pressure measurement probe; e--diffuser; f--joint; g--pressure measurements and heat flow probe insertion hole

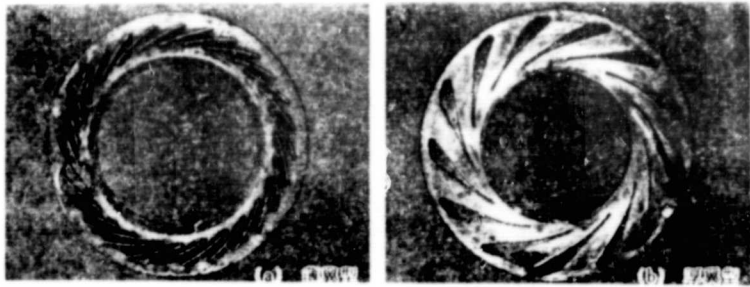


Figure 4.10. Diffuser models used in compressors (fans).  
a--thin blade; b--thick blade

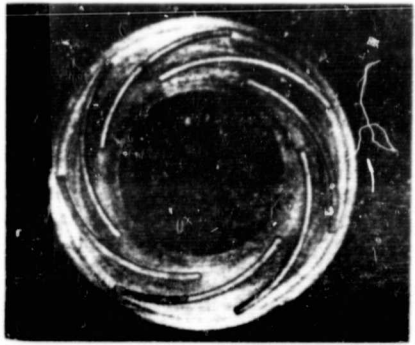


Figure 4.11. Diffuser model of centrifugation pump

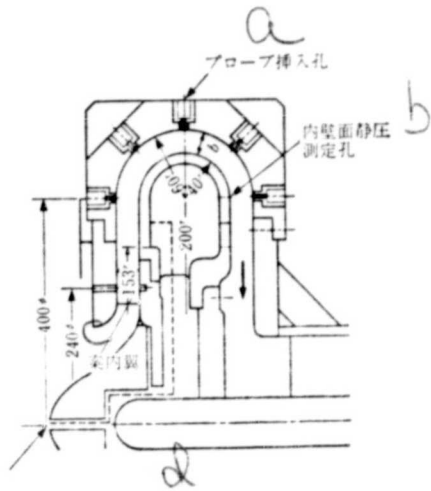


Figure 4.12. Deflected flow path model  
a--probe insertion; b--static pressure measurement hole;  
c--guide blades; d--static pressure pipe outlet

diffuser (low relative velocity). Moreover, a diffuser for pumps is shown in Figure 4.11. There are differences between compressor diffusers and pump diffusers (the same differences are seen with runners). The reason for this is given below.

ORIGINAL PAGE  
BLACK AND WHITE PHOTOGRAPH

(a) Pumps require a stable operation at a total flow range. Therefore, they are designed with a low flow coefficient. The blade inlet angle is small. Therefore, the angle of spiralling toward the center of round blades is long and few blades are used.

(b) The blades in compressors are often made of thin plates (welded, etc.). Because of the fact that fluid power is strong with pumps, they are generally made from thick plates. This fact is a factor in the differences seen between the diffusers.

Figure 4.12 is a model test device pertaining to the deflected flow path set up between the diffuser and guide paths. It was taken from Oshibo, et al., [16]. This device does not use runners and is made so that a swirl is produced from the guide blades. The entire emitted flow is measured.

The centrifugation diffuser models do not vary in properties from the case of pipe diffusers. However, in comparison /80 to the latter, the size of one flow path is usually small and the dimensions and form (particularly no variations in each flow path) are critical. The positions of pressure measuring holes on the surface of the blades are difficult to set. However, the same method as used for the bladed wind tunnel can be used (large introduction pipes along grooves in the blade surface (stainless steel, copper, etc.) so that the holes are of a small diameter and penetrate the blade surface. The pipes are made so that they span the blade being studied. The same is true with regard to static pressure measurement holes and probe insertion holes. The guides on the up current side and the guide blades on the down current side should be studied for a peripheral direction correlation. Moreover, variations (adjustments) may be necessary within the angle range of the diffuser.

#### 4.2 Measurement gauges and methods

/81

(1) It is necessary to determine the properties of the diffuser (efficiency and loss coefficient) as a whole and measurements of static pressure and the inlet and outlet and flow should be made. The dimensions and forms of the diffuser were previously mentioned and, therefore, the calculations can be made using equations (3.56)-(3.58). At the same time, it is possible to do the same thing for centrifugation bladed diffusers. Moreover, the total properties of the fluid machine (pressure and head, flow, driving power, total efficiency) can be determined by conventional methods. The state of the flow inside the fluid machine will be mentioned in detail, and when it is necessary to obtain data on improvement of properties, it will be necessary to determine the distribution of pressure, flow, velocity, flow angles, etc., and make measurements possible. This text reviews the necessary devices and gauges.

JIS B 8330 (method for fans) and JIS B 8340 (method for turbopower and compressors) is used [17]. The measurements of flow are made using a pitot tube, nozzle, orifice, etc., set up so that there is a direct connection (measurement pipe (with the emission side and inlet side)\*. The orifices and nozzles (Figures 4.13 and 4.14 [18]) are plates in which holes have been made in circles. The device has a narrow flow path area so that measurement pipes are inserted in a circle. By determining the pressure difference  $\Delta p$ , it is possible to obtain the flow  $Q$  (mass flow  $G$ ) (refer to equations (4.1) and (4.2)--here  $d$  is the diameter of the orifice or nozzle hole,  $\rho$  is the density of the fluid,  $\alpha$  is the flow coefficient and  $\epsilon$  is the compressible coefficient of the gas).

$$Q = \frac{\pi}{4} d^2 \alpha \epsilon \sqrt{\frac{2 \Delta p}{\rho}} \dots\dots\dots (4.1)$$

$$G = \frac{\pi}{4} d^2 \alpha \epsilon \sqrt{2 \Delta p \cdot \rho} \dots\dots\dots (4.2)$$

---

\* In the case of pumps, the open water surface may be used and a weir is employed.

The measurements of flow are simplified by using Pitot tubes. However, the Reynolds number  $Re = \frac{UD}{\nu}$  represented by the diameter  $D$  of the measurement pipe, the mean velocity inside the pipe  $U$  and the kinematic viscosity coefficient  $\nu$  is larger than within a constant range (Figure 4.5 [18] shows the orifice). When the velocity is low, the pressure difference is not suitable. Moreover, part of the pressure difference that is produced is the total pressure loss and cannot be recovered. It is therefore necessary to use excess air at a certain pressure (the pressure difference and loss are lower with a constant flow and hole diameter of a nozzle when orifices and nozzles are compared. The manufacture of orifices is less expensive).

/82

The measurement of a flow by standard Pitot tubes (Figure 4.16 [19]) is often carried out with a low velocity and large flow path width. However, there are also cases when there are many measurement points in the measurement tubes and there is therefore a disadvantage in that the difference is large as time proceeds. When a diffuser model device is used, the measurements should be made with orifices and nozzles.

Measurements of pressure differences, such as those seen in flow measurements with orifices, etc., are commonly carried out by a manometer (water or mercury is used with U-shaped column or the Gottingen method is employed). Furthermore, JIS has set no special regulations. However, a gauge for dynamic measurements (mentioned later) is being developed. The pressure is represented by an analog (or dial) or a digital system. This will make measurements of fluid machines easier.

/84

In general tests on compressors, it is necessary to measure the temperature of the gas, driving power (inlet of compressor or output of motor) and the r.p.m. Thermometers may be used for temperature and are set up in the low velocity side. When the velocity is high, however, it is necessary to use a total temperature device similar to the total pressure probe.





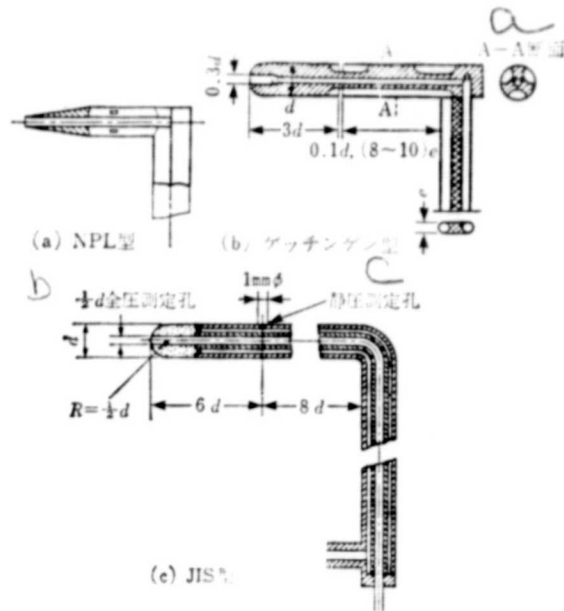


Figure 4.16. Standard Pitot tube  
 (a) NPL model (b) Getchigen model (c) JIS model;  
 a--A-A cross section; b-- $1/2d$  total pressure measurement hole;  
 c--static pressure measurement hole

It is not necessary to measure the r.p.m. and force in tests on model diffusers. Therefore, flow, pressure and temperature are used as mentioned above.

In addition, although there are no conventional regulations with regard to these tests, there are typical and mean values that have been set for the positions of the pressure hole, etc. Therefore, tests should be carried out on the values for the inlet and outlet values.

(2) Internal flow (static measurements)

/85

The flow condition of flow paths is determined by determining the distribution of the static pressure, total pressure, flow angle, velocity, etc. This data is tested with the diffuser design values and it is important that future design studies be carried out. Measurement gauges for static flows (constant

flows) will be described (this is limited to a low velocity and ultrasonic velocity is omitted).

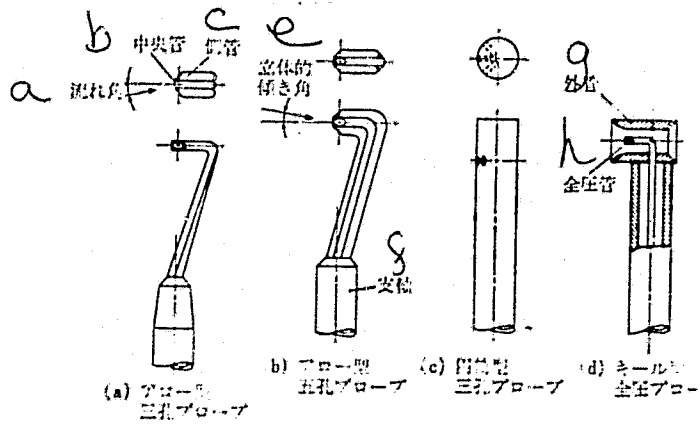


Figure 4.17. Each type of probe for internal flow measurement.  
 (a) arrow probe (b) 5-hole probe) (c) cylindrical probe  
 (d) total pressure probe

a--flow angle; b--central pipe; c--side pipe; e--angle;  
 f--bearing; g--outer pipe; h--total pressure pipe

Figure 4.16 shows the standard Pitot tubes. The direction of the flow is determined and the maximum pressure is obtained. However, in order to determine the direction of the flow, further studies are necessary. In addition, the flow may be disrupted and special probes must therefore be used. Figure 4.17 (a)-(d) shows photographs of each device. The photos show the probes combined with devices and probes are all set up so that they rotate around the center axis of the cylinder.

The arrow probe in Figure (a) is made from two side pipes around one center pipe and is used so that when the probe rotates, the probe is adjusted to the flow direction to determine the flow angle. Moreover, the central pipe values are equal to the total pressure (dynamic or static pressure are previously determined in wind tunnels and the probe readings are used to determine the flow angle). The probe may be perpendicular to the bearing so that the flow can be detected. Moreover, it can also be used in two-dimensional determinations of

velocity inside the boundary film [20].

The five-hole probe in Figure (b) is made so that 4-sided pipes are attached to the center pipe. By means of this probe, it is possible to make three-dimensional measurements of the flow. That is, the angle of the flow in a perpendicular direction can be determined. The probe may also be used so that it is slanted. The effect of the angle of inclination can be determined in a wind tunnel, making three-dimensional measurements possible. This probe is larger than that in (a) and may interfere with the flow. The stainless steel or copper pipes in (a) and (b) have a diameter of 1 mm and can be as thick as 0.6 mm. However, the form is difficult to make and response of pressure is poor. The five-hole probe is made in circular form also.

The cylindrical probe in (c) is set up so that there are three holes in the surface of the cylinder. It is used as in Figure (a). The end is relatively large and may affect the flow. The velocity of the flow in a perpendicular direction can be determined with a three-dimensional flow and it is, therefore, possible to determine a more precise flow distribution than with that in Figure (a). The probe in Figure (d) is made from outer pipes around a thin pressure pipe and is used for determinations of total pressure. That is, it is possible to determine the angle of the flow up to  $60^\circ$ , and obtain an accurate value without any flow separation [21]. Therefore, it is very practical. Moreover, the probes shown in the figures and photos have an inner pipe diameter of 5 mm and can be as small as 3 mm in diameter.

As was previously mentioned, there are many types of probes that range from simple to very complex, and various tests are

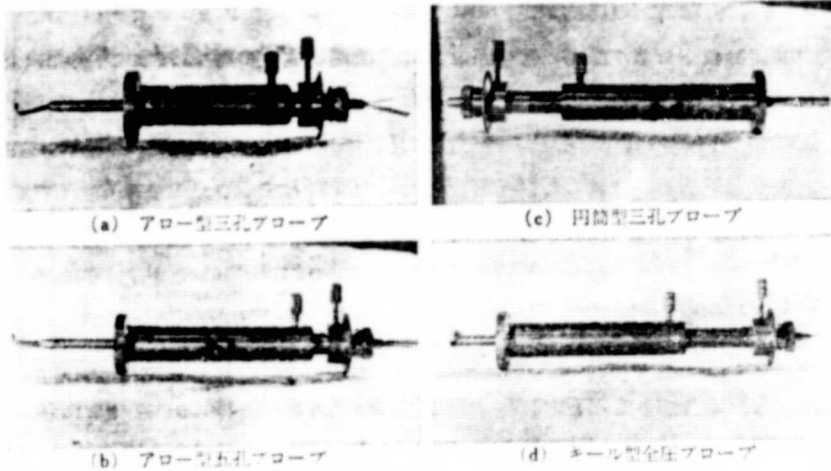


Figure 4.18. Outside of measurement probes  
 (a) arrow probe (b) 5-hole probe (c) cylindrical probe  
 (d) total pressure probe

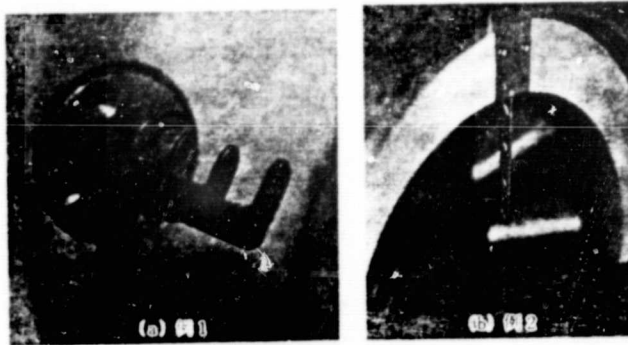


Figure 4.19. Teeth probe  
 (a) Example 1 (b) Example 2

ORIGINAL PAGE IS  
 OF POOR QUALITY

now being carried out. For instance, NACA (NASA)\* has been studying composite probes for measurements in compressors and turbines [22]. In addition, tests are also being carried out on probes that have several connections for large flow paths [17], guide path flow areas [23], etc. (Figure 4.19).

The flow path of a diffuser is usually small and unstable. Therefore, changes in flows should be determined because they

\* National Advisory Committee for Aeronautics and National Aeronautics and Space Administration.

are one cause of separation, swirl loss, etc.\*. This is res- /88  
tricted to the case where probes can be inserted and it is still  
difficult to carry out. It is therefore necessary to make sure  
that the probes have no detrimental effects.

(3) Internal swirl (dynamic measurements [24,28])

The diffuser is considered to be a device that gives a  
static flow and there are also flows that have abnormal separa-  
tion and lost velocity. There are many cases where an abnormal  
flow passes through the outlet, annular diffuser, bladed  
diffuser, etc. Therefore, in order to determine the cause of  
this flow, it is necessary to devise a gauge for measuring  
dynamic changes. Recent progress has been made in semiconductor  
technology and electronics.

The heat line velocity gauge is developed for measurements  
of changing velocity [29]. It is now being used. However,  
further improvements have been made and new devices are being  
developed. The heat flow velocity gauge is used by insertion  
in the current to be measured and obtaining the current value.  
Then variations in temperature and resistance with the flow  
current are read and the flow current is determined (constant  
current type).

Moreover, the temperature of the heat line changes with the  
current and the velocity can be determined from the current value  
(constant temperature type). The former method has little delay  
due to the volume of heat in the flow line and response is good.  
Therefore, measurements of changes in frequency of 100 kHz are

\* Swirl loss is the phenomenon where the lost velocity produced  
in the path moves the blades. There is also the phenomenon  
where the flow of the machine changes. These both cause  
separation and a reduction in inertia.

possible [28]. Moreover, the heat line is determined from the perpendicular velocity component and consequently the angle of the flow can be determined from two or more lines (Figure 4.20, two-dimensional measurement [30]). In addition, three-dimensional measurements with three or more lines are being carried out [25]. The heat line measurements are relatively simple and there is little obstruction due to flow. However, treatment for low strength is necessary. The head flow gauge (heat line and current sections) are used industrially and are very convenient.

Metallic and non-metallic films may be used in pressure determinations [27]. The pressure detection section (receiving section) can determine changes in pressure. This thin film has holes in the flow path curve and is used so that it extends along one surface [31]. Moreover, it can also be used as the probes listed in section (2).

Matsui, et al., [32] have developed a changing current probe (water currents). This is made from holes in pressure plates (pressure holes) and is constructed so that the air passes to the pressure converter (converts changes in the film to electricity (possible to measure changes of up to 100 Hz.

Furthermore, in tests on compressors, etc., it is possible to measure the changing pressure up to several 1000's of Hz (frequency of runner at several 10,000's of rpms) [28,31].

In addition to probes penetrating the flow, it is also possible to use laser Doppler gauges [33,38] (called LDV). These use the light reflected by particles in the flow and measure the velocity from changes in frequency (Doppler shift)\*. The fluid machines can be used with the method in which laser rays irradiated in the flow are reflected to the light source side. However, there are problems with output of the light source. The two-focus LDV recently developed uses two beams of laser light, so that the focus is connected at two points in the flow path and the output of the light source can be reduced [28,34].

/90

(4) Visible method [35,40]

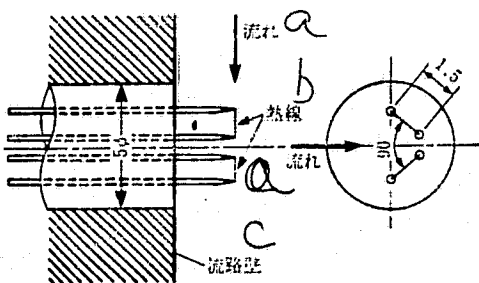


Figure 4.20. Heat line velocity gauge  
a--flow; b--heat line;  
c--flow

The flow of a fluid cannot be directly observed with liquids or gases. The visible method involves local and qualitative observation of the flow as a technological approach\*\*. Moreover, several types of techniques have been developed and are being studied.

There are many types and explanations of visible methods. We will explain the categories listed in the reference [38] (refer to 4.1). These methods all involve typical explanations as detailed explanations are impossible.

/91

\* The Doppler shift effect represents changes in apparent frequency of vibration produced by the object (high when the object is near, and low when the object is distant).

\*\* Qualitative indicates that a method for qualitative determinations is being used.



The oil film method (one type of wall trace method in Figure 4.1) involves the application of oil to the surface of the flow path and then tracing of the flow line along the walls. The condition of the flow inside the boundary film near the walls is recorded.

The surface of the flow path is connected to a light yarn, such as a metal probe in the Taft method and the flow is traced by movements in the yarn (mainly gases). It is necessary to use a very light yarn in this method.

Figure 4.21 shows the Taft method used in two-dimensional /92 designs by Ychishoku, et al., [41]. When the angle is large, peeling occurs on the flow path wall side.

The tracer method involves use of a substance different from the sample, such as a gas, liquid or solid, in the flow (tracer). This is mainly added by injection or production. The flow can then be observed. Of these methods, the direction injection method is the method where a tracer is injected directly. The substance that is injected may be ash, vapor or solid powder when the sample is air, or liquid particles (drops, colored liquid, bubbles, etc.) when the sample is water.

Moreover, when the sample is a liquid, the open water surface is used. The solid powder is floated on the surface and acts as a tracer. Figure 4.22 is the case where a colored liquid is injected to the runner (water test) and an image of the flow is obtained\*.

---

\* The fluid particles flowing from one point are called flow that curves instantly in a certain space (seen with dust). The fluid orbit is the orbit where the particles flow in the fluid. The flow usually shows the same flow line and flow orbit.

TABLE 4.1 VISIBLE METHODS

Visible Method	gas	water	Explanation
wall tracer method	○	○	Flow direction based on oil drop arrangement surface temp. using sensitive material flow direction with no electrodecomposition using electrodes
Taft method	○	○	Flow direction from short yarn (taft) direction Flow direction from tufts Direction of flow
Direct inj.	○	○	Tracer injection direction Intermittent tracer injection Perpendicular tracer injection Flow orbit, line with suspension of liquid flow particles Tracing flow on surface after tracer suspended in liquid
Tracer method	○	○	Boundary layer flow by reaction of fluid and substance Tracing of coloration tracer Time line with light emitting particle as tracer
Elec. Sup. methd.	○	○	Time line with hydrogen gas from decomposition as tracer Time line and orbit with discharge from high voltage puls. Time line from tracer on metallic wire with oil
Shadowgraph method Schlieren method Mac Sender method Laser holography Moare method Stereo method Fluid deviation method Thermography Presgel method	○	○	Density gradient changes (secondary density component) Fluid density changes (primary density component) Two-dimensional flow based on density using light interference 3-dimensional flow using density changes from interference Observation of changes in liquid surface " Velocity gradient of diffraction of flow with polymer solution Surface temperature determination with infrared rays Determination of pressure changes with color concentration

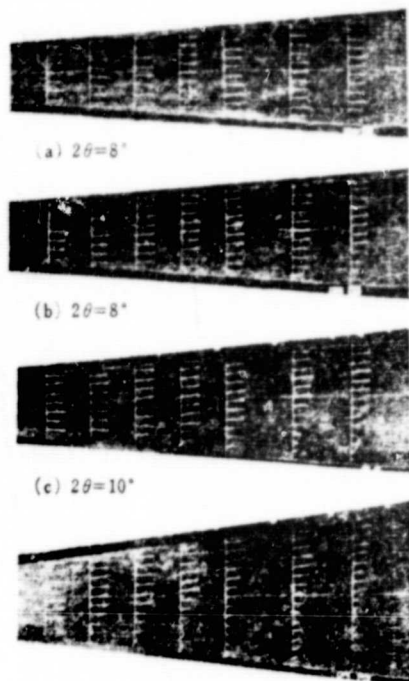


Figure 4.21. Observation of diffuser flow by Tuft method

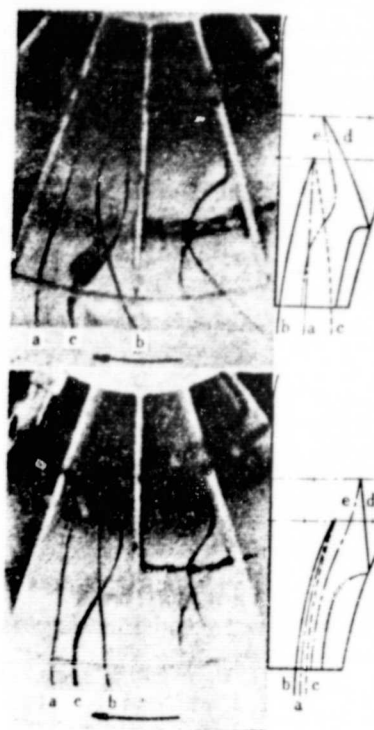
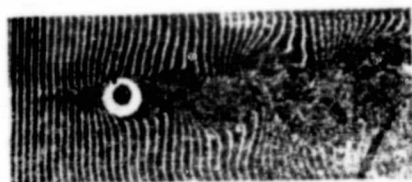


Figure 4.22. Observation of flow by colored water method

Kline, et al., [43] have studied two-dimensional diffusers and have made a map of the flow region (mentioned later). They used a colored liquid as the tracer and observed separation of the flow and transfer of the boundary layer. The electro-suppression method may be the hydrogen bubble method, smock wire method, etc. The production of the tracer can be electrically controlled and is, therefore, very useful for determinations of velocity, etc.

The hydrogen bubble method is the method whereby bubbles are produced in water by decomposition of the water. Figure 4.23 shows an example of the time line\* of a flow in a circle

\*The time line can be drawn for a certain flow using a tracer when the time and distance are known.



(a) タイムライン



(b) 流 線



(c) タイムラインと流線

Figure 4.23. Observation of flow by hydrogen bubble method.

(a)--time line; (b)--flow;  
(c)--time line and flow

by this method [39]. The tracing method involves the use of a light-emitting section by a high voltage that cuts the flow path with gases. Fister has used this method to draw a time line for a flow path between blades of centrifugal runners [38,44]. The Smock wire method involves using a tracer that produces vapor in oil applied to the surface of a metal wire to which a current is applied. /94

Optical determinations involve shadowgraphy. Schlieren method, Mach Sender interference, etc., methods that use measurements of the high speed velocity of turbine blades. Other methods have been developed.

With high velocities, there are marked changes in the density and the direction rate of the gas changes. Moreover, interference is produced due to changes when light passes through the flow. The above-mentioned three methods determine velocity of the flow using this principle. The Mach Sender interference method determines the changes in density, the Schlieren method determines changes in density (primary component) and the Shodagraph method determines the secondary component of density. Figure 4.24 is a photo [40,46] of a model of an axial flow turbine by the Mach Sender interference methods. Figure 3.25 is an illustration of part of the experimental compressors used for measurements of flow by the Schlieren method [47].

Furthermore, the device in 4.26 was developed by researchers who developed the device in 4.25 and has a reflection-type structure.



Figure 4.24. Measurement of turbine blade by Mach Sender interference.

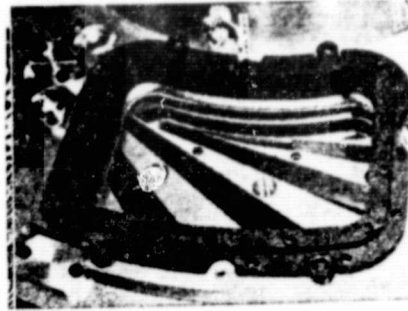


Figure 4.25. Measurement of diffuser by Schlieren method (1) (when viewed from the observation window)

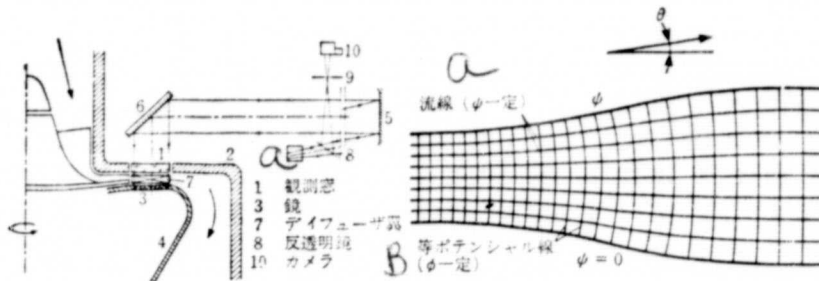


Figure 4.26. Determination of diffuser by Schlieren method (2) (measurement system)  
a--observation window,  
mirror, diffuser blade,  
reflection mirror,  
camera

Figure 4.27. Reverse (inverse) method for diffusers  
a--flow line ( $\psi$  constant)  
b--equipotential line ( $\phi$  constant)

### 4.3 Theoretical analysis

Calculations of the secondary diffuser form by the inverse method may be carried out in theoretical analyses of diffusers. /95 Stanits, et al., [49] have studied methods for determining flow path form by giving velocity above the center wire of the diffuser (Figure 4.17). The figure shows the intersection of potential lines and flow lines drawn on a diffuser flow path chart. The velocity is  $U$  and function of the flow is  $\psi$ . The velocity potential is  $\phi$  and the angle with regard to the center line ( $x$  axis) is  $\theta$ . The form  $(x,y)$  of the flow path walls is given by the following two equations (stream filament method) using the above-mentioned  $\phi$  and  $\psi$ . The velocity can be easily determined from the lattice  $\phi, \psi$ .

$$x = \int_{\phi} \frac{\cos \theta}{U} d\phi \dots\dots\dots (4.3)$$

$$y = \int_{\phi} \frac{\sin \theta}{U} d\phi \dots\dots\dots (4.4)$$

Yang, et al., [50] have studied calculations when the boundary layer has been emitted at the outlet using the above-mentioned methods and have shown that a large surface area ratio is obtained with a slender axis.

#### REFERENCES

- [1] For instance, Harada: Fluid Dynamics (1962).
- [2] Japan Mechanical Engineering Society: Mechanical Engineering Catalog (ed. 6) vol. 8, 5/1976.
- [3] Bofu (Murada and two other translators); Aerodynamic Tests on Mechanical Engineering (1970).
- [4] Sprenger, H.: Diss.\* Zurich, No. 2803 (1959).
- [5] Ui, Nippon Kikai Gakkaishi, 9-4, 211 (4-71).\*\*
- [6] Keni and Ko Mura: Turbomechanics 9-4, p. 211 4/71).
- [7] Tanaka: Research on Machines 23-1, p. 247 (4.71).

/96

- [8] Shimaya and Kagimoto: Turbomechanics 4-10, p. 645 (11.76)
- [9] Senoo, Y., Ishida, M.: Proceedings, the 2nd International JSME\*\*\* Symposium, Fluid Machinery and Fluids, Tokyo, p. 61 (1972-9).
- [10] Sugii: Kiron 32-237, p. 734, 5/66.
- [11] Herrig, L. J., et al.: NACA RM L51G31.
- [12] Jensen, W.: Trans. ASME (J. of Basic Eng.) p. 607 (1964-9).
- [13] Sugii: Kienshu no. 179, p. 153 (10/67).
- [14] Feiereisen, W. J., et al.: same as [9], p. 81.
- [15] Sakurai, T.: Trans. ASME (J. of Eng. for Power), p. 388, (197507).
- [16] Okubo and three others: Kikoron . (Proceedings, the 15th Thesis Presentation), p. 149, 1976-8.
- [17] Oyama Japan Society of Mechanical Engineers (525), p. 145 (7/80)
- [18] same as [1], p. 165
- [19] same as [2], p. 35
- [20] Sakurai: Kiron 36-29, p. 1886 11/70.
- [21] MIT: Pressure Measurements (MIT publication).
- [22] Schulze, et al.: NACA TN 2830 (1952).
- [23] Sakurai; Kienron (Hitachi Conventional, p. 24 (11/65).
- [24] Matsuki: Kienshu (525), p. 1 7/80.
- [25] Matsuki: Turbomechanics 9-12, p. 709 12/81.
- [26] Matsuki: Turbomechanics 10-1, p. 47 (1/82).
- [27] Shomiya: Turbomechanics 4-9, p. 551 (10/76)
- [28] Shimo: same as above, p. 546
- [29] for instance, Schubauer, G. B.: NACA Rep. No. 524 (1935).
- [30] Senoo, Y., Ishida, M.: ASME publication, Paper No. 74-GT-64 (1974-4).

- [31] Eckardt, D.: ASME publication, Paper No. 74-GT-90 (1974-4).
- [32] Matsui: Turbomechanics 4-9, p. 558 (10/76).
- [33] same as [2], p. 36
- [34] Schodl, R.: ASME publication, 74-GT-157 (1974-4).
- [35] same as [2], p. 42.
- [36] Iji (ed.) Flow Visualization Handbook (1977).
- [37] Turbomechanics Association: Turbo Machines (Visualization of Flows) 3-3 5/1975.
- [38] Nakayama: Kienshu (312), p. 43 2/67.
- [39] Nakayama: Kienshu (525) 37 7/80. /97
- [40] Akirashi: Turbomechanics 8-5 p. 290, 5/80.
- [41] Kimura, et al.: Kienron (290 Convention), p. 95 (8/68).
- [42] Imo: Kienron, 153, p. 199 (4/66).
- [43] Kline, S. J., Rumstadler, P. W. Trans. ASME (J. of Appl. Mech.), p. 166 (1956-6).
- [44] Fister, W.P BWK 18-9, p. 425 (1966).
- [45] Aerodynamic Engineering Association: Aerodynamic Engineering Handbook) p. 50 (Corona, 1955)
- [46] Iayam, et al.: Mitsubishi Heavy Industries Technological Report (p. 1) 3/1978
- [47] Philbert, M., Fertin, G.: ASME publication, Paper No. 74-GT-49 (1974-4).
- [48] Ribaud, Y., Avram, P.: Paper presented at the 2nd International Symposium on Air Breathing Engines, Sheffield (1974-3).
- [49] Stanitz, J. D.: Trans. ASME, No. 75, p. 1241 (1953-10).
- [50] Yang, T. T., Hudson, W. G.: ASME publication, 72-WA/GT-6 (1972-11).

- 
- \* Diss. Abbreviation of Dissertation
- \*\* Kishi: Abbreviation of Japan Society of Mechanical Engineers and Journal
- \*\*\* JSME: Abbreviation of Japan Society of Mechanical Engineers
- \*\*\*\* Kikokyo: Abbreviation of Japan Society of Mechanical Engineers Study Material.



## GENERAL PIPE-TYPE DIFFUSER PROPERTIES

Pipe diffusers are usually conical and two-dimensional. However, there are other types and the properties vary with the application conditions (inlet pipes and capillaries, inlet flow velocity distribution, boundary layer, etc.). The forms and flow dynamics have been studied to a great extent and there are few cases of convenient general computations and diagrams at the present time. Therefore, we will make an effort to study the properties of these diffusers in the future from the aspect of effects of various variables on their performance.

This chapter and Chapter 6 deal with data obtained based on the above-mentioned facts. We will attempt a physical explanation whenever possible. We hope to obtain some understanding of the diffuser problems from this discussion.

5.1. Conical diffusers

Conical diffusers are basic diffusers. They have been studied theoretically and experimentally, and their properties should be explained. The problems with these diffusers appear to be related to the formation of boundary layers with a large axially symmetric flow.

(1) Overall properties

The variables that determine the form of the conical diffuser are the three variables of length ratio  $l/r_1$  (length is  $l$  and inlet radius is  $r_1$ ), width angle  $2\theta$  and surface ratio  $A_r$  (two of these are used for individual cases). Depending on the case, the individual variable may differ and, therefore, a chart showing the correlation is given in Figure 5.1. Moreover, these correlation equations are shown in 5.1.

$$A_r = \left(1 + \frac{1}{r_1} \tan \theta\right)^2 \dots \dots \quad (5.1)$$

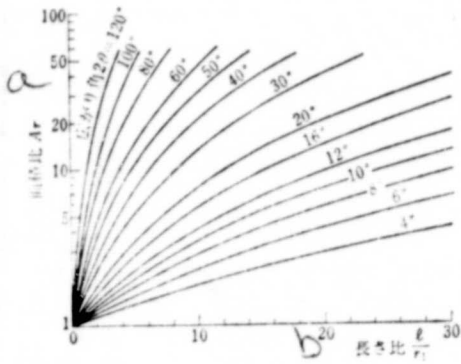


Figure 5.1. Angle of conical diffuser and correlation with length ratio and area ratio. a--area ratio; b--length ratio

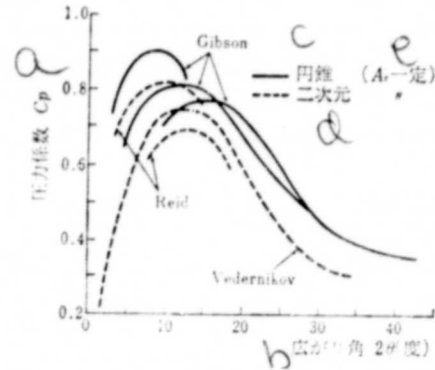


Figure 5.2. Correlation between angle and pressure coefficient. a--pressure coefficient  $C_p$ ; b--angle  $2\theta$  (degrees); c--conical; d--two-dimensional; e-- $A_r$  is constant

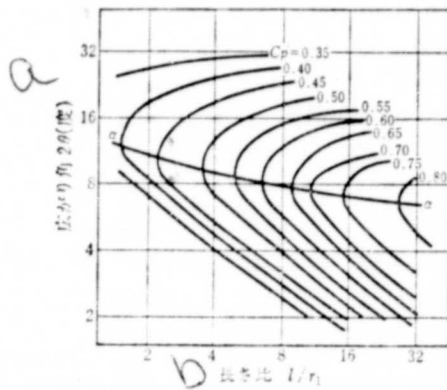


Figure 5.3. Form and pressure coefficient of conical diffuser. a--wide angle  $2\theta$  (degs.) b--length ratio  $l/r_1$

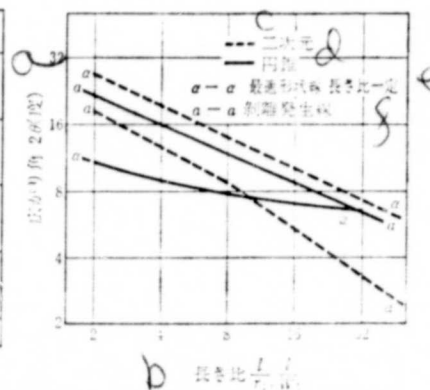


Figure 5.4. Separation and optimum form of two-dimensional and conical diffusers: a--side angle  $2\theta$  (degs.); b--length ratio  $\frac{l}{r_1} \frac{l}{w_1}$ ; c--two-dimensional; d--conical; e-- $\alpha$ - $\alpha$  optimum form length ratio constant; f--a-a separation curve

Conical diffusers are known to have a higher efficiency than angular diffusers or two-dimensional diffusers with the same surface area ratio. Figure 5.2 shows the comparison as the correlation between the wide angle  $2\theta$  and pressure coefficient  $C_p$  (taken from Kline, et al., [1]). The cross section is round and the length of the periphery is minimum with the same flow path cross section. In contrast with other diffusers, the periphery length is larger and a secondary flow is produced and loss occurs. (However, in two-dimensional tests, the effects of depth of the path were noted and, therefore, it is difficult to compare conical and two-dimensional diffusers from this aspect).

The above-mentioned graph of Kline was used by McDonald and Fox [2]. They adjusted the experimental results for conical and two-dimensional diffusers and placed the  $\frac{l}{W_1}$  or  $\frac{l}{r_1}$  ( $W_1$  is the inlet width of two-dimensional diffusers) on the axis of abscissas and the wide angle  $2\theta$  on the axis of the ordinates for these two types of diffusers to study the efficiency and pressure coefficient. The properties of the diffusers were then statistically discussed\*. Moreover, the results of studies on conical diffusers are shown in Figures 5.3 and 5.4. Figure 5.3 places the  $\frac{l}{r_1}$  and  $2\theta$  on the ordinate axis and shows that there is a curve for the pressure coefficient within this plane. When this pressure coefficient  $C_p$  is at a maximum, the curve  $\alpha-\alpha$  is obtained. When the wide angle is maximum, it is within a range of  $12-7^\circ$  and is smaller than the data of the BHRA in Chapter 3 (approximately  $12^\circ$ ).

---

\* When the wide angle is small, the flow path expansion rate is two fold that of two-dimensional diffusers with conical diffusers at the same angle and same length (equations (5.1) and (5.2)). Therefore,  $\frac{l}{W_1}$  and  $\frac{l}{r_1}$  can be used. However, in this case, the surface area ratio is large and this correspondence is sometimes inaccurate.

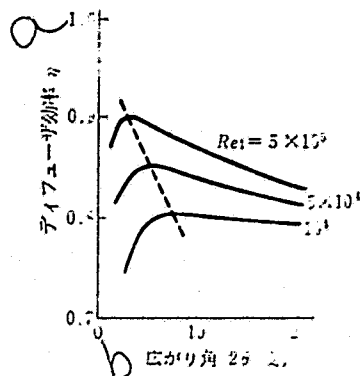


Figure 5.5. Inlet Reynolds' number, angle and efficiency (conical) a--diffuser efficiency  $\eta$ ; b--angle  $2\theta$  (degrees)

Moreover, Figure 5.4 also shows the conditions (a-a curve) noted when peeling occurs in the diffuser. Furthermore, the  $\alpha$ - $\alpha$  curve and a-a curve are recorded with broken lines for two-dimensional diffusers. The  $\alpha$ - $\alpha$  curve ( $C_p$  maximum form) with regard to conical diffusers is also the curve that falls to the lower right, as in the case of two-dimensional diffusers and the gradient is less than in the case of two-dimensional diffusers. When the length ratio ( $l/W, l/r_1$ ) is small and the wide angle is large, the area of the conical diffuser is greater than that of two-dimensional diffusers. Moreover, the angle

is limited. Furthermore, the angle during separation is lower than that with the maximum pressure and in two-dimensional diffusers, the opposite tendency is seen.

## (2) Theoretical calculations

Furuya [3,4] improved the calculation theory for conventional disrupted flow boundary layer (refer to Chapter 2, Gruschwitz and Buri) and introduced a method where separation of the boundary layer is determined. When used for the flow of conical diffusers, the main velocity  $U$ , thickness of the layer  $\theta$ , and form coefficient  $H$  are consecutively solved and then H.1.8 is made the peeling conditions ( $H = 1.4$  with flows that have not been deaccelerated above a plate).

Figure 5.5 is the theoretical calculations for conical diffusers obtained by Schlichting and Gersten [5]. When the area ratio is 1.4, the inlet Reynolds number ( $Re_1 (= U_1 D_1 / \nu, U_1$ : is the inlet mean velocity,  $D_1$  is the inlet diameter, and  $\nu$  is the viscosity coefficient) and the angle  $2\theta$  shows a correlation with efficiency  $\eta$ .

Therefore, when the  $Re_1$  is high,  $\eta$  is large and the maximum angle  $2\theta$  (optimum curve) is low. When  $2\theta$  is small,  $Re_1$  changes and  $\eta$  changes to a large extent. The experimental data is not compared directly in Figure 5.5. However, this tendency is seen in the experiments of Squire [6]  $A_r=4, 2\theta=4\sim 10^\circ$ .

### (3) Angular diffusers

The flow of angular diffusers is similar to that of conical diffusers when the diffuser has many sides. However, there are few research examples. Patterson has given the results for diffusers (surface area ratio of 4, according to Gibson) and considers  $2\theta = 6$  degrees as the optimum wide angle. However, the optimum angle in the tests of Satki [7] was 6 degrees.

/103

## 5.2 Two-dimensional diffusers

### (1) Overall properties and flows

Two-dimensional diffusers are diffusers that have a constant flow path depth and are made so that two planes form the expansion angle. The variables that determine the shape of these diffusers are the same as in the case of conical diffusers and area length ratio  $l/W_1$ , wide angle  $2\theta$  and surface area ratio  $A_r$  (of these two may be used in individual case). Their correlation is shown in Figure 5.6. These correlations can be represented by the following equation:

$$A_r = 1 + \frac{2l}{W_1} \tan \theta \dots\dots\dots (5.2)$$

In the 1950's, Saiki [7] studied various diffusers and used an area ratio of 1.5-4 and angle of 5-30 degrees for two-dimensional diffusers. He noted that there was an increase in efficiency when the optimum angle moved to the small side (15 degrees to 8 degrees) with an increase in the surface area ratio (Figure 5.7). Although this is different from the figure, the same tendency is seen in Figures 3.11 and 5.4.

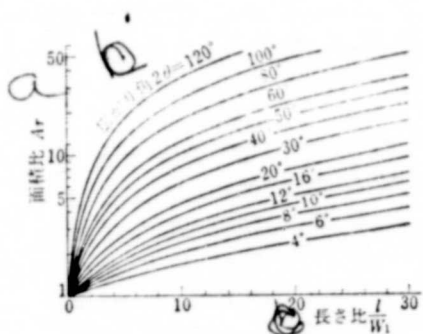


Figure 5.6. Correlation of length ratio, wide angle and surface area ratio of two-dimensional diffusers. a--surface area ratio  $A_r$ ; b--angle  $2\theta$ ; c--length ratio  $l/W_1$

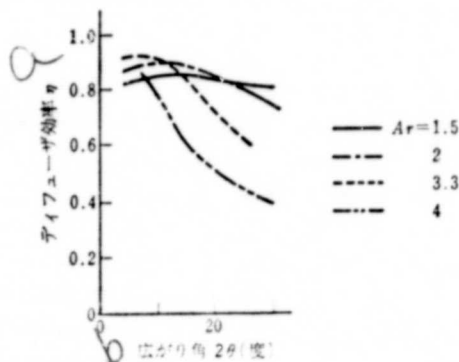


Figure 5.7. Wide angle and diffuser efficiency (two-dimensional). a--diffusers efficiency  $\eta$ ; b--wide angle  $2\theta$  (degrees)

The aspect ratio of two-dimensional diffusers (ratio of the depth  $b$ , inlet width  $W_1$ ) was studied by Furuya and Takeyama [8]. They varied the aspect ratio by 0.375-2.5. However, the effect of depth in the total range of the experiment was mainly on the pressure coefficient  $C_p$  and diffusers with a small depth have a low pressure increase. This is due to the effect of boundary layers of the side walls (parallel walls). Therefore, the properties of two-dimensional diffusers should be studied with the aspect ratio.

At the end of the 1950's, Kline showed that flow conditions and diffuser properties can be studied within a wide form range. Therefore, this study will be explained next.

Fox and Kline [9] represented the results with the length ratio  $l/W_1$  and wide angle  $2\theta$  on the coordinate axes (Figure 5.8). (They called this the flow regime map). In this figure, the flow region is divided into four areas:

- (a) area where peeling does not occur (below A-A curve),
- (b) area where peeling occurs on flow path wall (below B-B curve),
- (c) region of complete peeling (below C-C curve),
- (d) region of spray flow separated from both walls (above C-C curve).

The flow region map is used for two-dimensional diffuser designs. The following conditions are used.

The inlet boundary layer is thin, compressibility is not present, the order of disruption of the inlet is not extreme, the inlet Reynolds number is greater than  $10^5$ , and the aspect ratio at the inlet is more than four.

When a curve representing the maximum  $C_p$  is drawn in this figure, it is seen with a maximum of region (a) at approximately 10% of the  $2\theta$  angle (refer to Figure 5.4) and properties are at a maximum when the peeling area is reduced somewhat. /105

Kline, et al., [1] showed that the four types of diffuser design conditions should be used (refer to diffuser design digest).

1. find the form with which the pressure increase ( $p_2 - p_1$ ) is given and the total loss  $\Delta p$  is minimum;
2. determine the length  $l$  with the maximum ( $p_2 - p_1$ ) with  $A_r$  being given;
3. determine the  $A_r$  with a maximum ( $p_2 - p_1$ ) with the length  $l$  being given;
4. determine the form with the maximum ( $p_2 - p_1$ ) with the inlet conditions being given.

For instance, the optimum is at a 10% increase in the A-A curve with a constant path length ratio of  $l/W_1$ . When the form is selected, the optimum is to the right of the figures

$$\left(\frac{l}{W_1} = 25 \sim 30, 2\theta = 7^\circ\right)$$

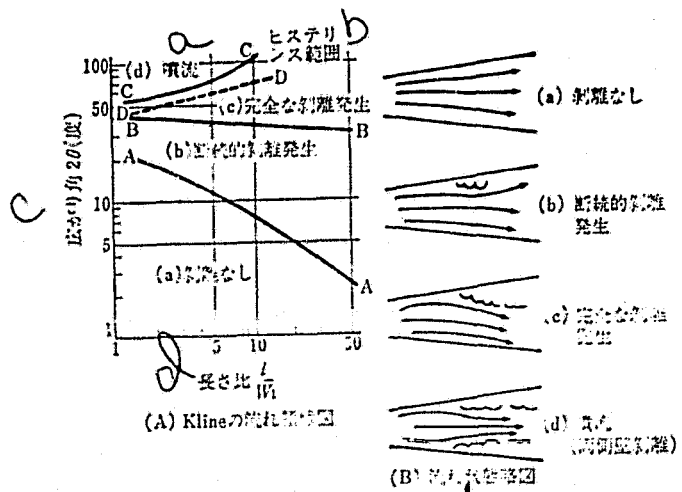


Figure 5.8. Two-dimensional diffuser and flow.  
 (a) ( flow region map of Kline) (b) flow conditions  
 A--no peeling; B--partial peeling; C--complete peeling;  
 D--spray flow (peeling at both walls)  
 a--spray flow; b--hysteresis range; c--wide angle 2θ degrees);  
 d--length ratio l/W<sub>1</sub>

(2) Theoretical calculations

Example of theoretical treatment of two-dimensional diffusers will now be given.

Nishi and Saimo have studied the hypothesis of the separation point by the boundary layer theory [10]. Sami and Nishi have introduced a simple method for calculating the correlation between the deacceleration rate and disrupted flow boundary layer (1970's) [11]. In the research of the former, the H of form coefficient is large at 1.8 in cases of internal flows. Furthermore, attention is focused on the pressure increase, and it is clear that the following correlation is established between the blockage rate  $B = \left( \frac{2\delta^*}{W} \right)_2$  and the form coefficient H<sub>s</sub> at the diffuser outlet.

$$H_s = 1.8 + 3.75 B \dots \dots \dots (5.3)$$



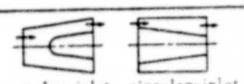
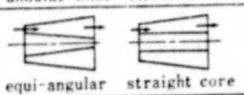
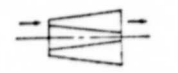
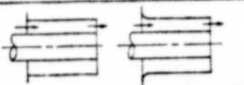

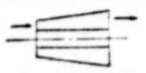
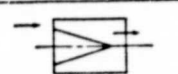
### 5.3 Annular diffusers

There has been relatively little research on annular diffusers and the majority of this was done since 1960 (considered to be the background for practical use of airplane engines). As shown in Figure 5.9, there are many types of annular diffusers. Therefore, simple examples will be given.

In 1940, Nelson and Popp [12] of NACA used two diffusers with equal wide angles (wide angle of cone where length is equal to area ratio) of 6-12 degrees.

These two types are the annular-inlet diffusers where the diameter is constant and the inlet is annular and the circular-inlet diffusers where the inlet is round and there is a flow line hub. The properties of the diffuser with a small angle will be explained with the correlation with the properties of the conical diffuser with the same path area ratio. The difference in properties with different angle and forms is low and efficiency is 85-89%.

Figure 5.9. Annular diffuser forms.  
 a--sketch; b--research;  
 c--and; d--et al.;  
 e--Kingen, et al.;  
 f--(Note: The double annular diffuser is a dump diffuser with an inner and outer case).

略図	研究者名
 annular-inlet    circular-inlet	Nelson および Popp
 equi-angular    straight core	Howard
	Kunz
	Okiishi および Serovy
 Dump diffuser	Klein
	Stevens および Williams
	金元

In the 1960's, Howard [13] studied annular diffusers. Howard carried out studies on equiangular annular diffusers and on straight core annular diffusers. From the results, he placed the peeling line and the  $C_p$  curve in the plane where the length ratio  $l/h$  ( $h$  is the difference between the diameter of the inlet and diameter of the outlet) and the surface area ratio  $A_r$  is on the coordinate axes (Figure 5.10 (a) and (b)). /107 In the figure, the curves of Reneau and McDonald for two-dimensional and conical diffusers are also given. The slope of the curve is different from the other two diffusers. When the length ratio is long, the optimum surface area ratio is smaller than with conical diffusers (therefore, the maximum  $C_p$  is also smaller). This appears to be due to the fact that the flow path is larger than in conical diffusers and there is, therefore, an increase in the friction loss.

Okiishi and Serovy [14] also studied the boundary layer of annular flow paths and Kunz [15] studied the equi-angular annular diffuser.

Klein, et al., [16] studied the dump diffuser (wide expansion type) used in engine combustion in the 1970's. They noted /108 that there were changes in the loss and optimum form, depending on whether the inlet flow was a swirl flow or another type of flow.

Stevens and Williams [17] have studied the annular diffuser with a constant diameter (beginning in the 1980's)[18]. They have noted that efficiency increases with an increase in the disruption of the inlet flow. Moreover, Kingen, et al., [18] have studied diffusers with three narrow angles of 16, 24 and 36 degrees and have noted that peeling (reverse flow) is produced with about the same area ratio (1.5-1.8).

The annular diffuser has more variables that determine the form than the conical or two-dimensional diffusers. Therefore,

study of data is more difficult and statistical results have not been obtained thus far.

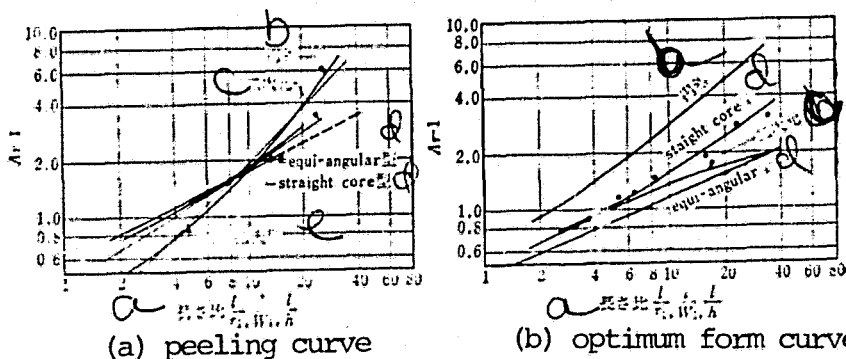


Figure 5.10. Properties of annular diffusers (Reneau, McDonald and Sovran)

a--length ratios ; b--conical; c--two-dimensional; d--type; e--expanded model

#### 5.4 Cross section and center lines

##### (1) Cross sections (profile of diffuser)

The form of the cross section including the center axis is called the profile of the diffuser. The form of the cross section perpendicular to the center axis is called the (horizontal) cross section form or flow path cross section. There have been many studies on the diffuser cross section form and on the curve form of mirror-type diffusers (Figure 5.11).

Gibson has carried out studies on the two-dimensional and axially symmetric diffusers with equation (5.4). The results are compared with the properties of two-dimensional and conical diffusers with straight walls (surface ratio  $A_r$  of 2-9, equal angle with angle  $2\theta$  of 10-30 (axially symmetric or 20-40 degrees (two-dimensional))).

$$\frac{1}{W_1} - \frac{1}{W} = kx, \quad \frac{1}{D_1} - \frac{1}{D} = kx \quad (5.4) \quad /109$$

(k is constant.....)

In the results, it is clear that the efficiency of the diffuser is 68% and 46% with rappa\* and two-dimensional diffusers respectively (two-dimensional diffusers have  $A_r = 0$  and  $2\theta = 26$  degrees) in comparison to the 36% of conical diffusers ( $A_r = 9$  and  $2\theta = 30$  degrees). The efficiency of the mirror type diffuser is 70% and, therefore, the properties of the diffuser can be improved with this type of profile.

Saiki [7] has studied two-dimensional diffusers with various profiles using an  $A_r$  of 3.33 and  $l/W_1 = 8.33$ .

(a) L type:  $2\theta = 16^\circ$  with straight walls

(b) C type: the pressure gradient  $dp/dx$  is constant ( $x$  is the distance of the axis,  $Q$  is the flow and  $i_d$  is the theoretical value),

$$\frac{1}{W_1^2} - \frac{1}{W^2} = \frac{dp}{dx} \cdot \frac{2bx}{\rho Q^2}, \quad \frac{dp}{dx} = \frac{(p_2 - p_1) i_d}{l} \dots \dots \dots (5.5)$$

(c) S type: the theoretical pressure increase curve is a sine wave

$$\frac{1}{W_1^2} - \frac{1}{W^2} = (p_2 - p_1) i_d \cdot \frac{b^2}{\rho Q^2} \left(1 - \cos \frac{\pi x}{l}\right) \dots \dots \dots (5.6)$$

(d) E type: distribution of width is given by index function

$$W = W_1 \exp\left(\frac{c}{l} x\right), \quad c = \ln \frac{W_2}{W_1} \dots \dots \dots (5.7)$$

The forms of diffusers given by the above-mentioned equations are mirror diffusers and they rank on the order of E, S and C. According to the experiments, the efficiency increases on the order of L, E, C and S (however, when length ratio  $l/W_1$  is 8 or less, E is superior to L). Saiki has carried out studies on L, C and F diffusers with rectangular profiles ( $A_r = 3$ ,  $\frac{l}{W_1} = 4.31$ ) (the ratio of increase in area is  $\frac{dA}{dx}$  and is constant). From these results, the order of efficiency is L, C and F. These results show that the straight wall diffusers are superior to the other (mainly mirror diffusers).

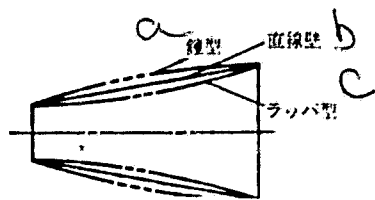


Figure 5.11. Profile of diffuser.  
 a--mirror type;  
 b--straight wall;  
 c--rappa type

Carlson, et al., [19] have studied /110 the three-two-dimensional diffusers of straight walls, rappa and mirror types with an  $A_r$  of 1.5-4.5 and  $\frac{l}{W_1} = 3 \sim 18$  and have studied the flow conditions. The form of the diffuser is given with the following equation ( $A_r(x)$  is the surface area ratio at position of distance  $x$  and  $\alpha$  is the coefficient).

$$A_r(x) = 1 + \frac{x}{l} (A_r - 1) \left[ 1 + \alpha \left( 1 - \frac{x}{l} \right) \right] \dots \dots \dots (5.8)$$

In the above-mentioned equation,  $\alpha$  is 2, 1, 0-1. ( $\alpha > 0$  is the mirror type and  $\alpha < 0$  is the rappa type). In the results, it was noted that efficiency increases on the order of mirror, straight wall and rappa types (however, the difference is small) and that the flow conditions vary with the type of diffuser but are approximately the same.

Stanitz and Yang have studied the theoretical form of two-dimensional diffusers and the results were previously mentioned in Chapter 4.

From the above-mentioned, it is clear that the results reflect the effect of the profile on properties (that is, the deceleration (boundary layer formation) increases near the inlet and, since the conditions at the inlet vary, a theoretical constant cannot be established).

(2) Changes in the flow path form and length

The profile of the diffusers affects diffuser properties. The cases of conical, angular and two-dimensional diffusers have been mentioned. Moreover, the effect of the aspect ratio (ratio of short cross section or of width and depth) on the two-

dimensional diffuser has also been mentioned. Now we will give other examples.

The studies of Sprenger [20] on diffusers have involved testing various cross section forms. When the efficiency  $\eta$  (defined in equation (3.56)) is defined for the case of thin boundary layer where there is no curve in the center axis and is read for various outlet forms, the following are obtained.

/111

Conical diffuser with  $A_r=4$ ,  $2\theta=8^\circ$  :  $\eta = 91\%$ , the profile at the outlet with a uniform angle is a vertical-horizontal ratio of 2 or 1/2 of the ellipse:  $\eta = 90\%$ . Ellipse with the same vertical-horizontal ratio of 4:  $\eta = 86\%$ .

As was previously mentioned, there is a tendency for properties to deteriorate when the profile is slanted. When the center curve is not curved, this deterioration is not as obvious (when there is a curve, the effects on profile are marked, as mentioned in (3)).

The authors of [21] studied logarithmic spiral diffuser models and varied the aspect ratio of the inlet of the flow path at 1.15 and 0.57. Then they made theoretical and experimental calculations. However, when depth was low, there was a reduction in efficiency and the effects of the Reynolds number were extreme.

At the BHRA [22], there have been studies on long profile-diffusers (angle of  $10^\circ$  and  $25^\circ$ ). These have been compared with conical diffusers. The results indicate that the difference between the two is low when the same conditions are used with an angle of  $10^\circ$ , but that when the angle is large, the pressure coefficient  $C_p$  is very low at 0.05-0.15 with rectangular outlets in comparison to conical diffusers.

### (3) Curve of center axis

Diffusers with curved center axes have been studied by Kline, but there are also several other examples. The system of curved diffusers studied the most frequently are diffusers where the flow path width is axially symmetric and perpendicular to the central line (two-dimensional) as in Figure 5.12. Here the difference in the angle in the direction of the outlet and inlet is represented as angle  $\beta$ .

Saiki [7] has studied diffusers with  $A_1=3.33$ ,  $-l/W_1=16.67$  ( $2\theta=8^\circ$ ) and has used angle  $\beta$  from  $10-60^\circ$ . As a result, he has noted that there is a linear reduction in efficiency  $\eta$  with an increase in the angle and that the efficiency is approximately 12% lower in comparison to diffusers with  $\beta = 60^\circ$ .

/112

Porokkis (USSR) has studied diffusers with  $-l/W_1=8.33$ ,  $2\theta=3.5\sim 14^\circ$ ,  $\beta=21^\circ 15'\sim 63^\circ 42'$ . The angle  $2\theta$  and the angle  $\beta$  results in a reduction in the efficiency  $\eta$  when the values are large (in combination of small  $2\theta$  and  $\beta$  angle,  $\eta$  is 89%. The maximum combination value was 61%. Furthermore, there is a reduction in the optimum angle with an increase in this  $\beta$  angle).

Fox and Kline [8] have studied curved diffusers and have made a flow region map for these diffusers. Figures 5.13(a) and (b) show the line (B-B) with complete peeling starting and line (A-A) where partial peeling started with (B-B) as the parameters. In general, there is a tendency for these curves to move to the low angle  $2\theta$  side with an increase in  $\beta$ .

Changes are not seen in the A-A curve within a range of  $\beta = 0-30^\circ$ . Moreover, the A-A curve is a maximum with  $\beta > 50^\circ$  ( $1/W_1$  where the lowest peeling occurs. The curve moves to the low  $2\theta$  side with a high efficiency or pressure coefficient.

/113

The studies of Sprenger on curved diffusers [20] have been used to study the effects of curves on the thickness of the inlet boundary layer. The differences in efficiency is 11% with conical diffusers with a rotation axis of  $30^\circ$ . It is 15% with a vertical-horizontal ratio of 2 and 4 (vertical and ellipse) and is 6% in the case of a ratio of 0.5 (horizontal length ellipse). The reduction in efficiency is different from the distribution of the profile.

On the other hand, there have been examples of direct tests. Sagi and Johnston [23] have studied the method where the form of the two-dimensional diffuser is studied by the inverse method (one type of Stanitz method for determining flow path shape when the distribution of velocity is determined) ( $\beta$  is  $30-90^\circ$ ). In this study, the diffuser in Figure 5.14 was used. The properties are good with a curve center axis ( $\frac{l}{W_1}=4, \beta=70^\circ$  and  $\eta$  is improved by 15%).

Next, we will explain the features of the flow in two-dimensional curved diffusers. The authors have used the diffuser that provides a flow path from two spirals at a constant depth [21]\* and the maximum expansion diffuser by introduction of a logarithmic spiral [24]. Moreover, the boundary layer seen with curved flows was studied (Figure 5.15)\*\* . This type of layer /114 was noted in cases where the diffuser had curved pipes. The secondary flow is weak on the concave surface (outside of the

---

\* The logarithmic spiral is the form where the expansion is low with bladed diffusers (equal to the flow line in bladeless diffusers). Therefore, it is mentioned as a starting point for the flow path of bladed diffusers.

\*\* There is a reduction in flow velocity in the boundary layer near the flow path walls and the flow is therefore at equilibrium with the main flow when the curve has a high curvature. The flow is formed by a pair of spirals shown in this figure.



curve) and is obvious on the convex surface (inside the curve). Therefore, there is a difference in the boundary layer formation above each flow path wall (the formation of boundary layers is faster above the convex surface).

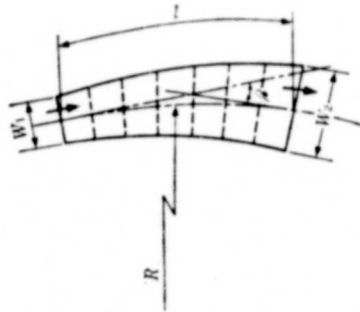


Figure 5.12. Design of two-dimensional curved diffuser.

Yamaki, et al., [26] have studied logarithmic spiral diffusers and have shown that efficiency is improved by setting up one or two blade guides in the convex sections of the flow path.

As was previously mentioned, the studies on curved two-dimensional diffusers are very important and more of these have been performed. The reduction in efficiency and peeling with the rotation angle or large expansion angle are obvious and there are many diverse methods for determining form. The effects of the Reynolds number and inlet boundary layer thickness are extreme and very important in application.

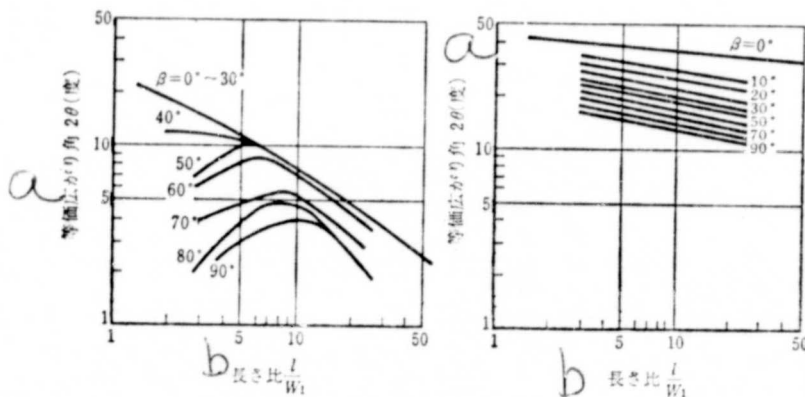


Figure 5.13. Flow region map for two-dimensional curved diffuser.

(a) A-A curve (beginning of intermittent peeling)  
 (b) B-B curve (beginning of total peeling)  
 a--wide angle  $2\theta$  (degrees); b--length ratio  $l/W_1$

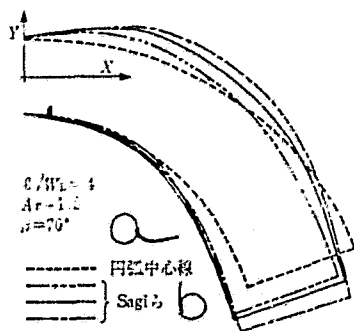


Figure 5.14. Two-dimensional curve diffuser of Sagi. a--curved central line; b--Sagi, et al.

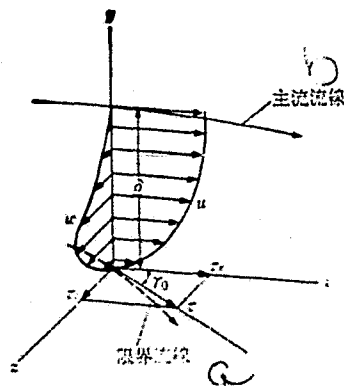


Figure 5.15. Boundary layer. a--boundary layer line; b--main flow line

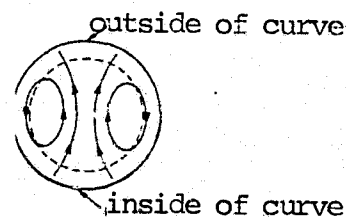
#### (4) Spatial curve of center line

There are cases where the center line of the diffuser is three-dimensionally curved and when these diffusers are used, spatial connections are formed by the position relationship with the fluid feed side and application side.

/115

There have been some studies on the case where several curved pipes or elbows\* are three-dimensionally connected and the group of Muranoue of Japan [27] has been studying this effect since the 1960's. According to this group, when the length  $L$  of the pipe between the elbow of two pipes is five times the diameter  $D$  of the pipes, there is marked interference between both elbows, and when the angle shown in Figure 5.16 is  $120-150^\circ$ , the pressure loss is maximum (when  $L \geq 0.65 D$ , however, the loss is less than two-fold with that of one elbow). This group [28] has also studied the case of wave-shaped pipes and coil pipes (Figure 5.17) which are used in combination with curved pipes.

\* This is not illustrated. However, elbows are formed with a curvature radius that is low (commercial elbows, etc.). These are differentiated from curved pipes with a large curvature radius (diffraction pipes and curved pipes).



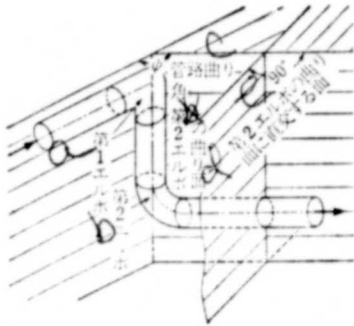


Figure 5.16. Two-dimensional curved pipe (elbow) system. a--1st elbow; b--2nd elbow; c--pipe curve; d--curved surface of 2nd elbow; e--curve crossing curved surface of 2nd elbow

Simizue, et al., [29] have studied the case where the spatial connection is large, as in the previous case [28] (expansion angle  $2\theta = 6$  and  $12$  degrees) and have determined the flow with various velocity distributions.

As a result, they have determined that for a surface area ratio of  $A_r$  of 4 to 8, the high efficiency seen with other diffusers (80% or more) can be obtained by combining the flow distribution with the properties of the secondary flow in the curved pipes (this design method is normally used and is very important).

## 5.5 Form of inlets and outlets

### (1) Inlet pipes

Pipe diffusers are used by connecting inlet pipes with a certain length and diameter equal to the inlet. The purpose of the inlet pipe is to regulate the flow going to the diffuser (make the flow uniform). On the other hand, a boundary layer



(a) 波型管(1)



(b) 波型管(2)



(c) 擬似コイル管(1)



(d) 擬似コイル管(2)

Figure 5.17. Connection of spatial curved pipes.

- (a) wave type pipe (1)
- (b) wave type pipe (2)
- (c) coil pipe (1)
- (d) coil pipe (2)

is formed by the inlet pipes. The properties of the diffuser and flow inside the diffusers are affected to a large extent by the inlet conditions and this fact must be considered in tests on diffusers.

For instance, Furuya [4] has carried out studies on diffuser properties with the velocity distribution being uniform at the inlet with a short pipe of  $\frac{L}{D_1} = 2.25$  ( $L$  is inlet pipe length,  $D_1$  is the diffuser inlet diameter) using conical diffusers and with conditions where the boundary layer is produced by a pipe with  $\frac{L}{D_1} = 24.5$ .

In addition, Sprenger [20] has studied the changes in length ratio of inlet pipes  $l/d_1$  from 0.85 to 10.85. The effects of the length and surface roughness of the inlet pipes on diffuser properties are often seen in the form of boundary layer thickness at the diffuser inlet and will be mentioned in detail later in this section.

## (2) Capillaries

When straight pipes (capillaries) with a diameter equal to the outlet diameter  $D_2$  are set up near the outlet of the diffuser, the pressure increase and current velocity are related and there is improvement in apparent properties of the diffuser. According to the tests of Patterson and Gibson and Peters in the previous chapter (Chapter 3), there is continuity of pressure elevation with a capillary length of (2-6)  $D_2$ . (Even in the tests of Furuya [4], the pressure elevation continued with (3-4)  $D_2$ . Furthermore, Patterson records that there is sufficient pressure elevation at the outlet without capillaries in diffusers with good properties.

## (3) Expanded outlet

/117

The results of Gibsons' study on curved wall diffusers were previously mentioned. According to Gibson, when the surface area ratio is large, there is a sudden expansion in the outlet (refer to Figure 3.15). This appears to be due to the fact that the disadvantages of the unstable flow due to intermittent peeling are eliminated when the curved walls have a wide expansion and the pressure increase in the capillaries is continuous.

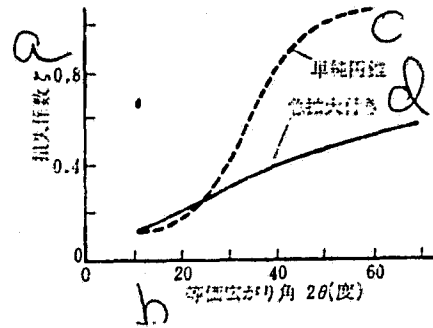


Figure 5.18. Properties of wide expansion (stepped diffusers)

a--loss coefficient; b-- $\eta$  equal to angle  $2\theta$  (degrees); c--simple conical diffuser; d--wide angle diffuser

Saki [7] has carried out studies on two-dimensional diffusers with a constant capillary width  $2\theta = 26^\circ$  with a uniform outlet width) using a two dimensional range of  $\frac{l}{W_1} = 5$ ,  $2\theta = 7 \sim 26^\circ$ . However, according to his results, in contrast to the efficiency of a single diffuser ( $2\theta = 26^\circ$ ), of 62%, the efficiency of a diffuser with  $2\theta = 10.5^\circ$  is 82%.

Furuya and Sato [30] have studied the conical diffusers with wide expansions ( $2\theta = 10 \sim 60^\circ$ ) and have carried out theoretical studies on their properties. According to their results, the outlet area is made uniform by combining the conical section of  $2\theta = 10^\circ$  with the large expansion capillary and the loss is lower than seen with a simple conical diffuser. The angle is approximately  $20^\circ$  more than that of the simple conical diffuser (refer to Figure 5.18). As was previously mentioned, the effects are considerable when the diffuser surface area ratio is large.

(4) Intermediate guide blades

There have been various studies on the method where an intermediate guide blade is placed in the diffuser to divide the flow path. Woollett [31] of NACA in the U. S. set up /118 guide blades in a diffuser that was asymmetric with a surface ratio of 3 (Figure 5.19) and studied the properties obtained by this and other methods (those where the flow is cut horizontally with three nets, those where the boundary layer is emitted and the inlet, and those where the boundary layer is blown in). These results show that the properties obtained with the nets are poor, while the other properties are about the same and the nonuniformity of the outlet velocity is reduced by 1/3 in comparison to the case where no dividers are set up. In the experiments with a high velocity flow, there is a reduction in efficiency with guide blades with an inlet Mach number  $M_1 = 0.75$ . However, the reduction is slight with other devices.

Furthermore, the studies of Sprenger [20] and other researchers have shown that the effects vary in tests on the effects of guide blades.

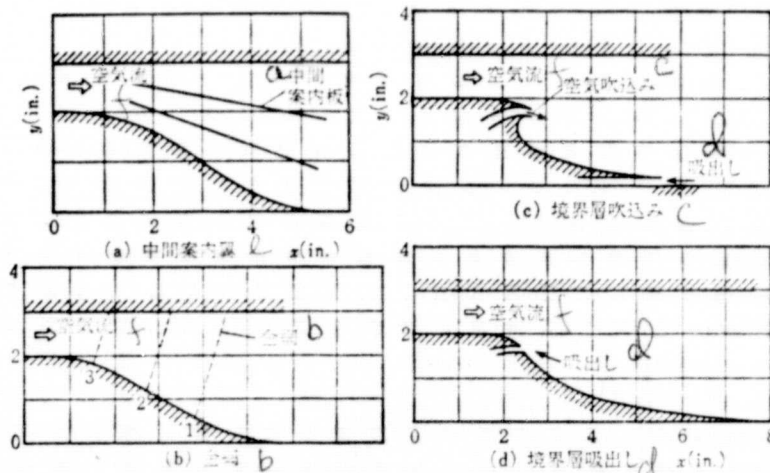


Figure 5.19. Methods for improving diffuser efficiency. (a) intermediate guide blades; (b) nets; (c) boundary layer blown in; (d) boundary layer emitted  $x(in.)$ ; (e) intermediate guide blades; (f)--air flow.

## 5.6 Inlet boundary layer and boundary layer control

### (1) Inlet boundary layer

The thickness of the boundary layer of the diffuser inlet, or the form coefficient, is an initial condition of boundary layer formation and is an important variable. The effects of the boundary layer thickness are extreme.

Sprenger [20] carried out studies on the curved diffusers with various ellipses and showed that when there is a correlation between the thickness  $\delta_1^*$  of the boundary layer at the inlet and efficiency  $\eta$  (equation (3.56")) the graph in Figure 5.20 is obtained. When  $\delta_1^*$  increases, the reduction in  $\eta$  is marked and when  $\frac{\delta_1^*}{D_1}$  increases from 0.5% to 5%, the reduction in efficiency is approximately 20% with conical diffusers. Under the same conditions, the reduction in efficiency of curved conical diffusers is 26% when the rotation angle  $\beta$  is  $30^\circ$  and /120 the reduction is 29% and 27% for vertically elliptical diffusers and horizontally elliptical diffusers respectively. The effects of  $\delta_1^*$  are therefore stronger in the case of straight diffusers. Furthermore, the increase in  $\delta_1^*$  results in a reduction in  $\eta$  and this reduction is marked when  $\delta_1^*$  is small. Therefore, there is a tendency for the reduction in  $\eta$  to gradually decrease with an increase in  $\delta_1^*$ .

Figure 5.21 is a graph showing the results of theoretical calculations of boundary layer formation by Schlichting and Gersten [5] using the conical diffuser ( $2\theta=8.9^\circ$ ,  $A_r=1.4$ ), and the dimensionless movement thickness  $\frac{\delta_1^*}{r_1}$  is placed on the axis of abscissas. This is the same as in Figure 5.20.

Waitman, et al., [32] (Kline group) have studied changes in the thickness  $\delta_1^*$  of boundary layers in two-dimensional diffusers with the two  $\frac{L}{W_1}=8$  and 12 and have studied

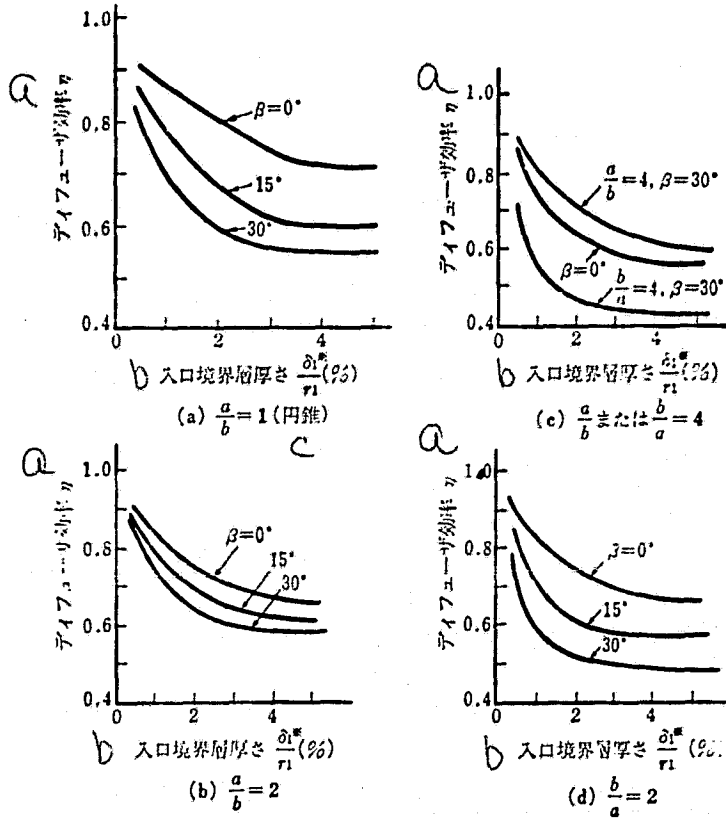


Figure 5.20 Performance of curved diffusers. (Inlet boundary layer thickness and diffuser efficiency). a--represents a vertical path on a circular radius, and b a horizontal path; c--  $a/b = 1$  (cone).

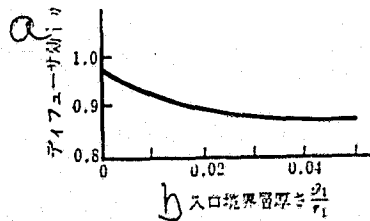


Figure 5.21. Inlet boundary layer thickness and diffuser efficiency. a--diffuser efficiency  $\eta$ ; b--inlet boundary layer thickness



changes in diffuser properties and the flow region. As a result, it is noted that the optimum wide angle moves to the small side when  $\delta_1^*$  increases. Therefore, the flow region hardly changes with the inlet boundary layer thickness.

Cockrell [33] has studied the correlation between inlet movement thickness  $\delta_1$  and pressure coefficient  $C_p$  for conical diffusers ( $2\theta = 10^\circ$ ). As a result, he noted that the lowest  $C_p$  is seen with  $\frac{\delta_1}{D_1} = 0.03$  and that there is an apparent increase with an increase in  $\delta_1$ . From the above-mentioned examples, it is clear that the correlation between the diffuser inlet boundary layer and efficiency or reduction in the pressure coefficient are the same and that the efficiency or pressure coefficient reduction is at a maximum with a  $\delta_1/r_1$  (or  $\delta_1^*/r_1$ ) of 3%.

## (2) Boundary layer suction or injection

The tests carried out by NACA [31] on boundary layer suction and injection have been previously mentioned. In the 1960's and 1970's, Furuya of Japan carried out studies on inlet boundary layer suction using conical [34] and two-dimensional [35] diffusers. In the studies on conical diffusers, tests were carried out by varying the ratio of suction flow  $q$  to main flow  $Q$  (suction flow ratio ( $q/Q$ ) with an  $A_r=4$ ,  $2\theta=10\sim60$ ). The results are shown in Figure 5.22. That is, when the suction flow ratio is 2-3% or more, the loss coefficient  $\zeta$  is made 0.2 or less with a large wide angle and efficiency can be increased to 90% or more (taking force of suctioning into consideration). /121

Moreover, in studies on two-dimensional diffusers, tests were carried out with  $A_r=4$ ,  $2\theta=30\sim180^\circ$  (wide angle) and when the inlet aspect ratio was four or more, the suction flow ratio was approximately 5% and the efficiency was

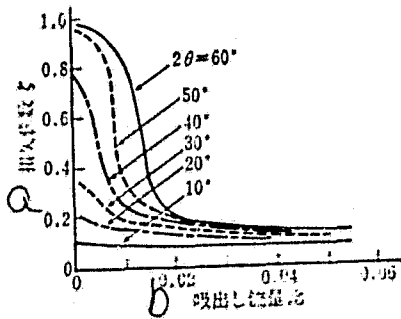


Figure 5.22. Suction amount and loss coefficient at diffuser outlet (conical)  
 a--loss coefficient  $\zeta$ ;  
 b--suction flow ratio

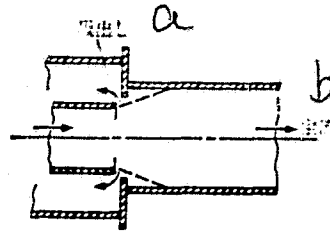


Figure 5.23. Diffuser of Adkins (boundary layer suctioning).  
 a--suctioning; b--main flow

approximately that of a diffuser with  $2\theta = 10^\circ$  when the wide angle was  $90^\circ$ .

Adkins [36] carried out studies on the special cylindrical and annular diffusers (do not have wide flow path walls and a wide flow is formed by the boundary between the flow and whirlpool) using a device for suctioning as shown in Figure 5.23. He obtained an efficiency of 80% or more with a suction flow ratio of 3%.

As was previously described, although boundary layer suctioning (or injection) is a unique technology in that a high efficiency diffuser is obtained, there are problems in that expertise and complex equipment are necessary.

### (3) Swirl (or whirlpool) producing device

Although the effects of flow swirls introduced to the diffuser will be mentioned in a later section, here we will comment on the case where a swirl producing (controlling) device is introduced to the diffuser.

In the test by Sprenger [20] on curved diffusers, studies were performed by attaching vortex-producing blades (or plates)

to two series along the convex side flow walls of the diffuser. According to the tests, efficiency was improved by 5-15%. /122 However, the form of the diffuser and direction of the vortex had an effect and a strong tendency was noted.

Im and Nishi [37] carried out studies on diffusers by attached vortex producing blades to the front of the conical diffuser inlet ( $A_r=4$ ,  $2\theta=8\sim30^\circ$ ), as shown in Figure 5.24. According to their results, the peeling phenomenon is prevented in diffuser with a  $2\theta = 16^\circ$  by using these vortex producing blades and the same pressure coefficient with diffusers with a  $2\theta = 8^\circ$  is obtained.

Kingen and Toshishoku [38] carried out studies by attaching columns to the front of the inlet of a two-dimensional diffuser with a  $2\theta=2.8 \sim 40^\circ$ . They attempted to prevent peeling caused by interference between the boundary layer and back flow of the columns. In these examples, the effects of improved efficiency are obvious. However, there are some problems, such as increase in loss and therefore further testing of preliminary equipment, etc., is necessary.

#### (4) Grooves and rough surface of walls

We have mentioned placing grooves in flow path walls and making these walls rough. Mixtures of fluids are seen in the boundary layer and peeling is therefore delayed.

Furuya, et al., [30] have shown that by making the wall surface of conical diffusers rough by making particle adhere to the down flow side from the position where peeling occurs, peeling is delayed and there is a reduction in loss. Figure 5.25 shows the results of tests with  $A_r=3.52$ ,  $2\theta=10\sim60^\circ$ . With  $2\theta > 10^\circ$ , there is a reduction in loss because part of the surface is rough. When the  $2\theta$  is  $>35^\circ$ , the entire surface is rough and the results are superior to those obtained with

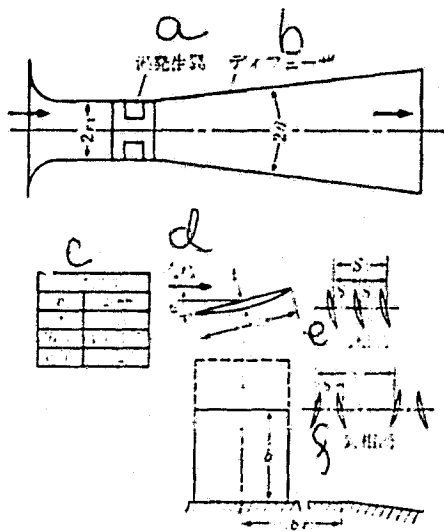


Figure 5.24. Vortex-producing devices.  
 a--vortex producing blades;  
 b--diffuser; c--vortex producing blades; d--flow; e--in-phase vortex; f--out of phase vortex

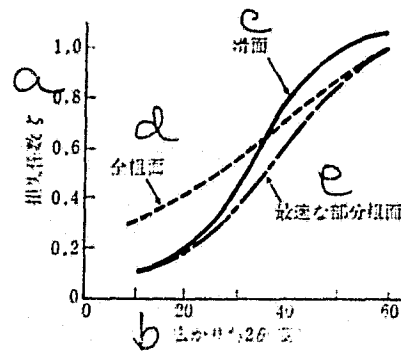


Figure 5.25. Loss coefficient in partially rough diffusers (conical).  
 a--loss coefficient  $\zeta$ ;  
 b--wide angle  $2\theta$  (degrees);  
 c--smooth surface; d--completely rough surface; e--optimum partially rough surface

smooth walls. The pressure loss seen in diffusers is produced due to friction on the flow path surface and peeling. When /123 the wide angle is large, the main cause is the latter and therefore the results are obvious.

Migai of the Soviet Union has carried out studies on wide angle two-dimensional (or conical) diffusers ( $\frac{l}{W_1}=1.95, 2\theta=22\sim60^\circ$ ) by attaching parallel grooves (or annular grooves) to the inlet side of the flow path (refer to Figure 3.16). He compared the results with those of grooveless diffusers. The groove results were maximum near  $2\theta=40\sim45^\circ$  and at  $2\theta > 45^\circ$  peeling could not be prevented. Moreover, there was little effect with  $2\theta < 20^\circ$ . Migai has also studied the effects of grooves where the same as in the previous examples and the number  $n$  of grooves was varied

between one and twelve. However, loss was reduced with  $n > 8$  and it was not necessary to set up grooves along the entire length of the diffuser.

## 5.7 Effect of Reynolds number and Mach number

### (1) Reynolds number

The formation of boundary layers is controlled by the Reynolds number and, therefore, the Reynolds number plays an important role in diffuser properties. The effects of the Reynolds number were previously mentioned and much testing has been carried out.

For instance, Saki [7] has studied diffusers by varying the Reynolds number  $Re_1$  at the inlet of two-dimensional diffusers with  $A_r = 3.33$ ,  $\frac{l}{W_1} = 16.67$  from  $10^3$  to  $10^4$ . However, in these results, there was an increase in efficiency  $\eta$  from 62 to 85% /124 with an increase in  $Re_1$  (Figure 5.26). (This appears to be the opposite tendency of the Reynolds number loss in Figure 2.5. Moreover, the increase in  $\eta$  is markedly reduced with an increase in  $Re_1$ ).

Furuya [4] has also studied the Reynolds number of conical diffusers with  $A_r = 2.64$ ,  $2\theta = 20^\circ$  by varying the inlet  $Re_1$  between  $(1-3) \times 10^5$ . However, he noted that the increase in efficiency was 84 to 89% with a uniform flow (thin boundary layer). Therefore, it appears that the changes in the reduction in efficiency with a change in the Reynolds number are greater in the latter case.

In the tests of Sprenger, et al., [20] on curved diffusers, when the Reynolds number was very high, the efficiency continued to change, and when the Reynolds number was low, efficiency decreased to a large extent (tendency stronger with diffusers

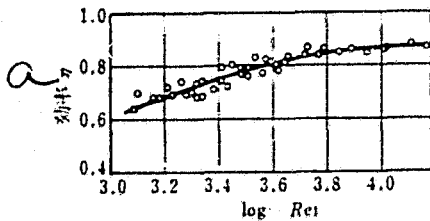


Figure 5.26. Inlet Reynolds number and diffuser efficiency (two-dimensional). a--efficiency  $\eta$

with poor formation conditions). The correlation between the

Reynolds number and efficiency (or pressure coefficient), varies with the form and flow conditions.

## (2) Mach number

Large devices are necessary for tests where the Mach number of an inlet is high and determinations are not simple. Most tests have been carried out by aeronautical research institutes in the U. S. and Britain. Young and Green [39] have studied two-dimensional diffusers with  $A_1=4$ ,  $2\theta=8\sim 31.2^\circ$  and increased the flow to sonic speed until choke was reached. The correlation between the inlet Mach number  $M_1$  and loss coefficient  $\zeta$  is shown in Figure 5.27. According to the figure, in any case, the  $M_1$ , which suddenly increased the loss, is high when the angle is large. When the angle is small, the loss increases with a lower  $M_1$ .

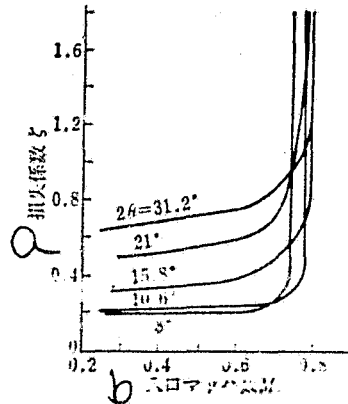


Figure 5.27. Inlet Mach number and diffuser loss coefficient.

a--loss coefficient  $\zeta$ ;  
b--inlet Mach number  $M_1$

Nelson and Popp [12] carried out studies on a high velocity in annular diffusers and compared the case of a wide angle  $2\theta = 6^\circ$  with that of  $12^\circ$  with a circular inlet diffuser (refer to 5.3). The  $M_1$  at which efficiency was low was higher with the former (0.8). Moreover, Woollett [31] made high velocity

/125

tests with two dimensional asymmetric diffusers (5.5) and noted that there was a reduction in efficiency with intermediate guide blade switch at  $M_1 = 0.75$ . The efficiency decreased up to an  $M_1 = 0.9-1.0$  with diffusers in which boundary layers were suctioned. From these examples, it can be said that properties are poor with narrow inlets.

Runstadler and Dean [40] carried out studies on two-dimensional diffusers with inlet aspect ratios of 1 and 0.25 using various inlet Mach numbers and inlet boundary layer thicknesses. They drew a  $C_p$  curve inside the plane where the coordinates were the length ratio  $\frac{l}{W_1}$  and the surface area ratio  $A_r$  using the blockage rate  $B$  of the inlet and  $M_1$  of the inlet as the parameters. According to the results, the pressure coefficient increased by several percent with an  $M_1 = 0.2-1.0$ . However, it decreased with  $M_1 = 1.0-1.4$ . However, the tendency for a reduction in efficiency and pressure coefficient was not marked. This example shows that when the blockage rate  $B$  is constant, this type of tendency will probably be seen.

### (3) Rate of disruption and changes in flow

When the Reynolds number is high, the rate of disruption  $\frac{u'}{U}$  ( $u'$  is the changing velocity and  $U$  is the mean velocity) /126 increases. Therefore, the Reynolds number affects the rate of disruption. Waitman and Kline [32] carried out studies by attaching rods to the front of an inlet of a two-dimensional diffuser ( $\frac{l}{W_1}=8, Re_1=2.4 \times 10^5$ ). They then drew the high flow with a high rate of disruption artificially. When there were no rods, the rate of disruption was 1.06%, while the rate of disruption with rods was increased to 10.1%. As a result, the pressure coefficient  $C_p$  increased from 0.65 to 0.79 with  $2\theta = 10^\circ$ . However, when we consider the pressure loss caused by the rods, this is not a desirable method.

Stevens and Williams [17] have studied the effects of disruption in annular diffusers and have noted that the rate of disruption is increased with porous plates set up in the upward current side. When no plates are used, the pressure coefficient  $C_p$  increases from 0.44 to 0.52 to 0.54 to 0.58. Therefore, the correlation between the rate of disruption and diffuser properties is related to the method of the disruption and cannot be quantitatively determined.

#### 5.8. Shear flow and swirl flow effects

##### (1) Shear flow

When a shear flow is present at the inlet (flow having velocity gradient perpendicular to flow), the pressure increase at the wall surface is unbalanced, and there is a reduction in properties. Moreover, methods for testing this shear flow have been used whereby pipes are connected to the inlet of the diffuser and nets with varying degrees of opening are set up inside the flow path.

Pohl [41] has carried out studies using two pipes with a rotation degree of 90 and 180° at  $R/a$  of 1.389 ( $R$  is the curved radius of the center line and  $a$  is the length of one side of the profile) using diffusers with  $A_r=2.5$ ,  $2\theta=10$ . When round pipes were used, the reduction in velocity was marked and when round pipes with a length 7.14-fold that of the side /127 of the outlet profile were set up, the velocity was irregular at more than 20% of the mean velocity. The properties of the diffusers itself cannot be analyzed.

Wolf and Johnston [12] carried out studies on two-dimensional diffusers with shear flows and studied the flow region and properties. They considered the velocity distribution with a uniform shear and nonuniform shear (wake, jet or step shear). When the shear flow occurred, the optimum form



was obtained with a lower area ratio than in the case of a uniform flow (data of Reneau).

Ushida, et al., [43] have carried out theoretical studies and measurements of conditions where the flow changes in the flow path using a two-dimension diffuser and shear flow with a velocity gradient in the direction of depth. According to the results, the pressure increase is small with a large pressure gradient  $dp/dz$  ( $z$  is the distance in the direction of depth) at the inlet. The velocity gradient of the main flow decreases in a downward direction. Moreover, it decreases with an increase in the wide angle. The boundary layer formation is marked, particularly on the flow wall on the low velocity side [44].

From the above-mentioned, it seems that the correlation between shear flow and flow can be explained quantitatively. However, there is still insufficient data.

Nakamura [45] has studied the case where a shear flow is applied to the inlet of a conical diffuser with  $A_r=4$ ,  $2\theta=10\sim30^\circ$  and has noted that the back flow is readily produced on the low velocity side and there is, therefore, a reduction in pressure. As a result, the wide angle that gives the same pressure coefficient as in the case of a uniform flow (equal wide angle during uniform flow) is larger than the shear flow (refer to Figure 5.28,  $\lambda_1$  in the figure is  $\frac{\Delta U}{U_1}$ ,  $\Delta U$  where  $\Delta U$  is the difference between the central flow and maximum or minimum flow). /128  
Nakamura [16] has also studied conical diffusers with capillaries and in this case he noted that there was improvement in the reduction in properties. The distance for pressure recovery behind the outlet of the diffuser is 5-8 fold the outlet diameter.

## (2) Swirl flows

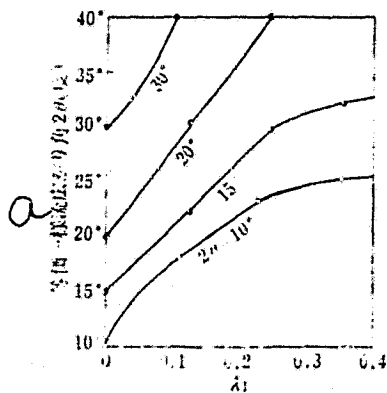


Figure 5.28. Equal flow wide angle with shear flow (conical).  
 $\alpha$ —equal flow wide angle;  
 $2\theta$  (degrees)

Swirl flows are seen with axial flow compressors and fans. There have been several examples of the production of swirl flows by blades in this study.

Patterson has shown that there is an improvement of several per cent in the efficiency when a swirl flow is produced in a diffuser according to the results of Vullers, Andres and Peters. Patterson feels that this was due to the prevention of peeling.

Imo [47] has carried out measurements of the swirl flow (free vortex flow) using conical diffusers with  $2\theta = 8-30^\circ$ . The pressure coefficient increases within a certain range due to disruption along the flow path wall caused by swirling. Therefore, the wide angle at which the maximum  $C_p$  is obtained is about  $8^\circ$ . Moreover, the maximum swirl strength at which the maximum apparent pressure increase (disregarding pressure reduction due to swirl) is seen is approximately  $\alpha = 8^\circ$  with  $2\theta \leq 20^\circ$  (angle of inclination of  $\alpha$  in axial direction).

### (3) Rotation

Rotation is seen with coolant systems and with flow paths of runners.

Muranoue [48] has carried out studies on flows produced in the axis of rotation of U-shaped pipes. Two-dimensional flows are produced inside these pipes and this phenomenon is more obvious with an increase in the rotation velocity and axial velocity.

Muranou [49] also studied the same thing with conical /129 diffusers ( $A_r=4$ ,  $2\theta=10^\circ$ ) and noted that peeling readily occurs due to the effects of Coriolis force\*. Moreover, according to studies on conical diffusers with  $2\theta = 7-15^\circ$ , the increase in loss coefficient or minimum loss coefficient occurs near  $2\theta = 10^\circ$ , regardless of the r.p.m.

From the above-mentioned, it is clear that the above-mentioned variables have effects of properties and flow conditions. However, these effects are not quantitatively clarified. There are many cases where it is difficult to determine the effects as a whole because of interference between the main factors of these effects.

The reader should refer to the references for further information.

#### REFERENCES

- [1] Kline, S. J., et al.: Trans. ASME (J. of Basic Engg.), p. 321 (1959-9).
- [2] McDonald, A. T., Fox, F. W.: ASME publication, 65-FE-25 (1965-66).
- [3] Furuya: Kiron 22-121, p. 667 (31-9).
- [4] Furuya and Suzuki: Kiron 23-125, p. 7 (32-1).
- [5] Schlichting, H., Gerstein, K.: fuer Flugwissenschaften 9-4/5, p. 135 (1961).
- [6] Squire, H. B.: Aeronautical Research Council R&M 2751 (1950).
- [7] Saki: Kyoto Diagaku Kogaku Kenkyuho Dai 2 go, p. 18 (1952).

---

\* Coriolis force is the force exerted on the fluid in a direction perpendicular to the flow line when the flow site rotates.  $m$  is the mass,  $\omega$  is the angle velocity and  $w$  is the relative velocity when  $2m\omega w$  is the force.

- [8] Furuya and Akiyama: Kienron (dai 34 ki Tsugo kokai Koenko) p. 67 4/1957
- [9] Fox, R. W., Kline, S. J.: Trans. ASME (J. of Basic Engg.) 84-3, p. 303 (1962-9).
- [10] Nishi and Imo: Kiron 42-362 p. 3206 10/76.
- [11] Imo and Nishi: Kiron 43-367, p. 997 (3/1977).
- [12] Nelsen, W. J., Popp, E. G.: NACA RM L9H09 (1949).
- [13] However, J. H. G., et al.: ASME publication, 67-WA/FE-21 (1967-11).
- [14] Okiishi, T. H., Serovy, G. K.: ASME Paper, No. 67-WA/FE-10 (1967-11).
- [15] Kunz, H. R.: Trans. ASME (J. of Basic Engg.) 87-2, p. 535 (1965-6).
- [16] Klein, A., et al.: Paper presented at the 2nd International Symposium on Air Breathing Engines, Sheffield (1974-3).
- [17] Stevens, S. J., Williams, G. J.: Trans. ASME (J. of Fluids Engg.) 102, p. 357 (1980-9).
- [18] Kingen, et al.: Kiron 47-422, p. 1940 (10/1981).
- [19] Carlson, J. J., et al.: Trans. ASME (J. of Basic Engg.) p. 151 (1967-3).
- [20] Sprenger, H. : Diss. Zurich, No. 2803 (1959).
- [21] Sai: Kiro 36-291, p 1886 (11/1970).
- [22] BHRA: Internal Flow--A guide to losses in pipe and duct system. Part II, Performance of Straight-Wall Diffusers, p. 77 (1971).
- [23] Sagi, C. J., Johnston, J. P.: Trans. ASME (J. of Basic Engg.) p. 715 (1967-12).
- [24] Sagi: Kiron 37-397, p. 992 (5-1971).
- [25] Kento: Kishi 62-490, p. 46 (11/1959).
- [26] Yamamoto, et al.: Kiron 47-416, p. 763, 4, 1969
- [27] Muranoue: Kiron 35-272, p. 763 (4/1979)
- [28] Seimizu, et a.l: Kiron 47-417, p. 762 (5/1981)

- [29] Seimizu, et al.: Kiron 47-417, p. 729 (5/1981).
- [30] Furuya and Sato: Kiron 26-162, p. 163 (2/1960).
- [31] Woollett, R. R.: NACA RM E56C02 (1956).
- [32] Waitman, B. A., et al.: Trans. ASME (J. of Basic Engg.) 83-3, p. 349 (1961-9).
- [33] Cockrell, D. J.: J. Roy. Aeron. Soc. 68-648, p. 844 (1964-12).
- [34] Furuya, et al.: Kiron, 31-224, p. 553 (4/1965).
- [35] Furuya, et al.: Kiron, 35-274, p. 1249 (6/1959).
- [36] Adkins, R. C.: Trans. ASME (J. of Fluids Engg.) p. 297 (1975-9).
- [37] Imo and Nisho: Kiron 37-3003, p. 2153 (11/1961)
- [38] Kingen: Kiron no. 800-17, p. 103 (10/1980).
- [39] Young, A. D., Green, G. L.: Aeronautical Research Council R&M 2201 (1944).
- [40] Runstadler, P. W., Jr., Dean, R. C., Jr.: Trans. ASME (J. of Basic Engg.), p. 397 (1969-9).
- [41] Pohl, K. H.: Ing. Arch. 29-1, p. 31 (1960).
- [42] Wolf, S., Johnston, J. P.: Trans. ASME (J. of Basic Engg.). p. 462 (1969-9).
- [43] Tohida, et al.: Kiron 38-305, p. 123 (1/1972)
- [44] Tohida, et al.: Kiron 40-338, p. 2863 (10/1974)
- [45] Nakamura, et al.: Kiron 46-408, p. 1476 (8/1980)
- [46] Nakamura, et al.: Kiron 46-414, p. 227 (2/1981)
- [47] Imo, et al.: Kiron 43-369, p. 1863 (5/1977)
- [48] Muranoue; Kiron no. 700-15, p. 53 (10/70)
- [49] Muranoue: Kiron 42-335, p. 828, (3/1976)
- [50] Sakiyama, et al.: Kiron 45-397, p. 1257 (9/1979).

### 6.1 Centrifugation bladed diffusers

The diffusers used in centrifugation fluid machines (compressors and fans) are diverse in form and application and practical research has been carried out. However, there has been little adjustment of form in comparison to pipe-type diffusers. Therefore, the various data and examples of new research results will be presented here and a method for analysis of flow form and practical application will be touched upon. Moreover, we hope that this will play a role in improvement of centrifugation designs.

In addition, basic and structural research on runners and diffusers has been carried out since the 1950's and in comparison to the research on pipe diffusers in the 1920's, this history is relatively new.

#### (1) Flow of runner outlet

In Chapter 3, we explained calculations for the flow of runners and diffusers and this treatment involved simplification of the flow. The actual flow is a three-dimensional flow that varies axially in the flow path and is an inconsistent flow that varies through the blades.

The properties of this type of flow affect diffuser properties. We will first explain the features of flows emitted from runners.

#### (i) Inconsistent distribution

The first feature of this type of flow is that it is inconsistent in spatial distribution (three-dimensionality). The fluid introduced from an axial direction is rotated in a radial direction is an inconsistent distribution of fluid velocity. Moreover, the number of blades after pressure and velocity distribution is, therefore, inconsistent in a peripheral direction.

This type of distribution is also seen with potential flows. The actual fluid machine produce peeling of flows and secondary flows and the distribution is further complicated.

Eckardt [1] has studied the flow of high speed runners in centrifugation devices by variable flow determination probes (high velocity of 300 m/s). The flow emitted from the runner is in the direction of the width of the flow path and, therefore, is high speed high angle flow on the side of the hub (high energy flow). It is a low energy flow on the side of the side plate (shroud). Moreover, when the flow is viewed from the runner side, it is a high energy flow on the pressure side and low energy flow on the negative pressure side.

(ii) Slipping

When there is no loss, slipping of the flow occurs (difference between relative flow direction and blade outlet direction). The slippage is represented by the slippage coefficient  $\mu$  and there have been various equations for its calculations. The most recent is that of Wiesner [2].  $\beta_2$  is the angle of the blade outlet and  $Z$  is the number of blades.

$$\mu = 1 - \frac{\sqrt{\sin \beta_2}}{Z^{0.7}} \dots\dots\dots (6.1)$$

(iii) Time changes in flow and loss

Since the flow inside the path of the runner has a distribution in a peripheral direction, the flow that is emitted is

seen from the stationary side (diffuser side) as a flow that changes over time. This time a flow is related to the gradual deterioration inside the diffuser and has been studied by Imanishi [3]. (Measurements of flow emitted from runner). As shown in Figure 6.1, the distance from the periphery of the runner is paced on the axis of abscissas and changes over time in the flow angle (difference between maximum  $\alpha_{\max}$  and minimum  $\alpha_{\min}$  are placed on the axis of ordinates.

The changes in flow diminish up to a distance of 5 m from the runner outlet (runner radius of 3.4%) and remain the same thereafter. The nonuniformity of the flow is reduced with an increase of several per cent in the runner diameter. However, it is difficult to reduce this disuniformity in the direction of the flow path width. /135

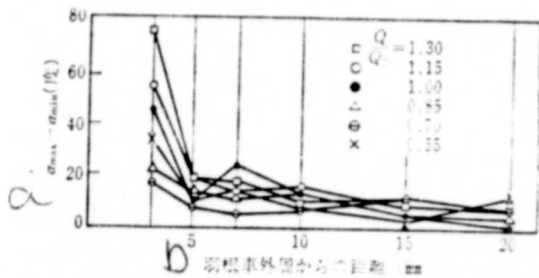


Figure 6.1. Diminishing changes at runner outlet. a--changes in angle (degrees); b--distance from runner (mm)

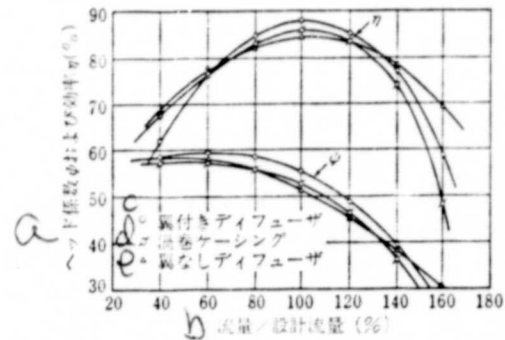


Figure 6.2. Properties of fans having bladeless and bladed diffusers. a--head coefficient  $\psi$  and efficiency  $\eta$  (%); b--flow-design flow (%); c--bladed diffuser; d--spiral casing; e--bladeless diffuser

## (2) Research on diffusers

The properties of fluid machines with bladed diffusers (pressure or head and efficiency) are higher than bladeless diffusers. Figure 6.2 shows a comparison of properties of fans



with a spiral casing only and the case of bladed and bladeless diffusers. The properties of bladed diffusers are high near design flow of 100%. However, there is a reduction with an increase in flow.

This is explained as an increase in pressure loss due to disuniformity between the inlet angle and flow angle. Basic explanations (quantitative explanations) use this theory today to a certain extent. However, today's theory is more detailed.

Next, there will be explanations of detailed measurement results. The flow was experimentally studied by Den of the /136 Soviet Union. Here, in Figure 6.3a and b, the measurements of flow and velocity were made using a bladed diffuser. (c) and (d) shows the results of studying distribution of static pressure measured in the upward current (15-20 points) and in the outlet (1-5 points). The flow as varied by three flows (numbers 1-3) and is shown for the center plate side and side plate side (dotted line and solid line). The flow is nonuniform with an upward current  $\frac{r}{r_2} = 1.05$ ,  $r$  is the radius of the runner outlet). However, it is uniform near the outlet ( $\frac{r}{r_2} = 1.36$ ). Therefore, the distribution of velocity and flow is nonuniform near the inlet and is almost constant at the outlet.

Next, we will explain the effects of the number of blades on the properties. In this text, the inlet angle  $\beta_4$  was made  $20^\circ$  and the outlet angle  $\beta_5$  was made  $31.1^\circ$  with the diameter of the outlet  $D_5$  and diameter of the inlet  $D_4$  being constant  $\frac{D_5}{D_4} = 1.12$ ,  $\frac{D_5}{D_2} = 1.39$ ,  $D_2$  is the runner diameter). When the number of blades  $Z$  was varied between 6 and 24, the correlation between the angle  $\alpha_4$  of the flow at the inlet and pressure coefficient  $C_p$  and the loss coefficient  $\zeta$  is shown in Figure 6.4(a). According to these results, the properties vary with the number of blades  $Z$  (when  $Z$  is high, the curve moves to the left side and the properties are of a low velocity and high pressure type). When  $D_4$  and  $\beta_4$  are varied and the number of blades  $Z$  is 11-22, the same tendency is seen (Figure (b)).

ORIGINAL ...  
OF POOR QUALITY

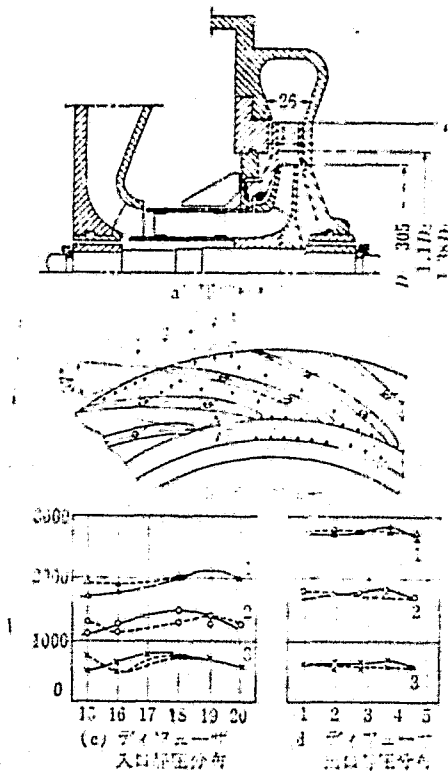


Figure 6.3. Static distribution of diffuser inlet and outlet.

(a) cross section compressor; (b) diffuser; (c) diffuser inlet static pressure distribution; (d) diffuser outlet static pressure distribution; a. Curves 1, 2 and 3 represent the flow coefficient  $\frac{C_{r2}}{U^2} = 0.174$ , 0.274 and 0.347

there was a reduction in efficiency with high flow-type properties being obtained.

(d) The correlation between the blade inlet angle ( $15^\circ$  to  $40^\circ$ - $19^\circ$ ) and properties is the same as that with wide type blades.

The difference between the blade outlet angle and outlet flow angle (deviation angle) is determined by the equation of Howell.

Shrustack (Soviet Union) has studied the effects of the blade form, angle of rotation and inlet angle of the compressor properties. In this research, a blade with a thick back end was used and the main results were as follows.

(a) When the number of blades was constant and the inlet angle was increased from  $15^\circ 10'$  to  $30^\circ 30'$ , the properties were those of a high flow type and efficiency decreased.

(b) When the inlet angle was constant and the number of blades increased from 19 to 31, the properties were those of a low flow type and efficiency decreased (Figure 6.5).

(c) When the blade inlet width  $b_3$  was increased ( $\frac{b_3}{b_2} = 0.87 \rightarrow 1.125$ ,  $b_2$  is the outlet width of the runner),

ORIGINAL FIGURE  
OF POOR QUALITY

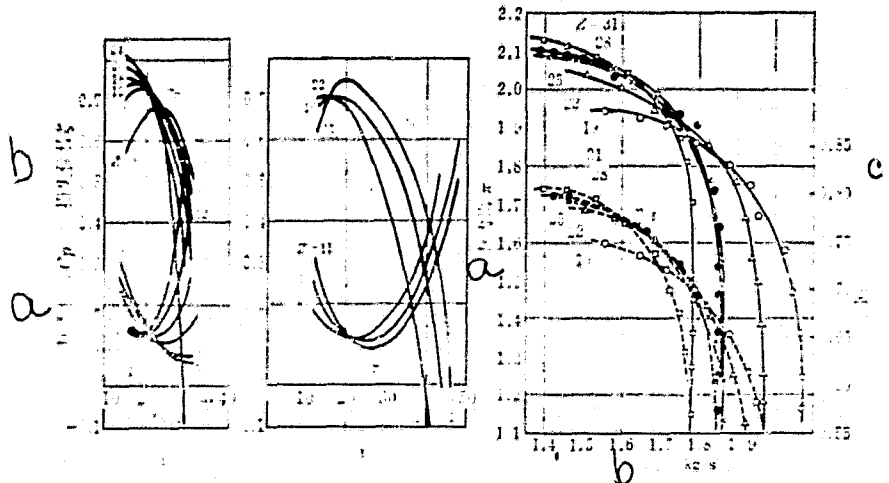


Figure 6.4. Correlation between diffuser number of blades and diffuser properties.  
a--pressure coefficient;  
b--loss coefficient

Figure 6.5. Correlation between number of diffuser blades and compressor properties.  
a--pressure ratio  $\pi$ ; b--flow amount ; c--efficiency of cross section

Figure 6.4 is a diagram of the properties of the diffuser, and Figure 6.5 is a diagram of the properties of the entire compressor. Measurements of the former are preferred for analysis of each structural part of the compressor. By visualization of the flow, it is possible to study properties which is what Nimo did [5]. In this study, he observed the flow of a water current in a bladed diffuser. The following results were obtained:

(a) Even when there is no impact flow (design flow point), there is a marked boundary layer.

(b) The boundary layer above the side wall is thin (same as with pipe diffusers).

(c) A secondary flow is seen in the blade flow path (Figure 6.6).

(d) The relative velocity of the back flow of the runner is low and, therefore, when the flow is viewed as relative flow velocity, which is the sum of the vectors with the peripheral velocity, it becomes a flow in a direction different from the main flow and a secondary flow is therefore produced.

(e) With large flows, there is a reduction in secondary effects and the flow orbit becomes two-dimensional.

The above mentioned results are constant. However, it appears that they will play a role in improvement of runner properties and diffuser efficiency.

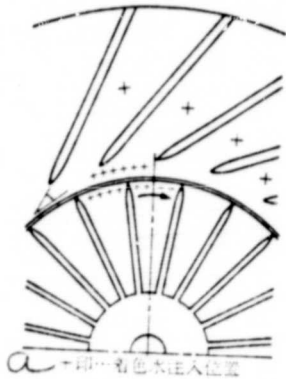


Figure 6.6. Visualization of bladed diffuser. a-- + indicates position of colored water injection

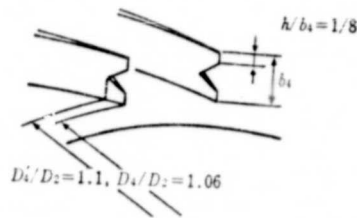


Figure 6.7. Diffuser blade form (V-shaped)

Yoshinaga [6] has studied the effects of diffuser form and flow and properties by combining bladed diffusers with runners (radius ratio of 1.35-1.6, equal wide angle of 5.1-15.5°, deacceleration ratio (inverse of area ratio) of 0.41-0.64). According to the results, the critical diffuser deacceleration ratio is 0.5 and the pressure distribution coincides with the calculated value for potential flows. Moreover, Figure 6.7 shows the inlet of a blade with a V-shaped current at a high velocity near the center of the path width. When /139 the flow changes as the diameter increases, the pressure and efficiency clearly improve.

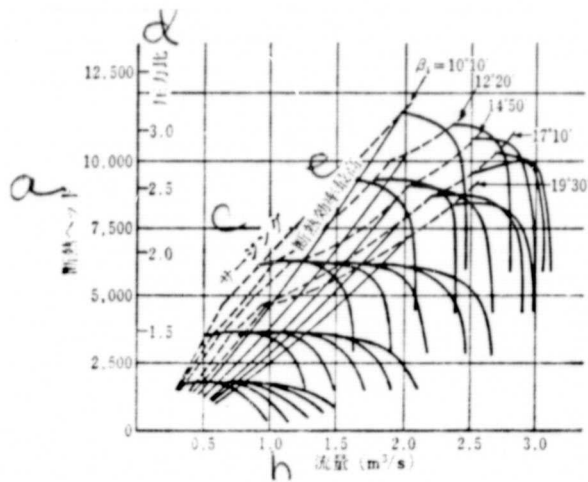


Figure 6.8. Correlation between diffuser blade inlet angle, r.p.m. and compressor properties. a--adiabatic head; b--flow ( $m^2/s$ ); c--purging; d--pressure ratio; e--adiabatic efficiency maximum value

The many above-mentioned studies show the properties of centrifugation pumps and how they are affected by diffusers. However, we will now mention the properties of bladed diffusers themselves in (3) and (4).

### (3) Effect of injection angle of blade inlet angle

The inlet angle of the blade should be the same as the angle of the flow from the runner or should be set with some angle of incidence. Changes in properties and problems with designs will be discussed.

Figure 6.8 gives the results of tests of Shung [7] where the inlet angles of blades were varied by  $10^{\circ}10'$  to  $19^{\circ}30'$ . The property curve shows 5 r.p.m. values. The axis of ordinates is the head or pressure ratio and the solid line shows the efficiency and the dotted line shows the beginning of surging. The head curve moves to the maximum flow side with an increase in the inlet angle. However, when velocity is  $\frac{1}{140}$  increased (pressure ratio of two or more), the curves does not move as much with a large angle. In addition, when the pressure

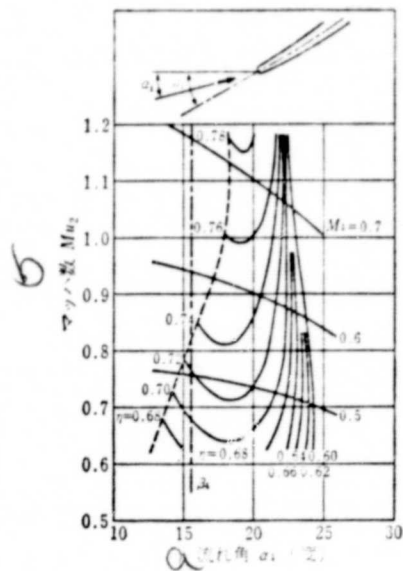


Figure 6.9. Correlation between diffuser inlet flow angle and properties (1).

$M_{u2}$  is the runner periphery velocity/suction inlet sonic speed.

$M_4$ : Mach number of inlet.  
 a--flow angle  $\alpha_4$  (degrees);  
 b--Mach number  $M_{u2}$

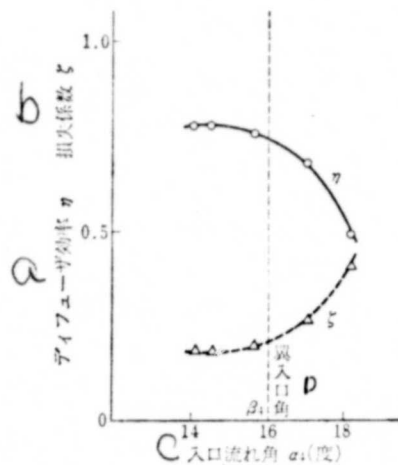


Figure 6.10. Properties and inlet flow angle (2).  
 a--diffuser efficiency  $\eta$ ;  
 b--loss coefficient  $\zeta$ ; c--inlet flow angle  $\alpha_4$  (degrees); d--blade inlet angle

ratio is 2-2.5 or more, the angle of efficiency crosses the surging curve and, therefore, the results are outside of the operation range (refer to 6.5 for effects of compressibility or Mach number).

Linsi [8] has studied the effects of varying the form of the runner, diffuser and spiral casing. Figure 6.9 shows the results of determining efficiency  $\eta$  and inlet Mach number  $M_4$  with the angle at the outlet  $\alpha_4$  on the axis of abscissas and the Mach number  $M_{u2}$  excluding velocity of blades at sonic speed on the axis of ordinates.

The angle of the inlet flow is 18-20° with maximum efficiency and when the inlet angle is used, it is 15.6° and when /141 the entire blade inlet section is used, it is 22.2°. Therefore, when 22.2° is the standard, the diffuser efficiency is at a maximum with an angle smaller by 2-4°.

The calculation of the inlet flow angle were carried out by the same method as given in Chapter 3. However, by these calculations, it is assumed that the flow in a constant flow is "one dimensional" in the direction of the flow path width. Therefore, this may differ from the actual flow. The author of [9] has studied the mean values by weighting using the radial directional component of the velocity  $c_r$ . This system was used to show the properties of the diffuser (Figure 3.5). In Figure 6.10, the efficiency is at a maximum and loss is at a minimum when the flow angle is 1-2° smaller than the conventional calculations (=blade inlet angle). Furthermore, the same tendency is seen in the round blade model tests (section (4)).

Sorgel has used bladed and bladeless diffusers in his study [10]. He used a straight line blade\* with various numbers of blades and blade lengths. The angle of incidence with the minimum loss coefficient\*\* (maximum angle of incidence is within a range of 0 to negative (minimum of -5°)). Therefore, with a small angle of incidence, the maximum properties are obtained with an optimum distribution of flow velocity.

---

\* The straight line blade is also called plate blade. It is a two-dimensional graph using a solid (substance).

\*\* The angle of incidence is the inlet flow angle-blade inlet angle. When the straight line blade is used, the same equation is used. However, the incidence angle is the opposite sign. The flow angle is measured from an axial direction with straight blades and is measured from a peripheral direction with centrifugal blades.

The author of [11] has carried out tests on the model shown in Figure 6.11(a) using the system of logarithmic spiral in Chapter 4. It is clear that the same flow conditions as with round blades can be obtained. Moreover, (b) in the figure shows a model without leading edges. The angle of incidence was varied with the velocity distribution by changing the form of the running path.

As was mentioned in Chapter 5, the boundary layer is rapidly produced in the convex section of logarithmic spiral diffusers. Therefore, when the flow conditions are like those in paths 4, 5, the deceleration gradient of the convex section is obvious and properties are decreased. In contrast to this, in the case /142 of paths 1, 2, the deceleration gradient is relaxed and formation of a boundary layer is controlled, thereby improving properties. The maximum properties seen with the angle of incidence at a negative value can be explained by the above-mentioned factors.

Kasugi [12] carried out tests on evaluations of the angle /143 of incidence of the flow. That is, taking the fact into consideration that the path is narrow and the flow distribution is not uniform and, therefore, the mean flow is obtained, the nonuniform coefficient of the flow (distortion factor) was defined. This was done by calculations of the flow angle. A 2.5° larger flow angle than with the mean conventional calculations was determined. Figure 6.10 illustrates this same fact.

#### (4) Research using round blade testing device

In order to study centrifugal diffusers, round blade testing devices (swirl flow producing devices) are not necessary). However, tests have been carried out on conventional fluid machines. It is very difficult to produce a two-dimensional flow with round blade testing devices. However, a uniform flow can



第6章 遠心型ディフューザ性能

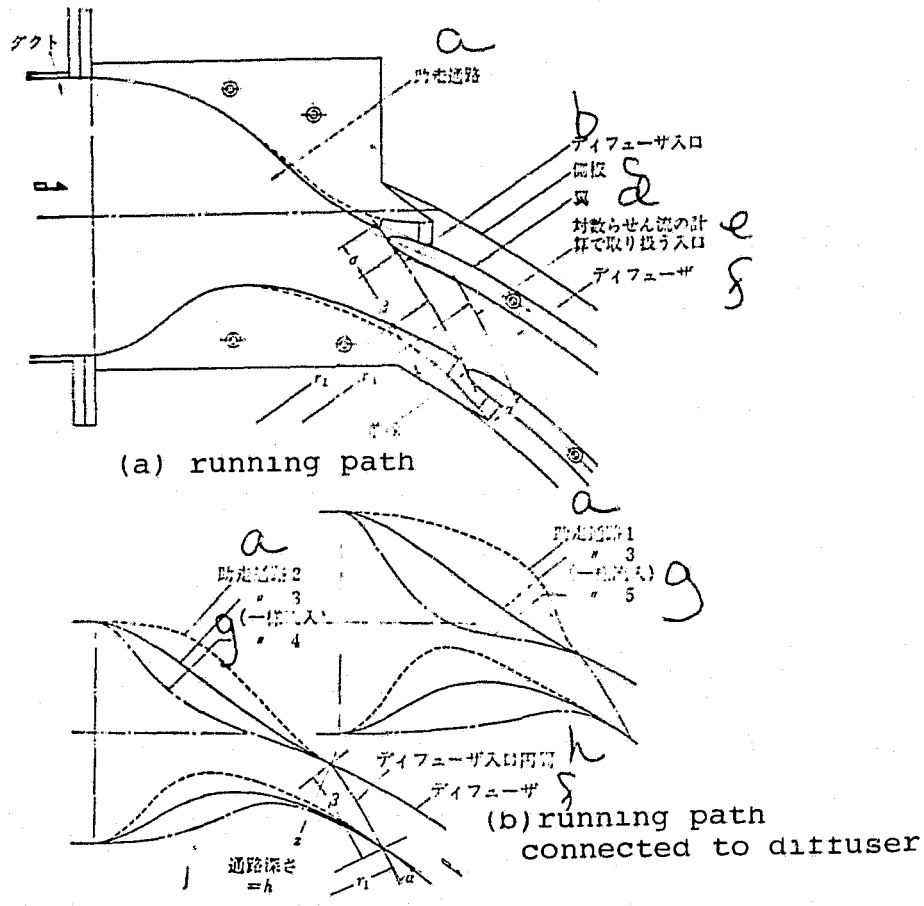


Figure 6.11. Tests on effect of inlet flow angles.

a--running path; b--diffuser inlet; c--side plate; d--blade; e--logarithmic spiral flow determinations; f--diffuser; g--(uniform flow); h--diffuser inlet periphery; i--path depth

be produced using a fluid machine itself. Next, two or three examples will be given.

The author of [13] has studied bladed diffusers using the round blade testing device in Figure 4.8 of Chapter 4. Figure 6.12 is one example of the properties (inlet angle  $\alpha_1^*$  and efficiency  $\eta$  and loss coefficient  $\zeta$  correlation). The number of blades affects properties and there is a tendency for the

/144

\* These tests did not use runners and therefore a 1 is assigned to the value.

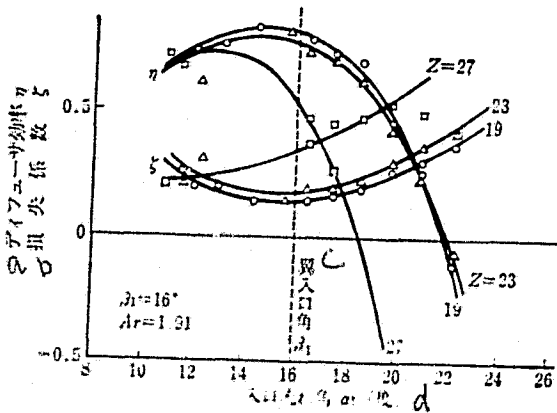


Figure 6.12. Properties of straight blade diffusers.  
 a--Diffuser efficiency  $\eta$ .  
 b--Loss coefficient  $\xi$   
 c--Blade inlet angle  $\beta_1$   
 d--Inlet angle  $\alpha_1$  (degree)

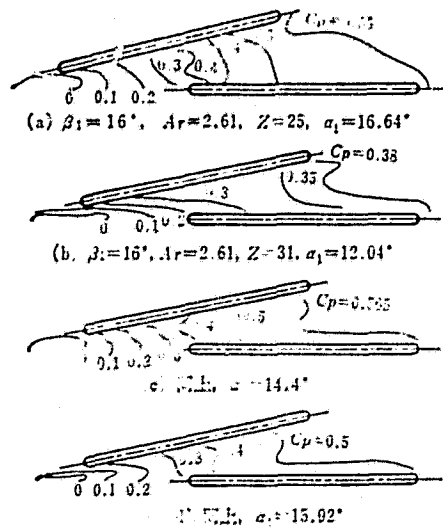


Figure 6.13. Pressure distribution of straight blade diffuser. (c) same as above; (d) same as above

angle of incidence to have the same effect as was previously mentioned. Figure 6.13 shows the curve of pressure obtained along the side walls. When the flow angle is smaller than the blade inlet angle, the pressure increase is maximum ( $C_p$  at outlet) and when the blades are increased, the pressure increase is considerable.

Sekichi, et al., [14] have studied the pump water wheel diffuser using a device similar to that in 4.8 (the form of the blade is a thickness ratio of 10% and 15%<sup>\*</sup>). The effects of the thickness ratio and the inlet angle and incidence angle on properties are shown below.

(a) The difference in distribution is mainly determined by the incidence angle, and thickness ratio and inlet angle have little effect.

(b) The rotation angle of the flow is mainly determined

\* The thickness ratio is the maximum thickness/blade length.

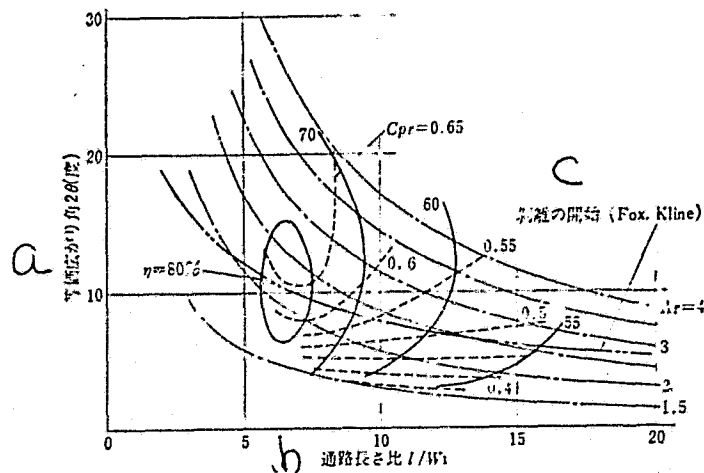


Figure 6.14. Properties of round blade diffusers. a--equal wide angle  $2\theta$  (degrees); b--path length ratio  $l/W_1$ ; c--beginning of separation

by the incidence angle.

(c) The value of  $\zeta$  is within a range where the angle of incidence is  $-5$  to  $0^\circ$ , which gives the minimum loss coefficient  $\zeta$  and is constant, regardless of the thickness ratio and inlet angle.

Figure 6.14 shows the results of several blade tests by the author [15]. When the length ratio  $\frac{l}{W_1}$  and equal wide angle  $2\theta$  [refer to 3.2 (1)] were placed on the coordinate angles, a curve was drawn with efficiency  $\eta$ , pressure coefficient  $C_p$  and area ratio  $A_r$ . In the figure, the maximum efficiency is seen near  $\frac{l}{W_1} = 6 \sim 7$ . When  $\frac{l}{W_1}$  is large, properties deteriorate. The /145 fact that the diffuser has a small inlet angle is significant. Moreover, when the length is small and the inlet angle is large, the efficiency decreases with an increase in the loss of blades. This is true for straight blades and round blades.

## 6.2 Bladed diffuser

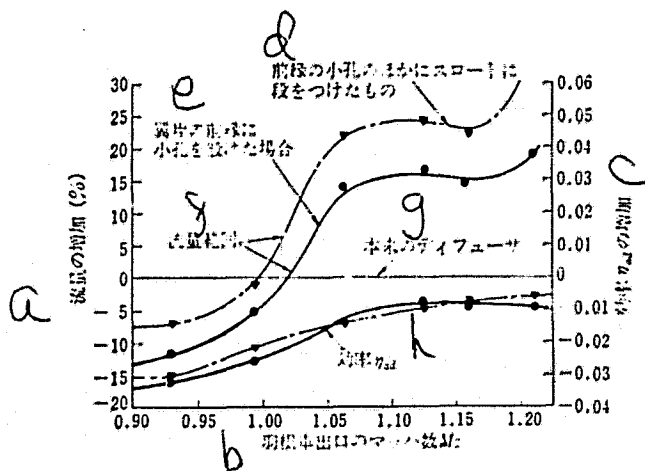
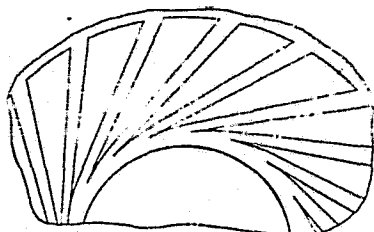
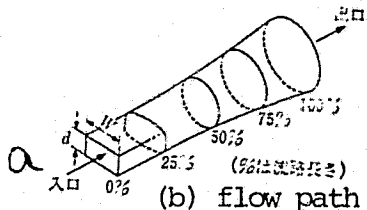


Figure 6.15. Properties of channel diffuser at high speeds. a--increase in flow (%); b--Mach number  $M_2$  at outlet of runner; c--efficiency  $\eta_{ad}$  increase; d--slots used in addition to small holes in leading edge; e--small holes set up in leading edge; f--flow region; g--original diffuser; h--efficiency



(a) diffuser front



(b) flow path form

Figure 6.16. Invention of Mason.

a--inlet; b--(% of flow path length)

The bladed application diffuser is a special diffuser and tests have been seen on actual development and basic and systematic studies.

### (1) Channel diffuser

The channel diffuser is used in high velocity and high pressure ratio compressors. Stahler [16] has studied this device.

/146

In this test, the flow was at ultrasonic speed and perpendicular impact waves were produced, as shown in Chapter 4\*. Moreover,

\* When the ultrasonic speed is reduced to subsonic speed, wave surfaces that change the velocity (impact waves) are produced. This increases the pressure of the flow (when perpendicular, the wave surface is perpendicular to the flow).

it is clear that the flow increases with increase in r.p.m. (Shung). Figure 6.15 is a graph of the Mach number of the runner outlet on the axis of abscissas and the center line in the figure shows the conditions of the diffusers (flow and adiabatic heat). The solid curve shows the properties where small holes are made near the leading edge of the blade, and the broken curves shows properties when a boundary layer trip is set up as small slits (holes)\*. The former provides a stable flow and the latter provides a constant peeling position. Therefore, the effective area of the slot is stable, and when the Mach number is 1 or more, the flow increases 20-30% and the efficiency decreases somewhat (1%). The efficiency of the diffuser is not shown. However, adiabatic efficiency of the compressor is about 79% with 33,000 rpm and 72% with 43,000 rpm.

The newest features of channel increase diffusers have been studied in detail\*\* (particularly in the U. S.). Therefore, the following examples will be given (improvements have been made so emphasis should not be placed on the examples).

Figure 6.16 shows the features of the invention of Mason /147 [17]. The profile of the channel is varied and Figure (b) shows the cases where the inlet is a flat slender section and the outlet is elliptical. Then changes in profile are determined by the following equation

$$\left(\frac{x}{a}\right)^s + \left(\frac{y}{b}\right)^s = 1$$

(provided that  $s = \infty$  at the inlet and  $s = 2$  at the outlet) (6.2)

---

\* This is used for small areas of slow paths (position in perpendicular line leading down from the front edge of the blade is called a slot).

\*\* The new technologies and features are being studied. This development is given in various patents and the patents should be referred to for detailed explanations.

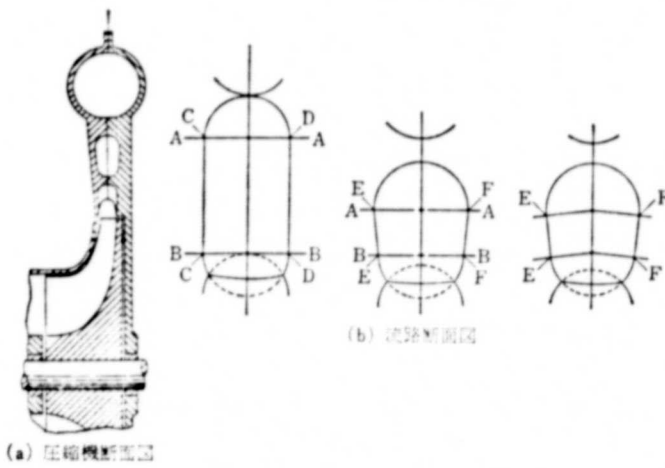


Figure 6.17. Invention of Fitzpatrick.  
 (a) compressor profile (b) flow path profile

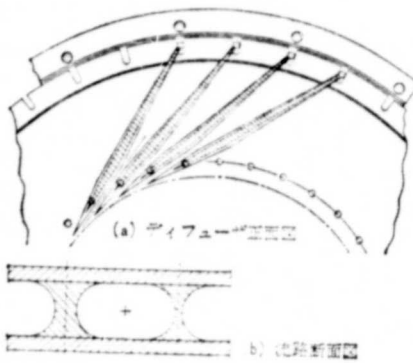


Figure 6.18. Invention of Balje.  
 (a) diffuser front view  
 (b) flow path profile

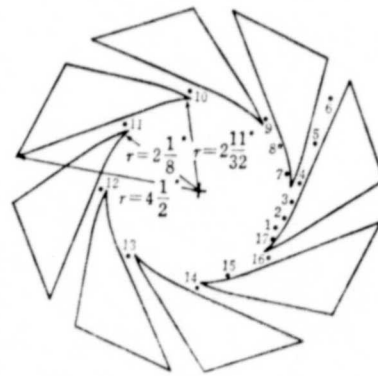


Figure 6.19. Vane-Island diffuser

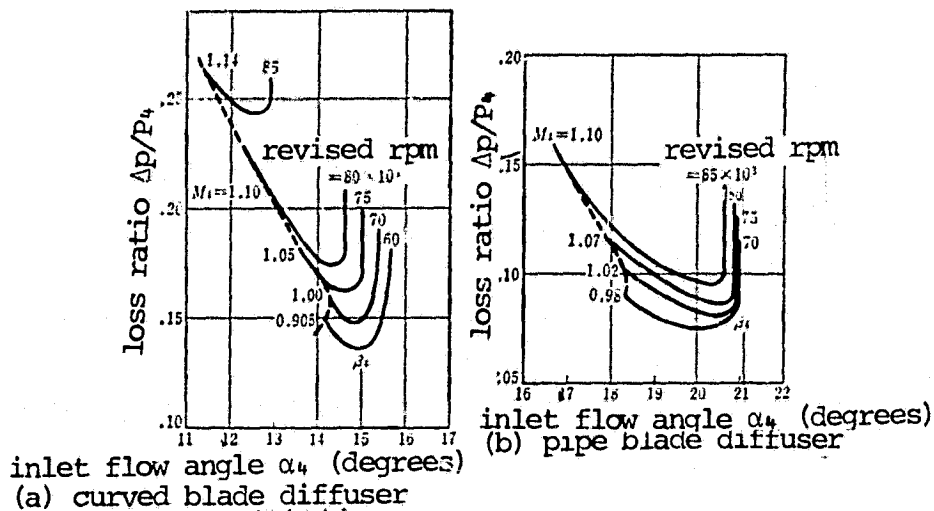


Figure 6.20. Comparison of pipe diffuser and conventional diffuser (1). (Stechkein (translators; Hamashima): Jet Engine Theory, (Corona, 1965).

Figure 6.17 shows the invention of Fitzpatrick [18]. Here there are two circles at the inlet and a circle at the outlet of the flow path profile. The advantages of this invention are the same as those in Figure 6.16. Moreover, it is possible to make large improvements in diffuser efficiency.

In the invention of Balje [19], a support is used for rotation\* by the gearing near the running edge of the material (blade) separating the path. Grooves are made in a radial direction in a circle around the periphery. The wheel is rotated around the center of rotation so that the inlet angle can be varied.

These inventions were taken from patent publications and, therefore, the results are not given. Please refer to the references for new developments in channel diffusers.

/148

The Vane-Island diffuser of Rayan and Yang [20] is shown in Figure 6.19. Tests were carried out with an inlet angle of

\* Refer to Chapter 7, page 182.

about 6°. The maximum efficiency was about 65% with five types of blades. The results of Runstadler, et al (refer to Chapter 5) are used as indices of channel diffuser designs. Moreover, when the position of the leading edge of the blade is 1.2 /147 fold the radius of the runner outlet, the loss coefficient is reduced (this value differs with the flow conditions but is usually considered to be standard).

As was previously shown, channel diffusers do show a correlation between form and properties. However, a general design policy has not been established. Various tests are necessary in the future.

## (2) Pipe diffuser

The pipe diffuser is a combination of individual pipes. Its cross section is round and the properties of the channel diffuser can be used.

Kenny [21] has studied the combinations shown in Figure 1.12 with high pressure ratio diffusers. Figures 6.20(a) and (b) show the values with regard to inlet flow angles (total pressure loss/diffuser inlet total pressure). The range of /150 operating flow is wider than with the curved blades and the pressure loss is also lower. Efficiency is 81.8% when pipe diffusers are used (Pressure ratio of 5). Moreover, it is 8.8% higher than with straight blades, and 6.8% higher than with curved blades.

In addition, improved pipe diffusers have an efficiency of 81.3% with a pressure ratio of 6. In contrast, the efficiency of curved blades is 73%. Furthermore, the profile is round and therefore the curve of total pressure (velocity) is concentric. The profile of curved blades or straight blades is long and slender, and the pressure curve is irregular.



Klassen [22] has studied a combination of four types of straight blade diffusers, bladed diffusers, two types of pipe diffusers, one with a wide angle of  $7.5^\circ$  and the other a conical pipe, using compressors with a pressure ratio of 1.9. The maximum efficiency with the conical and blade diffusers was 82%, while that with the rappa diffuser was 80% and with the straight blade it was 74% (Figure 6.21). The operation flow is 32% with conical, 23% with rappa and 81% with straight blades. Moreover, these three types of diffusers have little room (flow) up to production of surges. Therefore, it appears that the pipe diffusers are not superior to the other diffusers.

### (3) Tandem or slot diffusers

Tandem or slot diffusers come in various forms. Their features are mentioned here.

Shokuda and Mitsumura [23] use a compressor to study the three diffusers in Figure 6.22(a)-(c) (three tandem types\*, /151 two straight blade types and two round blade types). The efficiency and compressor efficiency with the three types of diffusers with inlet angles of  $22^\circ$  was 87 and 85% for the tandem, 83 and 82% for the straight blade and 83 and 82% for the round blade. The best properties were obtained with the tandem types. Moreover, the flow with the maximum compressor efficiency was on the order of round blade, tandem and straight blade types. However, more surging was seen with the round blade and, therefore, the tandem type (a) is most efficient.

Pampreen [24] has studied the tandem diffuser made from

---

\* The number of blades on the inside and outside are the same and the group of blades is constant with regard to position (optimum position).

3 and 2 blades using pressure ratios of 2.5 and 5 and has selected the number of blades so that they will differ with each diffuser. The 25 blade types used in axial compressors and the double blade type were used. The results indicate that a high compressor efficiency of 82-83% is obtained and that the property curve is flat with a pressure ratio of 2.5. Figure 6.23 (a) and (b) show the tandem diffuser properties with those of conventional diffusers. The properties of equal straight blade diffusers are also given (equal rotation angle). (The correlation between the inlet angle and incidence angle and total loss is shown). The tandem diffusers have a large drop in the curve and the operational flow is very wide. Moreover, they are very small diffusers.

Galbonof (Soviet Union) has studied designs for tandem diffusers. He has indicated the following.

/152

The outlet diameter  $D_6$  is 1.5-1.7 fold that of the inlet diameter  $D_4$ , and the surface area ratio is 3-4.4.

The flow path width expands in a radial direction and the wide angle is 4-6°.

The outlet diameter on the inlet side blade (= inlet diameter of blade on outlet side)  $D_5$  is the geometric mean of  $D_4$  and  $D_6$  ( $\sqrt{D_4 D_6}$ ).

The surface area ratio of the inlet side is 1.7-2.1, and the outlet angle is determined so this ratio is satisfied.

The incidence angle (-0.5~1.5°) and deviation angle\* (2-3°) should be considered in determination of the inlet angle and outlet angle.

---

\* Deviation angle-blade outlet angle-outlet flow angle  
[computations in Chapter 3 (diffuser outlet angle, etc.)].

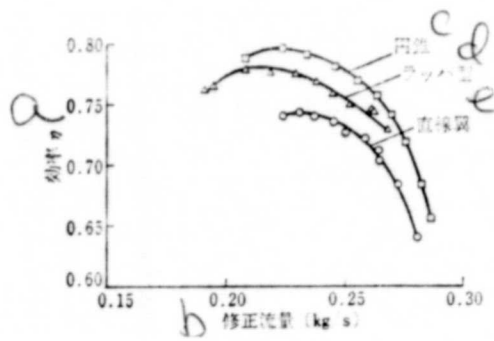


Figure 6.21. Comparison of pipe diffuser and conventional diffusers (Example 2) (Revised flow (kg/s is the same as in 6.20).

a--efficiency; b--revised flow; c--conical; d--rappa type; e--straight blade type.

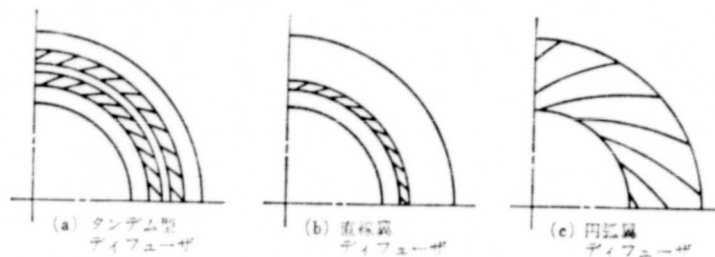


Figure 6.22. Various types of diffusers.

(a) tandem type; (b) straight blade type; (c) round blade type.

The peripheral direction of the running edge of the blade on the outlet side is the position that is 40-60% distance of 1 pitch from the back edge of the blade on the inlet side.

/153

Imo, et al. [25] have carried out studies on bladed diffusers (chord pitch ratio equal to inverse of pitch chord ratio). As a result, they have shown that the maximum pressure increase is seen with a low flow within a wide operation range. Moreover, they have also studied tandem diffusers where the pressure increase is high with a high flow on the outlet side [26]. That is, with round blades with a chord pitch ratio of 0.35 (chord pitch ratio in photographs in transformation to

straight blades) and round blades with a chord pitch ratio of 0.69, the position of the blade is only 9% of 1 pitch (Figure 6.24 (s)). Therefore, the pressure increase with a low flow and large flow is large.

From the above-mentioned research results, it is seen that the tandem and slot diffusers are technologies that improve fluid machines. However, their structure is very complicated and technical expertise is essential.-

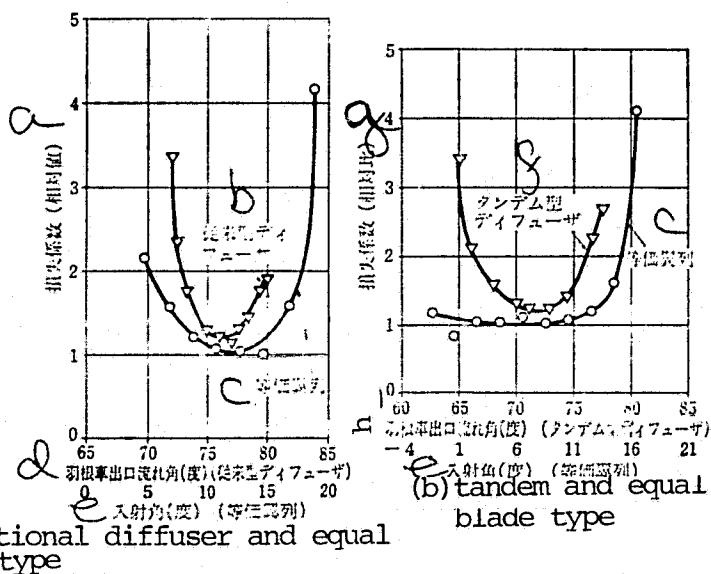


Figure 6.23. Tandem and other types of diffusers compared with blade type.

a--loss coefficient (relative); b--conventional diffuser; c--equal blade; d--angle of outlet flow of runner (conventional diffuser); e--incidence angle (degrees) (equal angle); f--tandem diffuser; g--loss coefficient (relative ratio); h--angle of outlet flow of runner (tandem).

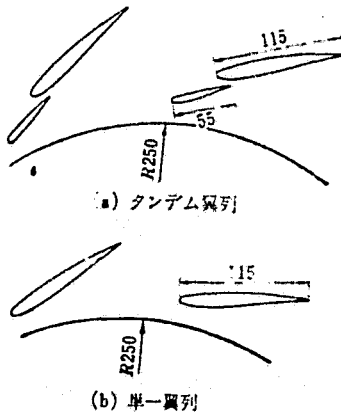


Figure 6.24. Properties of tandem and conventional diffuser. (a) tandem blade; (b) single blade.

### 6.3 Bladeless diffusers

The flow of bladeless diffuser is a centrifugal flow. /153  
 In comparison to other diffusers, it is relatively simple and has been studied often.

However, the research that has been carried out structurally has been done since the 1950's.

Runners can be used as devices for testing bladeless /154  
 diffusers (swirl flow generators). Moreover, model devices such as static guides and rotation screens are also used. Here we will report on the model testing device.

#### (1) Research and experiments on compressors

Figure 6.25(a) shows a model of a flow from a runner divided into jet velocity and wake velocity (Dean and Senoo [27]).  
 Figure (b) is the velocity triangle (j and w attached) to the /155  
 heat and wake models. According to this theory, changes in the radial direction of the flow can be determined. However, there is a difference in the absolute flows ( $c_{j1}$ ,  $c_{w1}$ ) of the jet and wake.

Therefore, mixtures are seen in the diffuser and the flow is constant with radial position  $\frac{r}{r_2}=1.06$  .

Shokumatsu [28,29] has studied centrifugal compressors with two openings shown in Figure 6.26 (a). According to these studies, there is no reduction in velocity or increase in pressure with a runner diameter increased to 9% (called runner region). However, there is an effect when the radius is increased (called total region). Therefore, the radial position of the boundary between the running section and total section (position where the boundary layer reaches center of flow path width is 1.07 fold the runner diameter. Figure (b) is the distribution in a peripheral direction of pressure at the design flow point. The flow is axially symmetric because of the spiral casing and distribution is not uniform.

From other examples it appears that when the diameter of the runner is increased by several percent, the flow is mixed.

Johnston and Dean [30] have introduced a simplified theory of Dean and Senoo. In this theory, the loss produced in the diffuser is the sum of the loss due to mixing and the two-dimensional flow frictional loss.

In tests on nonparallel diffusers, Tend of the Soviet Union has improved efficiency of bladeless diffusers with a small inlet flow angle. The angles of a narrow flow path width is varied by 0° (parallel wall) 3° and 5°. The flow is established with narrow outlet widths and there is improvement in diffuser properties and low flows (low flow angles). This is shown in Figure 6.17.

Next we will give examples of loss of flow and asymmetric flows.

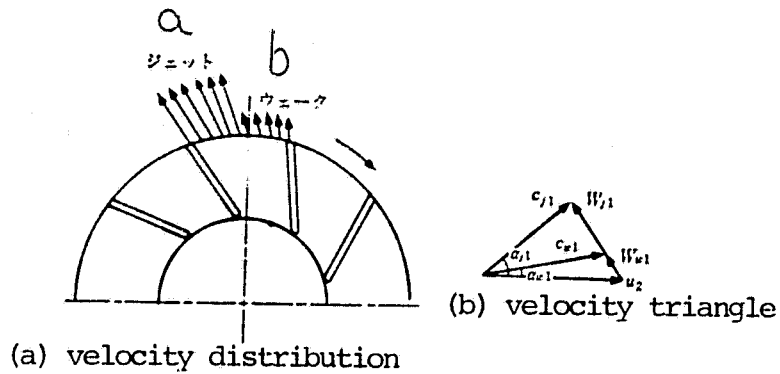


Figure 6.25. Flow of runner outlet.

a. jet; b. wake

図 6.25 羽根車出口の流れ

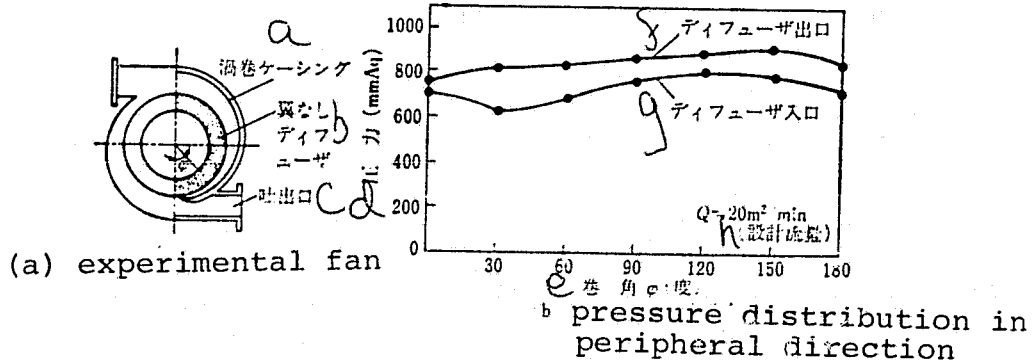


Figure 6.26. Parallel wall bladeless diffuser pressure distribution (1).

a--spiral casing; b--bladeless; c--outlet; d--pressure; 3--spiral angle (degrees); f--diffuser outlet; g--diffuser inlet. h--design flow.

Imo and Yamabuchi have used the 2-stage compressor with a low relative velocity (narrow path width with low flow). The frictional loss coefficient  $C_f (= \frac{\tau}{\frac{1}{2}\rho U^2}$ ,  $\tau$  is the frictional stress of the walls) is 0.011-0.017 with 1 stage bladeless diffusers and the mean friction a loss coefficient with 2-stage diffusers is 0.006-0.014. Therefore, the loss is smaller with 1 stage diffusers. This appears to be due to the fact that the diameter of the measurement position is larger in 2 stage diffusers (Johnston and Dean used the data of Gardow and showed that  $C_f=0.02\sim0.035$ , and Janssen showed that  $C_f=0.01\sim0.025$

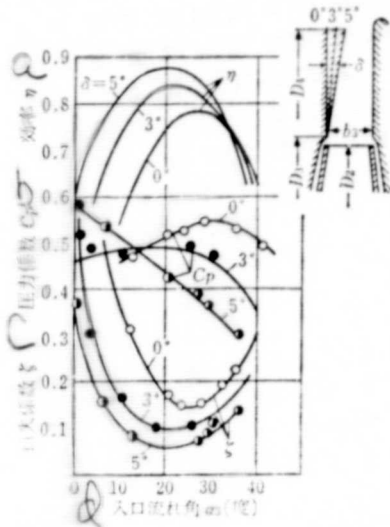


Figure 6.27. Properties of bladeless diffusers with nonparallel walls.  
 a--efficiency; b--pressure coefficient; c--pressure loss;  
 d--inlet flow angle, (degrees).

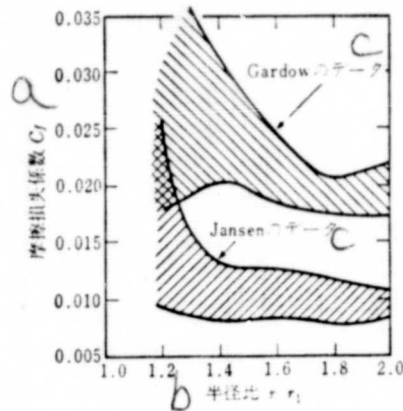


Figure 6.28. Mean friction coefficient loss of parallel bladeless diffuser.  
 a--friction loss coefficient; b--radius ratio;  
 c--data of.

(Figure 6.28). In any case, the loss is large with a low radial ratio. Therefore, the  $C_f$  is high with bladeless diffusers having a radius ratio of 1.4 or less).

Senoo and Ishida [32] have studied flows of bladeless diffusers using the compressor in Figure 4.4 and have analyzed the mechanism by which a slow is made uniform. The results indicate that because the time mean value of total pressure is greater



than the flow mean value with strong nonuniform flows, the efficiency of the runner is overevaluated when probes are used and the efficiency of the diffuser is therefore underevaluated (loss is overevaluated).

Moreover, Senoo and Ishida [33] have shown that the method /157 whereby pressure loss is determined using the sum of the mixed loss and friction loss is sufficient only when nonuniformity is low.

Senoo [34] has studied the case of asymmetry with different velocities and boundary layer thickness on both walls of the diffuser. He has calculated the increase in pressure and flow velocity distribution. Figure 6.29 shows a comparison with that of the references (Jansen). However, the two are in considerable agreement. When compared to the case of nonuniformity in the direction of the periphery, it appears that the flow is more unstable with nonuniformity in a radial direction and a reverse flow is readily produced.

Next, examples of bladeless diffusers will be given.

Lown [35] has designed a structure where bladeless diffusers rotate while the turbine attached to the long end of the diffuser is operating with air being leaked from the radial crevices between the runner and diffuser (Figure 6.30). The purpose of the invention is to prevent peeling of the boundary layer and improve efficiency.

Okamoto has measured changes in static pressure distribution with changes in flow [36]. As a result, he has determined /158 that the flow in an axial direction (called equilibrium flow) Figure 6.31 (b) is present and the pressure curve is approximately concentric with this flow. However, when the pressure is constant with any other flow (Figures a and c), the pressure

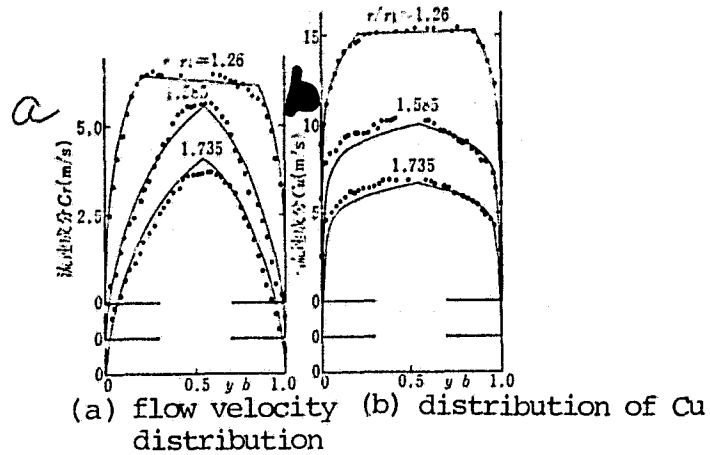


Figure 6.29. Distribution of velocity with asymmetric inlet (Comparison of measurement results and theoretical results). a--flow velocity distribution.

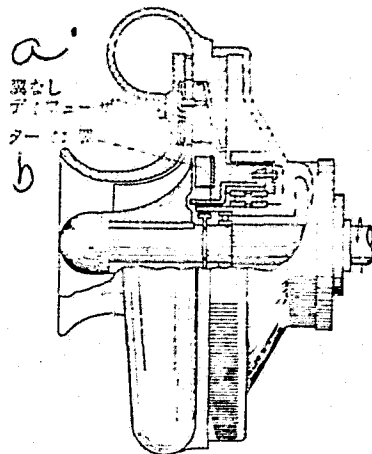


Figure 6.30. Rotating bladeless diffuser (Lown invention). a--bladeless diffusers; b--turbine blade.

curve is a unique form. The equilibrium flow is not the same as the design flow for fans.

Furuii [37] has studied bladeless diffusers also. In his tests, the nonuniformity  $B$  (ratio of mean flow in a diametric direction to mean value alone) of the flow at the inlet is large when the ratio  $\frac{b}{r_3}$  of the path width and inlet radius

is high and velocity is high (Figure 6.32). The results show that there is a marked reduction in efficiency. (This is characteristic of bladeless diffusers.)

(2) Research and theories on model devices

/159

The MIT group has studied a three-dimensional boundary layer (Figure 6.33). Gardow [38] has also used the same type of device as in Figure 4.6 (swirl flow generator) to study the flow of bladeless diffusers.

Jansen [39] has studied the improved device of Gardow. He has designed a flow with a uniform velocity (or a flow with a sufficient boundary layer production) and determined the flow in the diffuser. He has introduced a theoretical equation for flows. (Range of  $\alpha_1=19.6\sim 43^\circ$ ). Figure 6.34 is a graph showing the correlation with regard to all of 43 of the radial position  $\frac{r}{r_1}$  ( $r_1$  is the inlet diameter and the pressure increase  $(p-p_a)/\frac{\rho}{2} U_1^2$  ( $p_a$  is atmospheric pressure. The experimental results agree with the theoretical results.

The flow between two parallel plates has been studied to a great extent (assuming velocity distribution of boundary layer and frictional stress).

Pampreen [40] has studied the noncompressed boundary flow in bladeless diffusers (the flow path width is in reverse proportion to the diameter).

According to this study, the loss is lower than in parallel wall diffusers when the radial ratio  $\frac{r}{r_1}$  is less than 1.15.

Moreover, the radius position where peeling occurs is larger (study of Den).

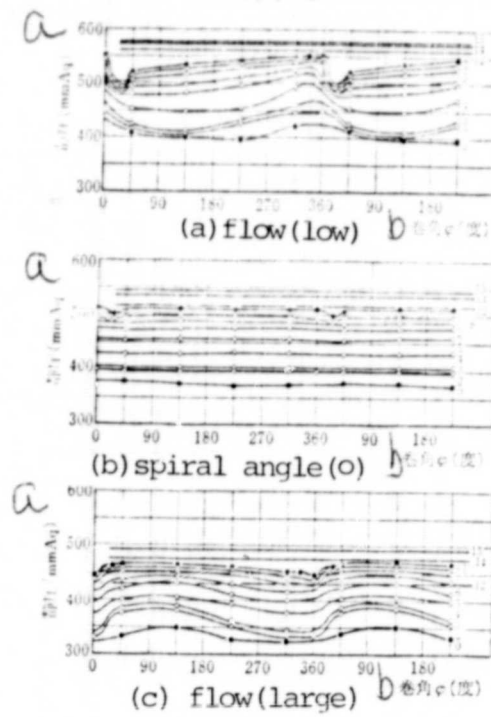


Figure 6.31. Distribution of pressure in parallel wall bladeless diffuser (2).  
a--static pressure; b-- spiral angle (degrees).

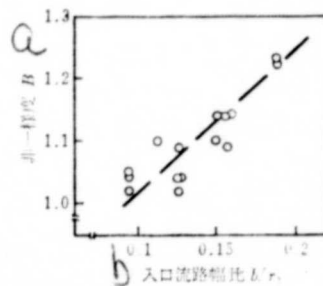


Figure 6.32. Correlation between inlet flow path width and nonuniformity.  
a--nonuniformity; b--flow path width ratio.

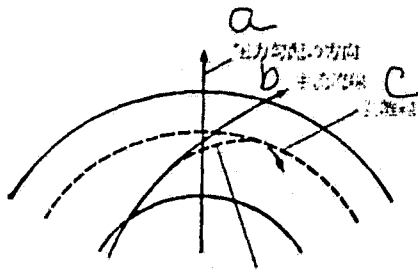


Figure 6.33. Boundary layer in bladeless diffuser. a--direction of pressure gradient; b--main flow line; c--peeling line.

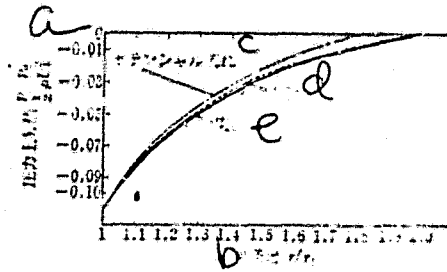


Figure 6.34. Increase in pressure with bladeless diffuser. a--pressure increase; b--radius ratio; c--potential flow; d--theoretical; e--experimental.

Ferguson [41] has studied the flow of swirl diffusers with noncompressed fluids and a constant flow width. He has used the one-dimensional method and calculated the flow using the efficiency and frictional loss and using boundary layer calculations. When the former method is used, the loss coefficient is very high (Dean and Senoo, Gardow and Jansen). Moreover, when boundary layers are used, they do not confirm the hypothesis of a velocity distribution in the direction of the main flow (Jansen and Mager and Kawaguchi and Furuya). Therefore, a one-dimensional design method is being used.

/160

Next, we will give special examples of research on bladeless diffusers. Broecker [12] has studied the production of a swirl flow and tested bladeless diffusers. Moreover, he has used the one-dimensional flow theory (Eckert, et al.) to compare the experimental results. Figure 6.35 (a) shows that when the width  $b$  is increased to  $B$  at the inlet of the diffuser [Refer to Figure (b)], the correlation between the radial ratio  $\frac{r}{r_1}$  and pressure increase can be obtained using the flow path width ratio  $B/b$  as the parameter. When  $B/b$  increases, there is a reduction in the pressure increase.

Vielhaber [43] has attached rods and plates to the periphery of the inlet of bladeless diffusers and measured the flow and efficiency (Figure 6.36 (a) and (b) use of runner for generation of swirl flow). The correlation between  $\eta$  the number of plates

or rods and  $\eta$  efficiency of the diffuser is shown in the figure. When the size and number of rods increases, the  $\eta$  decreases (with rods, efficiency is  $n > 4$ ). Moreover, efficiency decreases to a large extent with plates. In the figure  $\alpha_1 = 90^\circ$ . However, the reduction in efficiency is larger with  $\alpha_1 = 31.6^\circ$ . The elbow in bladeless diffusers is produced by "disruption" (peeling) at the inlet. This research is very important from the point of design and stability in measurements.

Moller [44] has studied the device in Figure 6.27 and has analyzed radial flows without a swirl. The flow at the axial direction shows peeling at the inlet. He determined an equation /162 that gives the pressure  $p$  (function of radius  $r$ ) that satisfies a flow path and flow with minimum pressure  $p_{\min}$  and position of peeling  $r_R$ . The Reynolds number (based on radius  $r$ ) that provides distance (transition) is about 2000 and is the same for round pipes. The ratio of inlet flow path width  $\frac{b}{r_1}$  is large at 0.5 or more. This is suitable for flows of low velocity compressors, etc.

Feireisen, et al. [45] have studied radial flows with the device in Figure 4.9. The curve for the pressure coefficient  $C_p$  in 6.38 was obtained. The  $\frac{2(r_2 - r_1)}{b}$  (length ratio) is on the axis of ordinates. The curve representing the optimum form is similar to a two-dimensional or conical diffuser and when the /163 surface ratio is the same, the pressure increase is larger than that with two-dimensional or conical diffusers. However, the flow of parallel wall diffusers is affected by obstructing devices set up in the inlet and a pressure increase is impossible with an area ratio of 4 or more.

There has been great progress in calculations of pressure increase and efficiency. Moreover, diagrams and equations for conditions (for instance flow angle) have been devised.

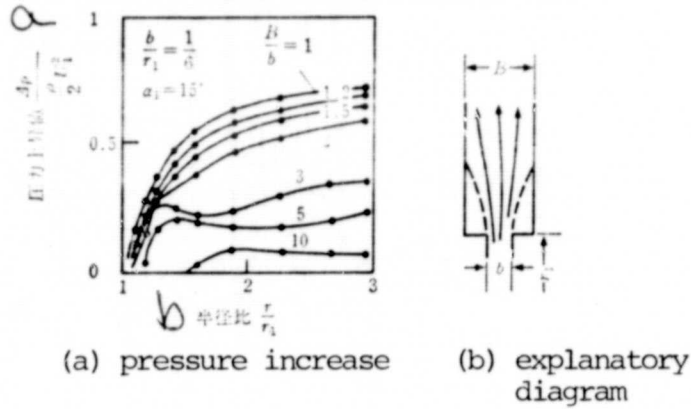


Figure 6.35. Ratio of radius and ratio of inlet width.  
 a--pressure increase; b--radius ratio.

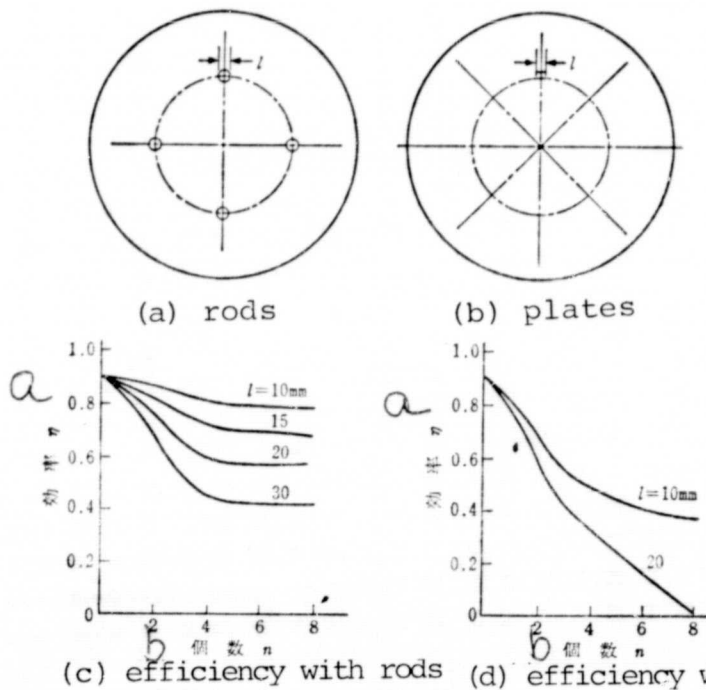


Figure 6.36. Correlation between obstruction and efficiency.  
 a--efficiency; b--number.

ORIGINAL PAGE IS  
 OF POOR QUALITY

ORIGINAL PAGE IS  
OF POOR QUALITY

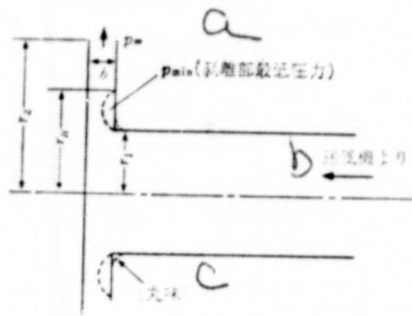


Figure 6.37. Bladeless diffuser tests (without swirl).  
a--pressure with peeling; b--from fan; c--rods.

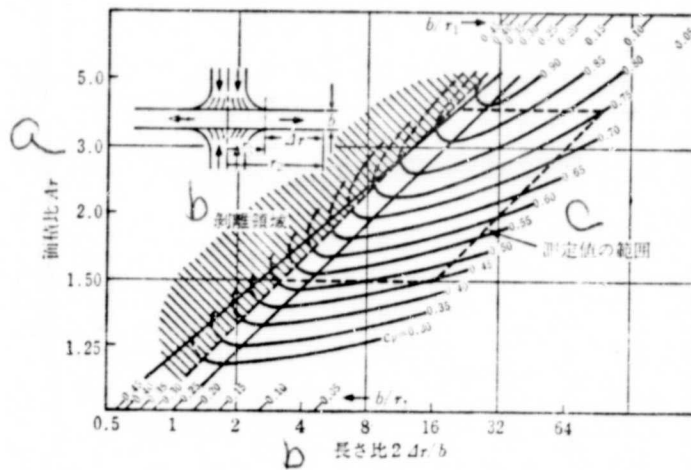


Figure 6.38. Property map of bladeless diffuser.  
a--surface ratio; b--peeling region; c--measurement.



### (3) Inconsistent flow of bladeless diffusers

A large scale inconsistent flow over time is indicated (swirl loss or surging). It has become clear that swirl loss is seen with bladeless diffusers (loss region is in the peripheral direction).

Jansen [46] has studied the fact that the flow in bladeless diffusers is unstable under certain conditions. The broken lines in Figure 6.39 show the maximum and minimum velocity section produced, and this condition extends at a constant velocity in the direction of the arrows. These are called cells 1, 2 and 3 from the left to right. Jansen showed that, when a flow /164 consists of two-dimensional viscosity and perturbation, a theoretical analytical method can be devised. In these tests 2 cases were used and one case was observed with strong-swirling. The flow becomes stable with the flow angle at  $\leq 0^\circ$  in the boundary flow line (Figure 6.33) according to the above-mentioned theory [39]. When  $\alpha_1$  is small and the Reynolds number is low, the radius ratio is high and instability occurs.

Baade [47] has shown that the changes in flow can be measured with a heat line device. As shown in Figure 6.40, in addition to change (2) based on an infinite number of blades and change (1) based on swirl loss, velocity change (3) (inconsistency of flow in runner) is also present. These changes occur even when the distance from the runner is large.

Imaichi [48] has studied swirl flows with axially symmetric fans. He has given a correlation between the reverse current and swirl loss. Moreover, he has determined a value for the radial direction of the reverse flow and has made determinations of swirl loss possible. The radial direction of the reverse current is the swirl loss produced when the reverse current occupies a certain range (according to these tests, approximately 15% of  $(r_2 - r_1)$  ).

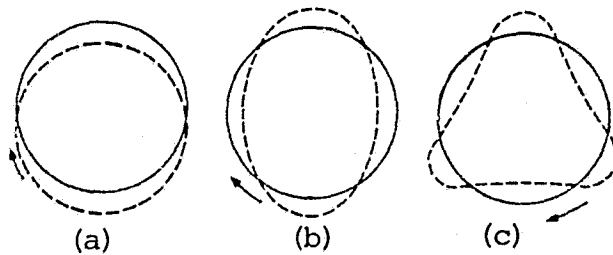


Figure 6.39. Swirl loss.  
 (a)--cell 1; (b)--cell 2; (c)--cell 3.

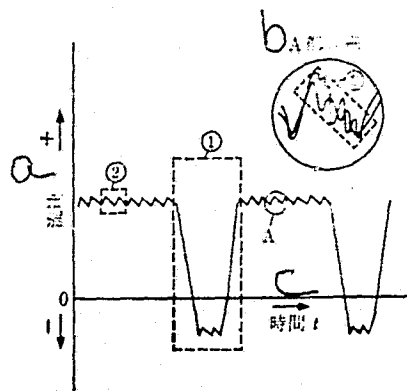


Figure 5.40. Time changes in flow with bladeless diffuser.  
 a--flow velocity; b--a section detail; c--time.

Research has been carried out on inconsistent swirls (swirl loss and surging). Further research is anticipated in the future.

(4) Semiaxial flow bladeless (or bladed) diffusers

There has been little research on axial flow (or mixed flow diffusers. The following are some examples. Research has been carried out on this type of compressor by NACA of the U.S. since the 1940's. For instance, tests have been carried out by Brown and Bradshaw [49] on an axial flow compressor with a runner diameter of 5.62 inches and diffuser diameter of 17 inches. The flow paths of the inlet cross to form an acceleration running section.

Otaro [50] has used the axial flow compressor in Figure 6.41 to study the axial flow bladeless diffuser where the head angle surrounds two conical surfaces. The flow is complex because it has a pressure gradient in the direction of flow and the direction of flow path width. The following properties are obtained.

(a) The pressure is higher on the center plate side than the side plate side.

(b) The position of the direction of path width of the highest velocity moves to the side plate side with an increase in radius.

(c) When the inlet angle is small, a counter current is produced at the center plate and the current resembles the boundary layer.

(d) The loss is greater than with centrifugation types and decreases with an increase in radius ratio.

Otaro [51] has also measured the three-dimensional disrupted flow boundary layer of semiaxial flow diffusers. In the studies he made the angle of flow equal in the direction of the flow path width using a rotation screen (net) and determined the flow path width using a rotation screen (net) and determined the flow on the convex surface (center plate side) and concave surface (side plate side). When the inlet angle is low, the boundary layer is marked and pressure increase is therefore low. /166

Friberg and Merigoux [52] have carried out studies (coolant gas tests) using the ultrasonic compressor in Figure 1.16 with a semiaxial flow bladed diffuser. The pressure ratio is 1.8, the total loss is less than 6% (pressure ratio of compressor

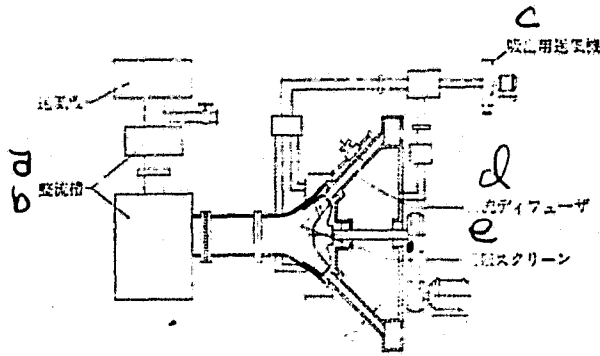


Figure 6.41. Axial flow diffuser testing device.  
 a--fan; b--rectifier tank; c--outlet fan; d--flow diffuser;  
 e--screen.

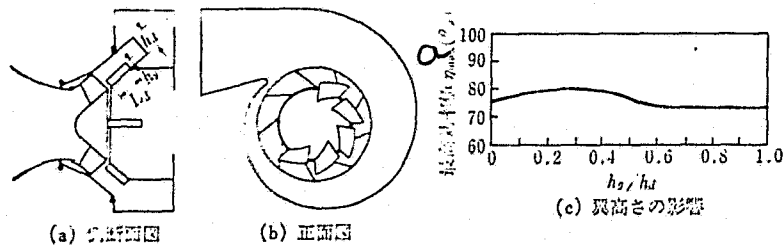


Figure 6.42. Axial flow compressor using diffuser (new proposal).  
 (a)--side view; (b)--front view; (c) effect of blade height;  
 a.--maximum efficiency.

is 2.3 and efficiency is 90% or more). The Mach number of the inlet is 1.2 and the Mach number of the outlet is 0.7.

In actual proposals for diffusers or compressors of semi-axial flow systems, the following examples are noted. Figure 6.42 a-c are the semiaxial flow compressor of Censhi [53]. Blades of height  $h_g$  and length  $L_d$  are set up inside a semiaxial flow path (width ( $h_d$ )) connected to the outlet of a semiaxial runner. The

outlet of the diffuser is connected to the spiral casing as in the case of centrifugal compressors. Semiaxial flow paths to which blades are not connected have been used, but are not preferred because a counter current is produced. In this proposal, the height  $h_g$  of the blade is 0.1-0.5 fold the width  $h_d$  of the flow path and within this range, efficiency of the fan is improved, as shown in (c).

#### 6.4 Axially symmetric flow paths

##### (1) Outlet side curved flow path

There has been little research on the flow paths used in stages of the centrifugation fluid machines and at inlet and outlets. The most recent research has been carried out in Japan. /167  
Examples of these studies will be given.

The outlet curved flowpath is a flow path that is axially symmetric and has a profile that is a reverse U shape which is used between diffusers and guide paths. It is the opposite of the inlet side curved flow path (flow path set up between guide path and next runner). Examples will be given.

Sekichi [54] has studied the curved flow path with the device in Figure 4.12. As shown in Figure 6.43, a swirl flow is produced inside the static guides (inlet angle  $\alpha_2=10\sim 35^\circ$ ; and the flow is then measured with the radius of the ends of the reverse U shaped curve being 200 mm, the curvature radius of the outside of the curve being 60 mm, and the widths of the flow path being 20 and 30 mm.

In this test, a reverse current is produced along the inside walls when the angle of rotation from the inlet is  $\phi = 90^\circ$ . However, the distribution of velocity in the direction of width is very irregular, but can be recovered to a certain extent at the end of the curve. The extent of recovery is worse with a flow path with a large width. The loss coefficient of the curved flow path and changes in the angle of flow were compared

with the calculations of Eckert (Chapter 2). However, all of the experimental values were larger (this may be due to the fact that Eckert used a one-dimensional loss coefficient).

Kishita and Senoo [55] have used the swirl generator made up of runners and booster\* runners. Tests were carried out with the ratio of diameter of curvature of the outside and inside being 1.4 and 1.8. The tests were performed with  $\alpha_2=10\sim90^\circ$ . The results show that the pressure loss with a strong swirl is due almost only to friction, but that in the case of a weak swirl, the friction loss is greater than the calculated value (that is, one-dimensional analysis is insufficient) and the effects of curvature on flow are extreme, particularly in that the peeling phenomenon can be prevented by changing the properties of the boundary layer on the outside walls. /168

The authors of [56] studied the case of no swirl in curved flow paths with a reverse U shape (inlet side curved flow path). These have been mentioned in Chapter 2. In this type of flow path, the ratio of outer curvature radius/inner curvature radius or of flow path width/mean curvature radius is greater than in the case of emission flow paths. Therefore, the flow readily becomes nonuniform, and the point of interference is very important.

## (2) Emission diffusers

The emission diffuser is a diffuser that has flow paths that are axially symmetric and from which an axial flow is emitted as a radial flow by being rotated. It is used for axial flow fans, etc.

Zaryankin, et al., (Soviet Union) have studied systematic changes in the form of this type of diffuser. That is, they

---

\*The range of operation of swirl-generating runners (changes in flow angle) is wide and therefore runners or fans can be used to reinforce pressure.

carried out studies by changing the dimension ratios of  $\frac{D_2}{D_1}$ ,  $\frac{D_2}{D_1}$ ,  $\frac{r_2}{r_1}$ ,  $\frac{L_1}{l_1}$ , and surface area ratio  $A_r$ , as in Figure 6.44 (a) and determined the correlation between the curvature radius ratio  $\frac{r_2}{r_1}$  and the loss coefficient of  $\zeta$  as shown in (b). In this figure, the range of the loss coefficient  $\zeta$  is 0.5-0.6 (in this model it is 0.4-0.75) and the efficiency of this type of diffuser is relatively low.

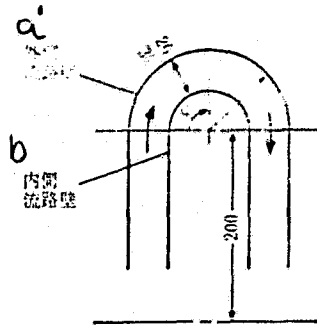


Figure 6.43. Outlet side curved flow path tests. a--outer flow path walls; b--inner flow path walls.

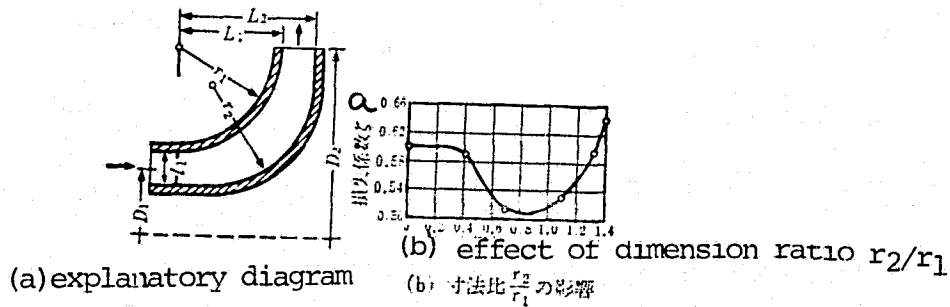


Figure 6.44. Tests on emission diffusers.

a--loss coefficient; b--radius ratio  $r_2/r_1$ .

Senoo, et al. [57] has applied the calculation method /169 for boundary layer formation and peeling to the two-dimensional diffuser and has studied the form of the emission diffuser (short length).

As a result, he noted that the evaluation method for peeling and the boundary layer calculation method for two-dimensional diffusers can be used because an inner and outer radius ratio of inlet = 0.7 (Figure 6.45), width direction length = 0.73 fold of inlet diameter, surface area ratio = 2.6, pressure coefficient = 0.63. For instance, evaluations of peeling were carried out with the following form coefficient  $H_s$  (outer flow path wall) ( $\delta^*$  is the thickness and  $b$  is path width).

$$H_s = 1.8 + 7.5 \frac{\delta^{*2}}{b} \dots\dots\dots (6.3)$$

According to these studies, the length ratio is approximately the same as that of annular diffusers and the same pressure coefficient was also obtained. A counter current is readily produced in the case of a swirl flow and therefore, when the surface area ratio is high, there is a marked reduction in properties.

### (3) Guide paths

Guide paths are paths having normal blades and are not axially symmetric. They have a function similar to the paths in above-mentioned (1) and (2). They will be briefly described here. There are a few examples of research on these paths; however, there are many diverse forms and the results do not always agree.

Figure 6.46 is the development of Sprecher [58] for using in-water generator pumps. It shows the three dimensional blades formed by connecting the bladed diffuser with guide blades. There have been few examples of use of this connected blade series because manufacture is difficult. Properties are very good when compared to conventional separated types (pump efficiency of 85% in this example). Therefore, they are sometimes





The reasons for this appear to be:

- (a) The total angle of rotation is low with S100,
- (b) The leading edge is in front of the 180° curve (curved flow path) and flow conditions are good,
- (c) The flow path length is long, and the rotation and expansion can be adjusted,
- (d) and the aspect ratio (flow path width ratio) is very good.

The authors have carried out studies on flows and the form of guide paths with the device in Figure 4.5. According to these tests, the total pressure loss is 0.7 - 1.2 fold the inlet operating pressure. This is due to the fact that in conventional types, the middles of the path between blades is wide and the flow peels as a result. When the blade form is improved as in Figure 6.47, the loss coefficient can be reduced to 0.4 or less. Moreover, the changes in the flow angle are small in curved flow paths when the flow is varied and operation of the next runner is efficient [61].

/171

Yoshikura has studied the potential flow in round blades where the flow is in the direction of the guide blades, as in multistage pumps, etc. [62]. (The device is a suction type consisting of blades for producing a swirl flow in the outside of the sample guide blades). In this study, the distribution of pressure from the experiments was approximately the same as the theoretical pressure distribution, but the values did not agree when the angle of incidence was increased.

From the above-mentioned it appears that, although it is difficult to obtain general theories, tests should be carried out in the future.

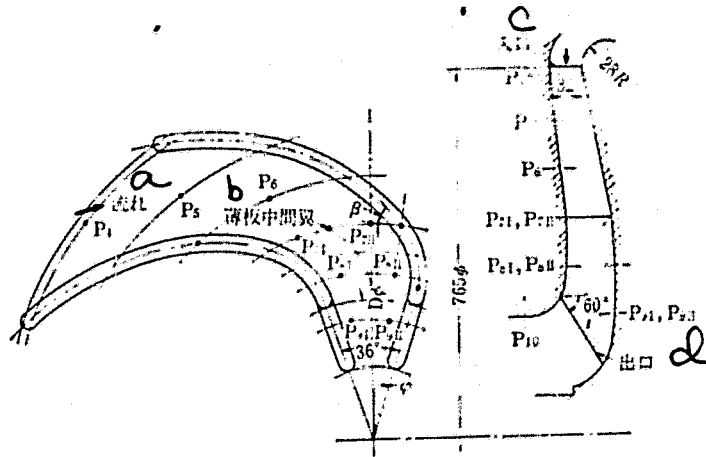


Figure 6.47. Potential flow guide paths.  
 a--flow; b--blades between thin plates; c--inlet;  
 d--outlet.

### 6.5 Effect of fluid dynamic variables

The fluid dynamic variables (Reynolds number, Mach number, etc.) have an effect on diffusers, but little research has been carried out.

Here we will give examples of research on fluid dynamic variables that affect centrifugation fluid machines in general or axial flow compressor straight blade groups.

/172

#### (1) Effect of Mach number (compressibility)

The effect of a high speed flow on fluid machine elements (changes in density, pressure, velocity distribution, condition of boundary layer, etc. due to compressibility of gas, that is, continuous changes, and intermittent changes, such as the formation of shock waves due to ultrasonic speed) have been explained with various examples. However, there are still many unknowns as treatment is more difficult than with low velocity flows.

Figure 6.48 is a diagram showing changes in property curves with high speed rotation of centrifugation compressors [63].

Curve (a) is the velocity produced in inducers (axial flow blade section of runner inlet side), and curve (b) shows the velocity with diffusers. The velocity of inducers and of diffusers is similar with high speed rotation. This is due to the fact that compression by runner proceeds and there is a reduction in volume flow to the diffuser, thereby making the diffuser in a state of low flow. Moreover, when the r.p.m. is increased, there is a gradual reduction in the increase in flow and the pressure of the compressors, or efficiency curve, suddenly falls. This is due to the fact that the flow becomes a sonic speed flow and choking (blockage) occurs making increase of the flow difficult.

Watanabe [64] has carried out studies on the effects of changes in inlet air conditions of centrifugation compressors on the properties of the compressor using the Mach number, while keeping inlet Reynolds numbers constant using a closed circulating pipe system. Figures 6.49 a and b show the correlation between the revised r.p.m.\* and the revised flow\* as the parameter. The data obtained with a constant Mach number  $M_{u2}$  of the runner peripheral velocity is placed on each curve. The adiabatic efficiency of the compressor decreases with an increase in  $M_{u2}$ .

/173

## (2) Effect of Reynolds number and disruption

The degree of disruption of the flow and the inlet Reynolds numbers effect on blades was studied by Wolf [65]. The correlation between the incidence angle  $i$  and resistance coefficient  $C_w^{**}$  is shown in Figure 6.50. It shows the case where the degree of disruption is low and when the degree of disruption is high due to a tripping wire. The difference in the size of disruption is not large when the resistance coefficient is low. However, the resistance coefficient is lower when the degree of disruption

---

\* Same as in Figure 6.20.

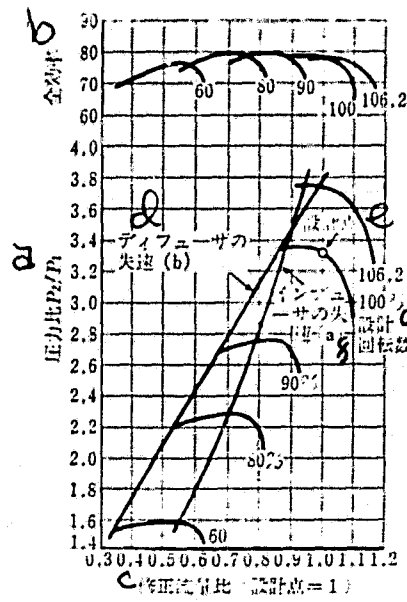


Figure 6.48. Properties of compressors at high velocity rotation.  
 a--pressure ratio; b--total efficiency; c--revised flow ratio (design point =1); d--diffuser velocity; e--design point; f--inducer velocity; g--design r.p.m.

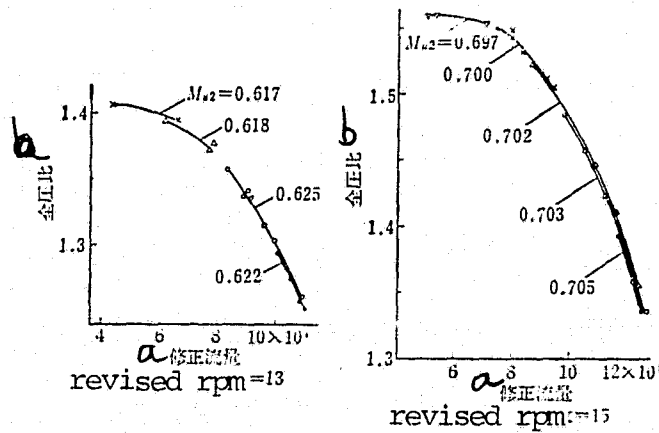


Figure 6.49. Effect of Mach number (compressibility) on properties of centrifugation compressors.

a--revised flow; b--total pressure ratio.

is low (there are cases where a high disruption is preferred for prevention of peeling, etc.)

Yugata and Shikita [66] have carried out studies on the effects of the Reynolds number on compressors and fans. Figure 6.51 shows one example. The correlation between the Reynolds number at the end of the operating blade in an axial flow compressor and the value that represents loss  $(1-\eta)$  is shown. The figure also includes that results of many other researchers. It is clear that the loss decreases with an increase in the Reynolds number and then gradually becomes constant. There are cases where the Reynolds number based on peripheral velocity of the runner is used. However, the loss produced in the fluid machine is the sum of many different losses and therefore, this picture shows a general tendency.

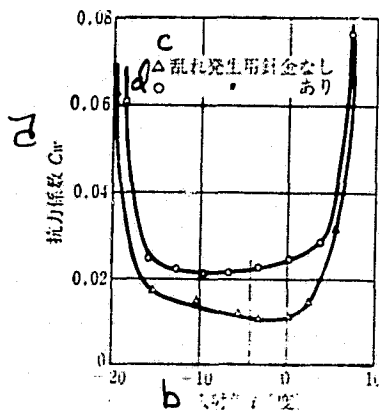


Figure 6.50. Correlation between disruption and blade properties.  
 a--resistance coefficient; b--no tripping wire; c--tripping wire for disruption; d--angle of incidence  $i$  (degrees).

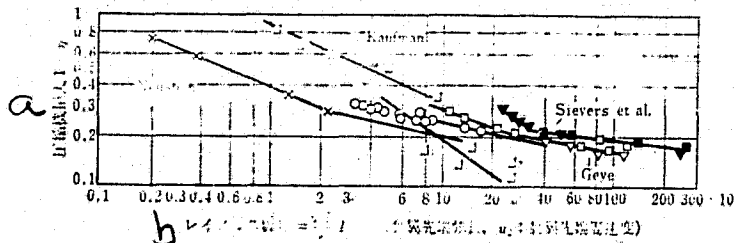


Figure 6.51. Correlation between Reynolds number and compressor loss.  
 a--compressor pressure loss; b--Reynolds number  $Re = u_2 l / \nu$ . ( $l$  is the initial blade and extension and  $u_2$  is the operating blade velocity).

(3) General conditions

We have briefly explained the properties of centrifugal compressors and given examples of studies on these devices.

Watanabe has studied the axial flow air devices (compressors, etc.) and high speed fluid dynamics. The data of the effects of Mach number on compressor properties is shown in Figure 6.52 and is one example of the research being carried out by the Soviet Union. The figure represents the flow and pressure as dimensionless. Moreover, the pressure coefficient and efficiency decrease near a Mach number  $M_{u2}$  that exceeds 0.7.

Mikai [68] has studied operating flow of centrifugation /175  
 devices and has measured changes over time in the pressure. According to his results, there is a reduction in pressure because a counter current is produced. The lost pressure is reduced from a pressure ratio of approximately 4 to 2 or less.

As was previously mentioned, the effects of fluid dynamic variables on centrifugation diffusers have been clarified quantitatively. However, further testing and research on special application conditions and fluids is necessary.

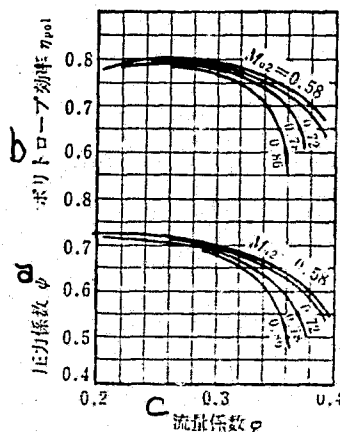


Figure 6.52. Correlation between Mach number and centrifugation compressor properties.  
 a--pressure coefficient; b--polito loop efficiency  $\eta_{pol}$ ;  
 c--flow coefficient.

## REFERENCES

- [1] Eckardt, D.; ASME publication, Paper N. 74-GT-90 (1974-4).
- [2] Wiesner, F.J.: ASME Paper, No. 66-WA/FE-18 (1966-11).
- [3] Sakinishi, et al.: Kienron No. 119, p. 101 (10/64).
- [4] Sepanof (Teruda, translator): Turbofans, p. 159 (1958).
- [5] Senoo, et al.: Kienron No. 153, p. 207 (4/1966).
- [6] Yoshinaga, Y., et al.: Trans. ASME (J. of Fluids Engg.) 102, p. 486 (1980-12).
- [7] Shung, H.: MAN Forschungsheft, No. 9, p. 33 (1960).
- [8] Linsi, U.: Brown Boveri Rev. 52-3, p. 161 (1965-3).
- [9] Sugii: Kienron No. 170, p. 223 (4/67).
- [10] Sorgel, G.: Maschinenbautechnik, 17-11, p. 576, (1968).
- [11] Sugii: Ken 37-303, p. 2161 (11/71)
- [12] Kawato, et al. Kobe Seido Giyo 31-3, p. 65.
- [13] Sugii: Kienron No. 179, p. 153 (10/67).
- [14] Sekichi: Kienron 40-335, p. 1929 (7/1974).
- [15] Sakurai, T.: Trans. ASME (J. of Engg. for Power), p. 388 (1975-7).
- [16] Stahler, A.F.: Transonic Flow Problems in Centrifugal Compressors (SAE Technical Progress' Series, Vol. 3).
- [17] U.S. Patent 3860360 (1975)
- [18] U.S. Patent 3905721 (1975)
- [19] U.S. Patent 393369 (1976)
- [20] Rayan, M.A., Yang, T.T. ASME publication, 80-GT-148 (1980-3).
- [21] Kenny, D.P.: ASME publication, 68-GT-38 (1968).
- [22] Klassen, H.A.: NASA TN D-7237 (1973).
- [23] Shokuda: Mitsubishi Nihon Heavy Industries Report 3-1, p. 8 (1962).
- [24] Pampreen, R.C.: Trans. ASME (J. of Engg. for Power), p. 187 (1972-7).
- [25] Seno: Kien 45-396, p. 1099 (8/1981)
- [26] Seno: Kienron 810-15, p. 195 (10/81)
- [27] Dean, R.C. Jr., Senoo, YI: Trans. ASME (J. of Basic Engg.) 82-3, p. 563 (1960-9).
- [28] Shokumatsu: Kien 27-183: p. 1780 (11/61).
- [29] Shokumatsu: Kien 27-183 p. 1789 (11/61).
- [30] Johnston, J.P., Dean, R.C. Jr.: ASME Paper, No. 65-FE-1 (1965).



- [31] Senoo: Kyushi University School of Industry Research Report 57, 1973).
- [32] Senoo, Y., Ishida, M.: Proceedings, the 2nd International JSME Symposium, Fluid Machinery and Fluidics, Tokyo, p. 61, (1972-9).
- [33] Ishida and Senoo: Kien 41-347 p. 2053 7/1975.
- [34] Seno: Kien 43-367, p. 987 3/1977).
- [35] U.S. Patent 3868196 (1975)
- [36] Okamura:: Turbodevices 8-6, p. 314 (6/1980)
- [37] Furui Kienron, No. 810-5, p. 201 10/1981.
- [38] Gardow, E.B.: MIT Gas Turbine Laboratory Report, No. 42 (1958).
- [39] Jansen, W.: Trans. ASME (J. of Basic Engg.), p. 607 (1964-9).
- [40] Pampreen, R.C.: The laminar incompressible boundary layer in a constant area vaneless radial diffuser.
- [41] Ferguson, T.B.: Radial Vaneless Diffuser (Dept. of Mech. Engg., the Univ. Sheffield, England), p. 160.
- [42] Broecker, E.: Heiz. Luft. Haust, 11-7, p. 173 (1960-7).
- [43] Vielhaber, K.: VDI\* Bericht, No. 75, p. 71 (1964).
- [44] Moller, P. S.: Aeron. Quart. 14, p. 163 (1963-5).
- [45] Feiereisen, W.J., et al.: Proceedings, the 2nd International JSME Symposium, Fluid Machinery and Fluidics, Tokyo, p. 81, (1972-9).
- [46] Jansen, W.: Trans. ASME (J. of Basic Engg.) 86, p. 750 (1964).
- [47] Baade, K.H: Unsteady flow in the vaneless diffuser of a radial compressor stage )Technische Hochschule Magdeburg, East Germany).
- [48] Imaichi, K. et al.: Rotating stall in a vaneless diffuser of a centrifugal fan (Faculty of Engg. Sci. Osaka Univ. Japan).
- [49] Brown, W.B., Bradshaw, G.R.: NATA TN 1426 (1947).
- [50] Otarō: Kienron (Kaishibu Dai 44 Kiteihi Sokai Koenkai)., p. 44 (3/1969).
- [51] Otarō: Kien 41-349, p. 2612 (9/1975)
- [52] Friberg, J., Merigoux, J.M.: ASME publication, 73-FE-35 (1973-6).
- [53] Practical New Publications Reports 1981-38240 (1981)
- [54] Sekichi: Kienron, 750-8 p. 41 (8/75).

- [55] Kishita: Kienron 800-14 p. 270 (8/1980).
- [56] Sugii: Kien 32-240, p. 1282 (8/76)
- [57] Senoo: Kienron, No. 778-1, p. 57 (3/77)
- [58] Sprecher, J.: Sulzer Tech. Rev. No. 3, p. 1 (1951).
- [59] Ellis, G.O.: Trans. ASME (J. of Basic Engg.) 82-1, p. 155 (1960-3).
- [60] Sugi: Kien 32- 237, p. 734 (5/1966)
- [61] Sugi Kienron (Hitachi convention), p. 24, 11/1965)
- [62] Toshikura: Kienron No. 810-18, p. 102 (8/81)
- [63] Rodgers, C.: Influence of impeller and diffuser characteristics and matching on radial compressor performance (SAE Technical Progress Series, Vol. 3).
- [64] Watanabe: Kienron, No. 160, p. 125 (10/66)
- [65] Wolf, H. Maschinenbautechnik, 13-12, p. 651 (1964).
- [66] Ugata: Turbodevices 5-5, p. 270 (3/1977)
- [67] Watanabe: Kienso (257) p. 33 (5/1976).
- [68] Mikai: Kikai no Kenkyu 29-4, p. 488 (1977)

## 7.1 Introduction

In addition to the knowledge and experience obtained on research and development pertaining to industrial technology, there still remains the need for further diagrams, discussion, reports, patents, etc. In Japan, we have been actively pursuing the collection of reports and data as well as discussions. There is little recording of patents in technological texts, and we will therefore discuss patents on diffusers.

Patents are given as specific inventions by new inventors of industrial products (the inventions are unique). [1] At the present time there are many patent laws in effect in Japan. There have been records of patents on centrifugation compressor and fan (called compressors below) diffusers over the last 20 years, and we would therefore like to view technological conditions in this field from the aspect of patents [2]. (This chapter will be limited to centrifugation bladed and bladeless diffusers and channel diffusers).

## 7.2 Inspection and adjustment of data

### (1) Terminology

The basic structure of centrifugation compressors with diffusers has been explained in Chapter 3. The terminology applied to each component is standard. [3]. However, various terms are actually used. The topic of patents in this section (called inventions) and terminology in the specification are varied. We will compare the terminology in this section. /180

Centrifugation type (axial flow type, radial flow type, etc.)

Diffuser (guide equipment, dispersion equipment, etc.)

Blade of diffuser blade (vane, blade, guide blade, etc.)

Bladeless diffuser (vaneless diffuser, etc.)

Bladed diffuser (bladed diffusers guide bladed diffuser, etc.)

Side wall of diffuser side walls (side plate, base plate, diffuser plate, etc.)

2 stage blade (double blade, tandem blade, etc.; tandem and slot diffusers)

Flow path width or diffuser flow path width (path width, flow path depths, blade height, etc.)

(Blade) inlet (also called inlet blade angle. A line drawn to the blade center line in the running edge is the angle in the direction of the periphery). In the U.S. this is also called the radial angle).

Inlet) flow angle (angle where the direction of flow is the peripheral direction of the blade inlet (or radial direction. The inlet flow angle is also called the flow angle and the outlet flow angle is called the outflow angle).

Incidence angle (there are cases where this is called the reverse\* angle. This represents the difference between the inlet angle and inlet flow angle.)

Runner \*impeller, rotor, blade, etc.)

(Runner) side plate (return plate, shroud, etc.)

Guide plate (return blade, retainer, guide vane, etc.)

Spiral casing (scroll, spiral casing, etc.)

## (2) Investigation methods

In Japan, patent publications take 15 years and utility proposals take 10 years to be removed. Furthermore, the applications up to 1970 were inspected. However, after 1971, the

/181

---

\* The reverse angle is the angle where the flow is the inflow with straight line blades (difference between feed angle and inlet flow angle). The difference between the blade inlet angle and inlet flow angle is the incidence angle.

patents were disclosed 1 year and 6 months after application. The stage patent verification is called patent publication and there are two types of patents, kokai and publications. The level of the patent during this period (or utility proposal) is not determined in patent publication materials. Therefore, the kokai patents are unexamined and the level of the patent (or utility proposal) at this time is not determined.

Inspection of patents is carried out by patent reports or kokai reports. Furthermore, there have been many parts of patent publications in recent years. In addition, patent reports have been computerized by special agencies and therefore, selection, patent applicant determination\*, etc. are possible. Both foreign and domestic patent applicants can make applications in Japan.

The patent controls of the U.S. do not apply to utility proposals. Moreover, there is no control over patent kokai and patent publications. They are presented simply in patents and registrations. The period for which patents are kept is 17 years after patenting. Moreover, there is a difference between priority claim in the U.S. and Japan.

The Official Gazette of the United States Patent and Trademark Office is used to inspect patents in the United States. The patent gazette differs from the Patent Report of Japan.

### 7.3 Tests on inspection results (technological trends)

#### (1) Technological Fields and Examples

Patents (and utility models) have classification codes /182 that represent their subject and technological details.\*\* The authors have listed the following 10 types of classifications A, B, C, .....J

\* Person presenting application (usually a company).

\*\* This is called the JPC (Japan Patent Classification) and the UPC (U.S. Patent Classification in the U.S. This is inconvenient for inspection of patents. Therefore, the IPC (International Patent Classification) was established and has been used since 1980 in Japan.

because details are not sufficient in technological inspection of diffusers.

Cl. A: Improvement of properties by control of boundary layers and diffuser blades (injection and suction of boundary layer, slot blades, prevention of boundary layers, etc.

Cl. B: Blades used in inlet flows (nonuniform flow in direction of path width, for three dimensions).

Cl. C: Control of properties by varying path width of diffuser to improve loss flow properties (instability of swirl velocity readily occurs with low flow angles and the path width is therefore narrowed).

Cl. D. Standardization of inlet radius with rotating blades\* (rotation around center axis of diffuser blades. The radial position of the inlet and outlet of the blade is varied. Changes in distance are undesirable and can thereby be prevented.)

Cl. E: Rotating devices of rotating blades (other than in D).

Cl. F: Changes in slot form to improve operation at ultrasonic speed (this form is used for high pressure and high velocity channel diffusers (gas turbines, jet engines, etc.)

/183

Cl. G: Method for manufacturing flow paths (special flow paths and their dimensional form).

Cl. H: 2-stage diffusers (of those in A, slot blades and operations).

Cl. I: Attaching short blades to inlet to control boundary layers (similar to layer prevention in A; however, the flow in the main flow region is guided and controlled.)

Cl. J: Bladed and bladeless regulator types (bladed diffusers that have narrow operation flow for high efficiency).

---

\* In patent terminology, the case of return to a constant direction (constant speed) is rotation and the case of return to left and right for adjustment is termed "revolution" (for detailed differentiation of operation and conditions).

Of the above-mentioned one example of classifications A, C, and F will be given in Figures 7.1 to 7.3. The details are given below.

CL. A (Example 1, Figure 7.1, Utility Sho 55-144896, Hitachi)..... This is a device where a low height loop is set up at the wall between diffuser blades and the loop inlet is extended from the blade inlet to the up flow side. The loss due to a low angle flow is reduced to flow caused by two-dimensional flow. /184

CL. C (Example 2, Figure 7.2, Japanese Patent Sho 43-29774, Zurutsua)..... This is a device where the side walls (side plates) rotate around the axis to connect the outside wall to the inlet diffuser. The pressure of both surfaces of this wall is balanced and the force for operation is reduced.

CL. F (Example 3, Figure 7.3, Utility 50-40006, Applicant: Shomatsu Seisajo)..... This is a device where a cam is set up inside the space near a slot of the triangular blade that covers the cam. The thin plate changes in form with rotation of the cam and the slot form is therefore changed with the changes in flow.

(2) Application period and technological details.

The correlation between the application period and number of classifications in Japanese patents (about 20 years) and U.S. patents (about 8 years) are shown in Figure 7.4.\* The following can be said from these figures.

(a) The number of applications was 68 in 20 years in Japan and 27 in 8 years in the U.S. This is not an accurate

\* As was previously mentioned, old data are retained for a number of years, depending on the patent rules. A comparison is made. The period from the application to the publication is now extended and there are problems with comparing published materials at the present time.

comparison, but the mean number per year is very different in the two countries. However, the Japanese applications are made by more foreign applications (19 out of 68) and therefore, the difference in the number of applications is even wider\*.

(b) There is a sudden increase (since 1977) in the number of applicants in Japan. The application fields are also increasing (because of increasingly sudden developments in technology). It also appears that Japan is falling behind in the field of fluid machines.

(c) The main applicants in Japan are 6 domestic and 7 foreign manufacturer. The number of applicants in the U.S. is 4, with 9 being primary and 6 being secondary out of 27.

/185

(d) The number of applicants in technological fields has increased.

Classification A (Boundary layer control: 14 (12 in Japan, centering on improvements in diffusers).

Cl. C (flow path width changes): 19 (all in Japan,, however, 8 are foreign. The number of applicants for fluid flow control in Japan is increasing.)

Cl.E (rotating blades): 10 (7 domestic, 3 in the U.S. Those who made many applications prior to 1974 in the U.S. are not included).

Cl. G (flow path manufacture): 19 (6 from foreign countries, 12 in U.S.; the majority are by U.S. manufacturers).

It appears that this reflects the fact that the industrial range in Japan is primarily conventional manufacture, in contrast to the large number of U.S. manufacturers involved in jet and gas turbine channel diffuser manufacture. Moreover, it appears that Japan is behind in research and development on fluid hydraulics, etc.

---

\* The number of applications in Japan is approximately 40 including utility models.



OF POOR QUALITY

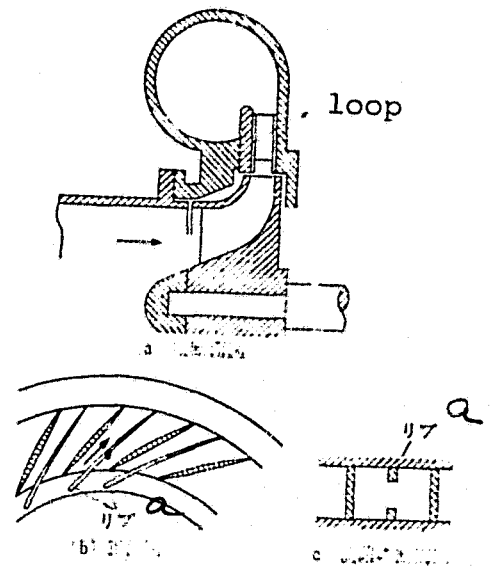


Figure 7-1. Example 1 (Cl. A, Utility 55-144896, Hitach).  
 (a)--cross section; (b)--front view; (c)--profile of low path.

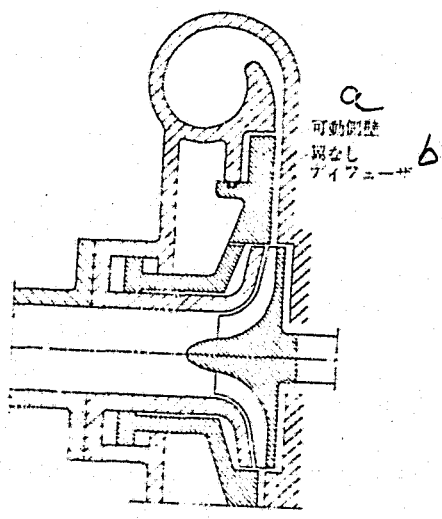


Figure 7.2. Example 2 (Cl. C Japanese Patent 29774 Zurutsua)  
 a--Movable side walls;  
 b--Bladeless diffuser

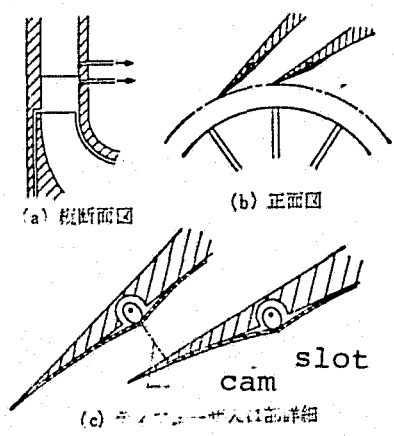


Figure 7.3. Example 3 (Cl. F, Utility 50-40007, Shomatsu Seisaho).  
 (a)--profile; (b)--front;  
 (c)--inlet of diffuser;

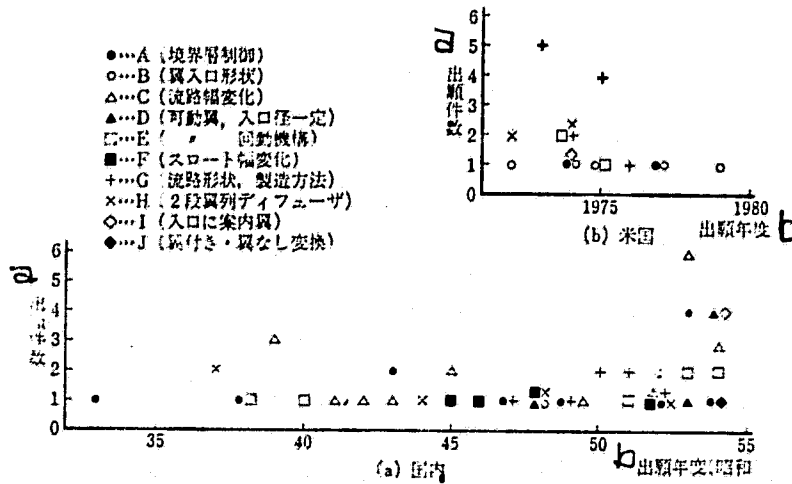


Figure 7.4. Classifications of patents and patent periods. a--number of patents; b--patent period (showa years) (a)--Japan; (b)--U.S.

A.--Boundary layer control; B.--Blade inlet form; C.--Flow path width; D.--Movable blades, inlet diameter consistency; E.--(movable blades, rotating mechanism); F.--Slot width changes; G.--Flow path form, manufacture; H.--(2 stage blade diffuser; I.--Guide blades; J.--Bladed and bladeless variations.

#### 7.4. Conclusion

The explanations of trends in Japanese patents and U.S. patents on centrifugation compressors were given in Section 7.3. However, these are not the only examples. Moreover, it can be said that the patents reflect research and development, but not the condition of new technology. The number of applications in Japan is markedly different from that in other developed countries and it can be said that patent invention application is considerably lower. In the future we hope to see improvement of patenting of technological developments.

## REFERENCES

- [1] For instance, Tekda Patent Information (Diamond, 9/76).
- [2] Sugii: Turbodevices 10-5, p. 312 (5/82)
- [3] Japanese Mechanical Engineering Society Terminology on Compressors and Fans: Kishi 67 -551, p. 1904 (5/74).

## Index\*

	<u>Page</u>
Adiabatic change	29
Adiabatic efficiency	48
Adiabatic head	48
Airfoil, airfoil vane	23
Angle of attack	9, 180
Annular diffuser	2, 64, 106
Annular fluid-channel	107
Applicant	181
Approaching fluid-channel	142
Approaching zone	155
Area ratio	100, 103
Arrow type five-hole probe	85
Arrow type three-hole probe	85
Aspect ratio	103, 104
Auxiliary guidevane	65, 117
Axial-flow compressor	14, 174
Axial-flow turbine	14
Axially symmetrical fluid-channel	67, 166
Backflow	157
Balance flow-rate	158
Bell type diffuser	108, 110
Bernoulli's equation (energy equation)	24
Blockage factor	106, 125
Booster	167
Boundary layer	3
Boundary layer calculation	169
Boundary layer control	68, 118, 182
Boundary layer equation	27
Boundary layer injection	118
Boundary layer parameter	39
Boundary layer suction	68, 118, 120, 159

\*Translator's Note: The page numbers are for the original Japanese text.

Boundary layer theory	26, 106
Camber	23, 144
Cartesian co-ordinates system	17
Cavitation	67
Cell, number of cell	164
Centrifugal, axial-flow, semi-axial-flow	5
Centrifugal compressor	46
Centrifugal force	68
Centrifugal pump	7, 12
Centrifugal-type diffuser model	78
Centrifugal-type diffuser, radial diffuser	62
Channel (type) diffuser	10, 66, 145
Choke	67, 124, 172
Chord length	33
Chord pitch ration solidity	153
Circular-arc blade (vane)	23
Circular cascade	5
Circular cascade test apparatus	143
Circulation	19
Classification of patent	182
Coefficient of viscosity	17
Combined probe	87
Complex potential	21
Compressibility	172
Compressible flow	19
Compressor, blower, fan	4
Compressor for refrigerator	8
Conformal transformation	19
Conical diffuser	2, 58, 64, 99
Constant-area diffuser	159
Continual return guidevane	170
Coriolis' force	68, 129
Critical (transition) Reynolds number	28, 162
Cross-section of fluid-channel	64, 110
Curved diffuser	3, 61, 65, 111

Curved fluid-channel	11, 67
Curved pipe, elbow	114
Cylindrical co-ordinates system	18
Cylindrical three-hole probe	85
Decelerating cascade	14
Decelerating fluid-channel	1
Degree of nonuniformity	158
Delivery casing	14
Delivery curved fluid-channel	12, 166
Delivery diffuser	67, 168
Design method of centrifugal compressor (blower)	46
Design method of diffuser	58
Deviation angle	152
Diffuser efficiency	26, 59
Diffuser for pump	79
Diffuser performance problem	64
(Diffuser) side wall	180
Diffuser test or measuring method	73
Diffuser vane	180
Diffuser with adjustable vanes	8, 182
Diffuser with airfoil vanes	150
Diffuser with circular-arc vanes	151
Diffuser with curved walls	117, 123
Diffuser with logarithmic spiral vanes	114, 142
Diffuser with non-similar end cross-sections	3
Diffuser with rough walls or grooves	65, 122
Diffuser with straight vanes	151
Diffuser with sudden expansion	65, 117
Diffusion ratio	138
Direct insertion method	92
Direct method, inverse method	32
Displacement thickness	28, 119, 169
Distortion factor	143
Diverging angle	3
Diverging duct	3

Double circular-arc blade	151
Double row diffuser	180
Draft tube	15
Drag coefficient	173
Dump type diffuser	108
Dynamic measurement of flow	134, 156
Dynamic (velocity) pressure	2, 24
Effective period of patent (right)	181
Efficiency, total efficiency	59
Electric motor blower	8
Entry without swirl	48
Equation of continuity	17
Equation of motion	17
Equation of state for perfect gas	29
Equi-potential line	20
Equivalent diverging angle	61, 106, 144
Equivalent straight cascade	151
Euler's equation of motion	23
(Fluid channel type) diffuser model	74
Flow angle	44
Flow-regime map	104, 112
Flow-rate coefficient	56
Fluid-channel between blades	62
Fluid-dynamic analysis method	94
Fluid-dynamic parameter	67, 171
Fluid machine	4
Francis (water) turbine	15
Free vortex flow	45
Friction loss coefficient	156
Friction stress	3, 28
Gas turbine	10
Gas constant	29
General fluid-channel type diffuser	58, 99

Head	7, 24
Head coefficient (pressure coefficient)	56
Hot-wire anemometer	88
Hub, shroud	67, 180
Hydrogen bubble method	93
Impeller exit flow	133
Impeller, runner	5, 180
Incidence	9, 68, 139
Incompressible fluid	17
Inducer	172
Inlet boundary layer thickness	67, 188
Inlet duct	116
Inlet flow angle	8
Inlet guidevane	8
Inlet Reynolds number	123, 173
Inlet shear flow	67, 126
Inlet swirl flow	68
Inlet vaneless diffuser	46, 51
Interference	78
Internal flow, external flow	14
Involute type return guidevane	171
Irrotational flow	20
Joukovsky's airfoil	23
Judgement for separation	169
Kiel (type) probe	85, 87
Kinematic viscosity	26
Kutta-Joukovsky's theorem	23
Laminar boundary layer	28
Laplace's differential equations	20
Law of similarity	31, 56
(LDV) laser-Doppler velocimeter	89
Leading edge, trailing edge	33, 180
	211



Length (to width) ratio	100, 103
Lift	9, 23
Logarithmic spiral	38, 113
Longitudinal profile	64, 108
Loss coefficient	26
Low flow-rate	172
Mach number	30, 118, 140, 146
Mach-Zender interferometry	94
Main flow, main stream	27
Magnifying ratio of transformation	23
Manometer	84
Manufacturing method of diffuser	186
Matching	7
Measurement of internal flow	85, 88
Mixed-flow type	13
Model test apparatus	154, 159
Moment of Momentum theory	43
Moment, torque	43
Momentum integral	29
Momentum thickness	28
Momentum theory	26
Movable wall	184
Multi-stage compressor	6
Navier-Stokes' equation	18
Newton(ian) fluid	18
Non-contact velocimeter	89
Nondimensional number	31
Normal shock wave	146
Obstacle at diffuser inlet	160
Official gazette for patent	181
One-dimensional flow theory	160
Operating flow-rate range	68, 151
Optical measuring method	94

Optimum diverging angle	60, 101, 103
Optimum incidence	141, 144
Orifice, nozzle	81
Patent information	181
Patent (invention) of diffuser	58
Path line	93
Performance of centrifugal-type diffuser	133
Performance of fluid-channel type diffuser	99
Performance test of compressor or blower	81
Pipe diffuser	10, 66, 149, 150
Pipe friction coefficient	25
Pitch chord ratio	33, 145, 153
Potential flow	19, 113, 171
Power coefficient	57
Pressure coefficient	59
Pressure loss	1
Pressure recovery efficiency	59
Pressure side, suction side	9
Probe	76
Publication (declaration) of application	181
Publication (disclosure) of application	181
Pump turbine	144
Pyramid diffuser	2, 60, 64, 102
Radial type	5
Rake probe	88
Reaction rate	49
Reduced flow-rate	173
Reduced rotational speed	173
Relaxation method	36
Request for examination	181
Return channel	6, 169
Return guidevane	11, 169, 170, 180
Reynolds number	25, 67, 123, 173
Reynolds stress	28

Rotating fluid-channel	68, 128
Rotating screen	154, 159
Rotating stall	163
Rotating vaneless diffuser	157
Rotor, stator	13
Roughness	26
Schlieren method	94
Secondary flow	62, 113, 138, 184
Semi-axial flow compressor	165
Semi-axial flow diffuser	67, 165
Separation	1, 160
Separation range	104
Shadow graph method	94, 146
Shape factor	64
Shape of circular cascade	53
Shape parameter	28, 106, 169
Shock wave	146
Shockless entry	138
Single-stage compressor	5
65-series airfoil	151
Slip	48
Slip factor (coefficient)	48, 134
Slot blade	9
Smoke wire method	93
Sound velocity	30
Source, sink	22
Spark method	93
Spatially curved diffuser	65, 114
Specific speed	57, 156, 158
Spiral casing	5, 155, 180
Stagnation state	30
Stagger angle	33, 145
Stall	68, 88
Standard Pitot tube	82
Static, dynamic, total temperature	30

Static measurement of flow	85
Static pressure	2
Steady flow	19
Straight blade (vane), flat plate blade (vane)	23, 141
Straightener, straightening device	74
Straightening	116
Streakline	93
Stream function	20
Streamline	20
Streamline analysis method	33
Streamtube	24
Suction casing	14
Suction curved fluid-channel	12, 34, 168
Sudden expansion	1
Supercharger	139
Supersonic	67, 146
Supersonic diffuser	166
Surging	139, 163
Surging margin	150
Swirl flow generator	143
Swirl flow, whirl	128
Swirl, swirl component	12, 68
Swirl (vortex) generator	121
Tail pipe	116, 127
Tandem type or slot type diffuser	66, 150
Theorem	31
Thickness ratio	144
Three-dimensional turbulent boundary layer	159, 165
Throat	146, 182
Time line	93
Total pressure	2
(Total pressure) loss coefficient	59
Transition	28
Traverse	82, 86
Trumpet type diffuser	65, 108, 150

Tuft method	91
Turbo type, displacement type	5
Turbulence	4, 68
Turbulence rate	108, 125, 173
Turbulent boundary layer	28
Turning angle, deflection angle	111, 144
Two-dimensional diffuser	2, 58, 64, 103
Two-dimensional fluid-channel	37
(Two-dimensional) straight cascade	14, 33
U-shaped curved channel	167
Unsteady flow	19, 25
Unsteady flow in diffuser	163
Utility model of diffuser	166
Vane (blade) angle	45
Vane block	10, 146
Vane inlet angle, vane exit angle	8, 180
Vaned diffuser	5, 66, 133, 135
Vaneless diffuser	6, 66, 135, 153
(Vaneless) diffuser with parallel walls	153
(Vaneless) diffuser with unparallel walls	155
Variation of vaned diffuser	8, 145
Velocity potential	20
Velocity triangle	48
Visualization test	90, 138
Vortex generator vane	122
Vortex motion	19
Vorticity	19
Wall trace	91
Waved pipe, coiled pipe	115
Wedge type vane	137
Width (depth) of fluid-channel	45, 180
Width ratio (inlet width ratio)	160
Wind tunnel	3